University of Alberta

Library Release Form

Name of Author: *Lesley Margaret Hill*

Title of Thesis: *Drylines observed in Alberta during A-GAME*

Degree: *Master of Science*

Year this Degree Granted: *2006*

_____

Signature

3906 Upper Dwyer Hill Rd.
R.R. #1 Kinburn, Ontario, K0A2H0

University of Alberta

Drylines observed in Alberta during A-GAME

by

Lesley Margaret Hill

A thesis submitted to the Faculty of Graduate Studies and Research in partial fulfillment of the

requirements for the degree of *Master of Science*

Department of *Earth and Atmospheric Sciences*

Edmonton, Alberta

Spring, 2006

Abstract

This thesis investigates drylines (or moisture fronts) in south-central Alberta during A-GAME (July-August 2003 and July-August 2004). Surface meteorological data were collected every 30 minutes at 4 sites along the FOPEX transect (from Caroline westward). In addition, mobile transects were performed allowing for even finer 1 minute resolution data. GPS-derived precipitable water estimates were also examined. The major findings of this investigation were:

1) During the 4 summer months, 7 dryline events occurred in the project area.
2) Five of these dryline events were associated with convective activity, including one severe thunderstorm with 2 cm diameter hail. Two of the dryline events had no convection associated with them.
3) The magnitude of the mixing ratio gradient across the dryline ranged from 0.9 to 4.3 g kg^{-1} km^{-1}, similar to measurements recorded in High Plains of the U.S.
4) GPS-derived PW estimates showed promise for locating the dryline.

Acknowledgments

I would like to thank first and foremost Dr. Geoff Strong, without you none of this would have been possible. Thank you for all you have invested in this project and me. Your enthusiasm regarding the stormy sky is rare and infectious, and it has been a great experience working with you and learning from you. I particularly enjoyed our time in the field; only someone like you would actually turn around *into* a hail shaft so that I could experience my first Alberta hailstorm.

Thank you to Dr. Gerhard Reuter, for your honesty and feedback during the writing process and your overall investment to co-supervise me. Thank you to Dr. Edward Lozowski, I consider myself very fortunate to have had such an excellent teacher and scientist to learn from inside and outside the classroom during my time at the University of Alberta.

I would like to thank my parents Tom and Ann Hill, all of your love, encouragement and support from across the country has meant more to me than I can put into words. You have taught me that anything is possible if I am willing to take chances and do some hard work along the way. Thanks to my siblings Mike, Scott and Joanne for keeping my feet on the ground even when my head is in the clouds. I am even thankful for the homesickness I often felt while attending the University of Alberta, because it was a constant reminder that I am lucky to have such a great group of people in my life to miss back home in the Ottawa Valley.

Thanks to all my close friends who always managed to lend an ear and offer words of encouragement even though they may have not been able to sympathize with my position. Special thanks to Marshall Elliott, who gave me unconditional support throughout the writing process beyond what I ever expected.

Thank you to Dr. Susan Skone at the University of Calgary, for supporting the thunderstorm research aspect of the A-GAME project. Thanks to her students in the Department of Geomatics Engineering involved in the processing of GPS data, among other things. Thank you to Craig Smith at the Climate Research Branch, for help with all things related to the FOPEX project. I am grateful to Claude Labine at Campbell Scientific Inc., and Gary Burke at Environment Canada for graciously supplying the equipment necessary for the mobile transects. Thanks to Ron Goodson for being so helpful by providing data and just as important, your time. Thanks to Dr. Terry Krauss at Weather Modification Inc. for your field support and generosity. Thank you Pat King for your participation in the A-GAME project of July 2003 – especially for spending so much time driving in and around the dusty foothills performing mobile transects. Special thanks to Julian Brimelow for your advice and support during my time at the University of Alberta. Thanks also to Neil Taylor and Stephen Knott for supplying me with the relevant Canadian literature regarding the dryline.

I would like to acknowledge Dr. David Sills, who has been one of the most influential people I have had the opportunity to work with since my first summer as a field assistant

in southern Ontario. By answering a random email from curious 1st year student seeking some advice, you pointed me in the right direction that got me to where I am today. I am grateful for every opinion and opportunity you have given me, in addition to your friendship.

Financial support during my studies was provided by the Canadian Foundation for Climate and Atmospheric Sciences through the Department of Geomatics Engineering at the University of Calgary, and also a Province of Alberta Graduate Scholarship.

Table of Contents

1 Introduction 1

1.1 Overview 1

1.2 The Dryline 1

1.3 Alberta Thunderstorms 10

1.4 A-GAME and FOPEX Field Projects 14

1.5 Objectives 16

1.6 Outline 18

2 Methodology 20

2.1 Overview 20

2.2 Detecting the Dryline 21

2.3 Identifying a Dryline Event During A-GAME 24

2.4 Summary 36

3 Results 38

3.1 Overview 38

3.2 FOPEX Dryline Signature 38

3.3 Dryline Events Observed During A-GAME 40

3.4 Thunderstorm Formation in the Dryline Vicinity During A-GAME 42

3.5 Moisture Gradients Observed by Mobile Transects 43

3.6 Case Study of 16 July 2004 Dryline Sampled by Mobile Transect 44

3.7 GPS-derived Precipitable Water Observations During 10 July 2004 FOPEX Dryline Event 51

3.8 Summary and Conclusions 61

4 Conclusions and Recommendations 63

4.1 Discussion and Conclusions 63

4.2 Limitations of this Study and Recommendations for Future Work 65

Tables 68

Figures 72

Bibliography 99

Appendix A 104

Appendix B 105

Appendix C 109

List of Tables

Table 2.1 Location of FOPEX transect stations 68

Table 2.2 Data recovery rates for FOPEX transect during study 68

Table 2.3 Locations of synoptic surface weather observations 69

Table 3.1 Overview of all A-GAME dryline events 70

Table 3.2 Stability indices for 16 July 2004 soundings 70

Table 3.3 Stability indices for 10 July 2004 soundings 70

Table 4.1 Summary of conclusions 71

List of Figures

Figure 1.1 Conceptual model of High Plains dryline....72

Figure 1.2 Map of the Great Plains (High Plains) 73

Figure 1.3 Annual mean thunderstorm days in Canada 73

Figure 1.4 Annual mean days with lightning in Canada 74

Figure 1.5 Multi-scale conceptual model of Alberta thunderstorms 75

Figure 1.6 Boundary layer evolution on Alberta thunderstorm day 76

Figure 1.7 A-GAME and SAN study area in southern Alberta....77

Figure 1.8 FOPEX study area in south-central Alberta 78

Figure 1.9 FOPEX transect topographic map....78

Figure 1.10 FOPEX elevation graph....79

Figure 2.1 Equipment mounted on mobile transect vehicle 80

Figure 2.2 Labeled synoptic and FOPEX observation sites in south-central Alberta....80

Figure 2.3 Process of computing GPS-derived PW 81

Figure 3.1 Typical dryline signature in FOPEX transect 82

Figure 3.2 Synoptic analysis charts for 16 July 2004 83

Figure 3.3 1800 UTC Olds-Didsbury Airport sounding on 16 July 2004....84

Figure 3.4 2200 UTC Olds-Didsbusy Airport sounding on 16 July 2004 84

Figure 3.5 Comparison of 1800 UTC and 2200 UTC soundings of 16 July 2004 85

Figure 3.6 Mixing ratio trends in FOPEX transect on 16-17 July 2004 85

Figure 3.7 Mixing ratio and wind direction trends in FOPEX transect on 16-17 July 2004 86
Figure 3.8 3-hourly synoptic moisture and wind field evolution on 16-17 July 2004 ... 87
Figure 3.9 Mobile transect mixing ratio observations on 16 July 2004 88
Figure 3.10 Mixing ratio field observed by mobile transect on 16 July 2004 88
Figure 3.11 Synoptic moisture field without and with mobile transect data on 16 July 2004 89
Figure 3.12 Cumulonimbus observed during mobile transect on 16 July 2004 89
Figure 3.13 1932 and 2210 UTC GOES visible satellite imagery on 16 July 2004 90
Figure 3.14 2130 UTC Strathmore radar imagery on 16 July 2004 90
Figure 3.15 Synoptic analysis charts for 10 July 2004 91
Figure 3.16 1900 UTC Airdrie sounding on 10 July 2004 92
Figure 3.17 2400 UTC Olds-Didsbury Airport sounding on 10 July 2004 92
Figure 3.18 Mixing ratio trends in FOPEX transect on 10-11 July 2004 93
Figure 3.19 Mixing ratio and wind direction trends in FOPEX transect on 10-11 July 2004 94
Figure 3.20 Synoptic moisture field without and with FOPEX data on 10 July 2004 95
Figure 3.21 3-hourly synoptic moisture and wind field on 10-11 July 2004 96
Figure 3.22 2310 UTC Strathmore radar imagery on 10 July 2004 97
Figure 3.23 1931 and 2301 UTC GOES visible satellite imagery on 10 July 2004 97
Figure 3.24 Mixing ratio and GPS-derived PW trends at AB4 and Sundre on 10-11 July 2004 98

List of Symbols

r	water vapour mixing ratio
m_v	mass of water vapour
m_d	mass of dry air
e	water vapour pressure
p	air pressure
g	acceleration due to gravity
z	geopotential height
R	dry air gas constant
T	air temperature

List of Abbreviations

A-GAME	Alberta GPS Atmospheric Moisture Evaluation
AGL	Above ground level
ASL	Above sea level
CAPE	Convective Available Potential Energy
CAPPI	Constant Altitude Plan Position Indicator
Cb	Cumulonimbus
CIN	Convective Inhibition
CRB	Climate Research Branch
FOPEX	Foothills Orographic Precipitation Experiment
GOES	Geostationary Earth Orbital Satellite
GPS	Global Positioning System
LI	Lifted Index
LIMEX	Limestone Mountain Experiment
MDT	Mountain Daylight Time (-0600 UTC)
MSC	Meteorological Service of Canada
PW	Precipitable Water
SAN	Southern Alberta Network
UTC	Coordinated Universal Time
WMI	Weather Modification Inc.

Chapter 1

Introduction

1.1 Overview

This thesis focuses on drylines in south-central Alberta and the relationship of this surface boundary with thunderstorm development. Prior to stating the thesis objectives, the background information and the motivation for this thesis is provided below. The field projects that supplied that data and means to address the objectives of this thesis are also described.

1.2 The Dryline

The dryline, first identified by Fujita (1958) as a moisture front, is defined as a boundary layer convergence zone, giving rise to a sharp moisture gradient between relatively moist and dry air masses that develops in the lee of the Rocky Mountains and typically parallels the terrain contours (Schaefer, 1974). The initial estimation of dryline location typically corresponds to the 12°C dewpoint temperature isodrosotherm (9 g kg^{-1} isohume) when examining the surface moisture field over the High Plains (Schaefer, 1986). The dryline boundary can be hundreds of kilometers long and up to tens of kilometers wide, and the moisture gradient associated with the dryline can persist for a number of hours.

The dryline has been studied in great detail in the High Plains of the United States since the late 1950's, as it is a favoured area for thunderstorm development (Rhea, 1966). As discussed below, the moist air east of the dryline boundary is capped by a stable inversion that, under certain conditions, allows significant Convective Available Potential Energy (CAPE) to build up in the boundary layer. The release of this energy can result in deep convection near the dryline.

Dryline research carried out for the U.S. High Plains includes extensive observational studies that have collected data from sources such as instrumented aircraft on low-level flights (e.g. Ziegler and Hane, 1993) and a mobile surface mesonet (e.g. Pietrycha and Rasmussen, 2001). The International H_20 Project (IHOP, Weckwerth et al., 2004) is an example of such a project in the Southern Great Plains, where a single dryline event can be monitored using high resolution (spatial and temporal) data collection devices such as *multiple* mobile radar systems, low flying aircraft, mobile mesonet vehicles, and mobile sounding systems. Numerical simulations (e.g., Sun and Wu, 1992) have expanded the knowledge base even further, exploring dryline interactions with other phenomena such as horizontal convective rolls (Peckham et al., 2004), and the interaction of the dryline with other factors influencing the boundary layer, such as soil moisture (e.g. Trier et al., 2004).

Conceptual Model of the Dryline

Ziegler and Hane (1993) developed a conceptual model for a typical dryline over the High Plains of the U.S. (Figure 1.1). West of the dryline (I) the air is hot and dry, while

east of the dryline (III) the air is moist and warm, and capped by an inversion (the capping 'lid'). The capping lid is a layer of stable air above the relatively unstable moist air that allows significant sensible and latent heat energy to build up at the surface, which can lead to deep convection if that energy is released. The intersection of the intermediate mixing zone (II) with the surface marks the dryline boundary, roughly 10 km wide. It is in this zone that air from the lower levels of the moist air mass mixes with the dry air mass. The dryline can also be described as the intersection of the capping lid with the surface (Schaefer, 1974). An elevated moist layer is often observed downstream (east) of the dryline boundary due to the eastward advection of the elevated moisture plume from the mixing zone.

Pacific source air, in moving across the Rocky Mountains, drops much of its moisture content as rainfall on the windward slopes, arriving at the crest (~ 3 km above sea level (ASL)) with a considerably lower mixing ratio. In descending to the foothills (1-1.5 km ASL), it retains that lower mixing ratio, and warms at the dry adiabatic lapse rate. Hence, the air west of the dryline (zone I in Figure 1.1) is warmer and drier than the source maritime air. This dry air has a greater diurnal temperature range than the moist air east of the dryline. In the early morning, a shallow nocturnal inversion in the dry air is quickly eroded and surface heating throughout the day results in a deep (up to 500 hPa) mixed layer west of the dryline. The hot, dry air is slightly unstable or neutral as it is adiabatically mixed.

During the afternoon east of the dryline (zone III), the convectively unstable moist air is capped with a low-level stable layer (typically between 700 hPa and 800 hPa) and neutral

air aloft. Convergence between the low-level westerly flow in the dry air and the weaker easterly winds in the moist air results in the warmer dry air rising above the relatively cooler surface air east of the dryline. The air above the inversion (zone IV) has the same general source as the surface air west of the dryline (Schaefer, 1974). The depth of the moist layer increases with distance from the surface dryline boundary as the inversion rises and the moist air at the surface may also be well mixed depending on location.

The issue of horizontal variation in virtual temperature (and hence air density) in the dryline environment is a topic with conflicting hypotheses (Sun and Wu, 1992). Rhea (1966) found that on average, there was a negligible difference in virtual temperature between the moist and dry air during a three-year dryline study in the Great Plains. Schaefer (1974) included cases of drylines across which only small virtual temperature gradients existed as a means to exclude classical fronts from that study. It has since been observed in many studies that gradients of virtual temperature can exist in a dryline situation (e.g., Ziegler and Hane, 1993; Crawford and Bluestein, 1997; Hane et al., 1997) and successful numerical simulations have been performed with simulated gradients in virtual temperature (e.g., Sun, 1987). Atkins et al. (1998) found that when examining high-resolution data of a single dryline case with a strong virtual temperature gradient, the dryline possessed many of the structural characteristics of laboratory-produced and weak atmospheric density currents (such as a sea/lake breeze). Even though the observed speed of the dryline was similar to that predicted for the propagation speed of a density current, Atkins et al. concluded that more data were required for the study. It was noted by Hane et al. (1997) that no relation between virtual temperature gradients and storm

development was observed in their investigation. Ziegler and Hane (1993) speculate that some of the conflicting observations regarding the state of the virtual temperature across the dryline boundary could be a result of different observation times (as a large diurnal variation of the sign and magnitude of the horizontal virtual temperature gradient exists). Due to conflicting research regarding the density changes across the well-studied High Plains dryline, the presence of such gradients associated with the dryline in Alberta will not be examined in this study. Given that the aim of this study is to address the absolute lack of *basic* local dryline knowledge in Alberta, focusing on a subtopic, such as density gradients, not fully understood in the High Plains after 40 years of research and discussion, may overwhelm a study of this scope.

Dryline Origin and Frequency

The dryline is most commonly found in the United States over the Great Plains (Figure 1.2), separating moist air from the Gulf of Mexico and the dry air of high plateau regions of the southwest and Mexico. The dryline boundary aligns approximately parallel to the contours of the gently sloping terrain in these areas east of the Rocky Mountains (Schaefer, 1986). The conceptual model discussed above describes the dryline boundary that is most frequently observed in West Texas and Oklahoma.

Schaefer (1974) explains that the development of a dryline begins with the migration of anticyclones over the northern Great Plains. As diverging air attempts to spread out horizontally, it is blocked to the west by the Rocky Mountain barrier. A cold front is initially associated with the edge of the spreading air, but as the conditions in the lower

atmosphere are modified by heating and orographic effects, the boundary can no longer be identified as a classical front. The dryline forms at the trailing edge of the continental air mass. After a few days, the air east of the dryline has significantly different properties than the neighbouring dry air as a result of the addition of moisture at the surface from various sources.

Rhea (1966) examined upper-air features commonly associated with active drylines over the U.S. High Plains, and found that over two-thirds of the cases studied were associated with a distinct upper-air temperature or flow pattern. The most common of which is an approaching weak shortwave trough and the presence of a maximum in the upper jet over the area is also common.

Obviously, drylines are most prevalent when great contrasts in dewpoint temperature exist in the same region. Over the southern Plains of the U.S., this is typically during spring and early summer, which is also normally the most active time of year for severe thunderstorms. Over a three-year study, Rhea (1966) found that, on average, drylines were present over the south-central U.S. on more than 45% of springtime days from 1959-1962. Schaefer (1974) came to a similar conclusion for the same region and season, detecting drylines on 41% of days from 1966-1968. Peterson (1983), using a smaller region of west Texas, observed drylines on 43% of the days between April and June of 1970-1979. A 30-yr (1973-2002) climatology for the High Plains by Hoch and Markowski (2005) observed drylines on 32% of days between April and June, with a peak frequency in May. It is not presently known how often a dryline forms in Alberta.

Dryline Motion

As described above, the inversion capping the moist air is intimately related to the dryline boundary. The nocturnal inversion that develops as the dry air cools at night is quickly removed as insolation brings about surface heating and mixing in the morning. The stable inversion capping the moist air at the dryline boundary; however, is not as easily eroded. Schaefer (1986) indicates that the heat required to break the inversion along the dryline boundary is nearly uniform, and increases to the east as the depth of the moist layer increases. Thus, when enough heat has been absorbed to break the inversion, mixing between low-level moist air and dry air aloft will result in the rapid drop of dewpoint temperatures. Strong vertical mixing of moist surface air and dry air aloft is responsible for the daytime eastward motion of the dryline. The mixing brings dry air with strong westerly momentum down to the surface. The dryline boundary then 'leaps' eastward to a point where no significant mixing between the two air masses has occurred and where the inversion is still intact. When the heat required to erode the inversion is beyond what is available, the dryline boundary becomes stationary. This could be brought about by reduced surface heating, for example by irrigation and enhanced transpiration in the area resulting in cooler temperatures. This impedes sensible heating and destabilization, and hence, slows the vertical mixing that is essential for eastward dryline motion (Hane et al., 1997).

Schaefer (1973) examined the diurnal nature of dryline motion. The dryline generally moves eastward during the day and retreats westward at night. The fastest motion occurs during the period of most rapid temperature changes (typically late morning and before

midnight) because the mean motion of the dryline is closely coupled to the diurnal temperature variation. The slowest motion is typically observed in the late afternoon and early morning hours. During the daytime, the eastward motion of the dryline is typically faster than what one would expect if advection were the only driving force, and there is little correlation between dryline displacement and surface wind speed. However, the speed of the retreating dryline at night is largely attributed to advection and thus is controlled by the surface wind field.

Under quiescent conditions, different sections of the dryline often move at different speeds or even in different directions. Hane et al. (1997) observed the development of a mesoscale bulge of a typical Great Plains dryline that arose, in part, from spatial variations in the surface temperature west of the dryline, and resulted in differences in motion of certain sections of the dryline. These variations in dryline speed and direction show that the driving forces may be local rather than synoptic. An additional cause for the rapid advance of certain sections of a dryline is the subsidence of dry air aloft with strong westerly momentum. Schaefer (1986) maintains that such bulges are commonly the result of increased advection in the dry air due to a mid- to upper-level jet in the vicinity, as turbulent mixing brings the upper air having strong westerly momentum down to the surface. Schaefer also suggests additional sources of increased momentum in the dry air such as standing mountain waves or convective rolls.

Convective Initiation at the Dryline

It is widely observed that the dryline is a favored location for thunderstorm development. As mentioned above, the most common time of year for drylines over the High Plains is May, which is also the peak time for thunderstorm days (Changnon, 2001), tornadoes (Concannon et al., 2000) and hail (Gokhale, 1975). The forced upward motion at the dryline boundary is sometimes sufficient to break the capping lid, aiding in destabilization and providing lift for low-level moist air leading to deep convection (Hane et al., 1997). Forecasting convective initiation along the dryline is often difficult due to the fact that important dynamical processes responsible for the initiation, movement and organization of convection along the dryline, or any other frontal boundary, are still not well understood (Atkins et al., 1998). Rhea (1966) observed considerable surface streamline convergence of the wind between moist and dry air in the majority of cases where thunderstorms developed near the dryline. Other ingredients necessary for the initiation of severe convection, such as low convective inhibition (CIN) and high CAPE, are also typically present over the Great Plains east of the dryline. It should be noted though that processes west of the dryline, such as the downward transfer of momentum, can also play an important role in initiation of convective clouds and thunderstorms along the dryline (Hane et al., 2000).

Rhea (1966) studied the development of thunderstorms in the vicinity of a dryline in the Great Plains over a three-year period. It was observed that over 70% of new radar echoes developed within 370 km of the dryline boundary. This is an exceptionally large distance, but Rhea further noted that the echoes that did develop closer to the dryline

typically became better organized than echoes developing further away from the area: 60% of the new echoes developed persistently in the same area until organized into line echoes.

The dryline bulge is also a favored area of thunderstorm development because the typical bulge results in maximum convergence as the winds in the moist air wrap around the dry air. Hane et al. (2001) found that although typical bulges develop in synoptically active conditions, surface processes such as horizontal advection and turbulent vertical mixing can be just as important in the development of dryline bulges. Dryline bulges may also develop as a result of different sections of the dryline moving at the different speeds and/or different directions, for the reasons mentioned above.

Other sources of convective initiation along the dryline include perturbations in the upper flow, such as a frontal zone that overtakes or merges with a dryline. Such a merger can initiate thunderstorms (Schaefer, 1986). Also, cloud lines, gravity waves, solenoidal circulations and horizontal convective rolls have been observed to interact with dryline boundaries and trigger convection (e.g., Schaefer, 1986).

1.3 Alberta Thunderstorms

The Rocky Mountain barrier has a significant influence on the weather of North America on many spatial and temporal scales (Smith et al., 1997). The impact of the Rocky Mountains on weather in Alberta during the summer season is revealed when examining

severe convective activity. The Alberta foothills are part of one of the most active thunderstorm areas in Canada (Figures 1.3, 1.4). Damage associated with summer severe weather in Alberta costs millions of dollars annually (Krauss, 2004). Alberta experiences the most hail days per year in Canada, with the seasonal peak observed in mid-July (Wojtiw, 1975), and Alberta also observes the second highest number of tornadoes annually in Canada after southern Ontario.

The 1985 Limestone Mountain Experiment (LIMEX) conducted in south-central Alberta (Strong, 1986, 1989) examined surface and sounding data collected during cases of severe and non-severe thunderstorms developing in the Alberta foothills, and led to the development of a multi-scale conceptual model for Alberta thunderstorms (Strong, 1986, 2000; Smith and Yau, 1993b). The capping inversion, which has been studied in detail in Alberta (e.g., Strong, 1986), is an integral part of the conceptual model and, as mentioned above, is intimately related to the dryline. However, the documented knowledge of the dryline in Alberta is limited to a few case studies of severe weather associated with the dryline using surface synoptic data, supplemented with radar and satellite imagery (e.g., Knott and Taylor, 2000; Dupilka and Reuter, 2005).

Conceptual Model of Alberta Severe Thunderstorms

Studies to develop a multi-scale conceptual model for severe thunderstorm outbreaks in Alberta (Strong, 1982, 1986, 2000; Smith and Yau, 1993b) have identified the typical synoptic conditions over Alberta associated with the initiation of thunderstorms along the foothills. This synoptic pattern results in conditions that satisfy the main requirements

for severe convection, including a significant supply of latent heat energy, strong convective instability, and large vertical shear of the horizontal wind (Smith and Yau, 1993a).

The conceptual model (Figure 1.5) for a typical Alberta thunderstorm day involves an approaching upper shortwave trough, preceded by a southwesterly flow aloft over the Rockies. The subsequent development of surface low in southern Alberta, through lee cyclogenesis as the trough approaches, results in easterly surface winds over the foothills through central Alberta. These easterly surface winds advect relatively moist air towards the mountains at low levels. In general, the main sources of moisture in the boundary layer are evaporation from an open water body, evaporation of falling precipitation, and evapotranspiration from a land surface. On the Canadian prairies, open-water evaporation is not considered to be a significant factor in overall local moisture (Strong, 1997; Raddatz, 1998), given that open water accounts for <10% of the total land surface. The primary source of surface moisture during the summer over the Canadian Prairies is evapotranspiration, particularly from grain crops with variability on a regional scale (Strong, 1997; Raddatz, 1998; Aguado and Burt, 2004). An additional source of moisture is that advected from the central U.S. to the Alberta plains during a southeasterly flow (Dupilka and Reuter, 2005).

The easterly upslope flow can be amplified by the thermally-induced mountain-plain circulation, a result of differential heating of the eastern slopes of the foothills (Smith and Yau, 1993b). The upslope flow does not continue far into the foothills due to orographic

blocking and a westerly counterflow of dry air sinking down into the foothills from higher elevations in the Rockies. The resulting convergence of relatively moist upslope flow along the foothills with dry air subsiding along the mountain barrier leads to the development of a capping inversion and an associated dryline in the lee of the mountains, as described in Section 1.2. The capping inversion (or 'capping lid', Figure 1.6), allows the buildup of sensible and latent heat energy in the boundary layer that can lead to deep convection (if released by the erosion of the capping lid). The capping lid is typically eroded in Alberta by a combination of cooling aloft, that is through horizontal advection of colder air (Knott and Taylor, 2000), and/or by adiabatic cooling from ascending air, along with strong surface heating and moisture convergence along the foothills (Strong, 2000).

Drylines in Alberta

The typical conditions for the development of severe thunderstorms over the High Plains and the development of the dryline (Rhea, 1966; Doswell, 1980) are very similar to those identified in the Alberta conceptual model. This is not surprising as the topography of Alberta is akin to that of the High Plains (Smith and Yau, 1993a). The important factors described by Sun and Wu (1992) required to sustain the moisture gradient across the dryline (low-level vertical wind shear, sloping terrain, and a soil moisture gradient) are also present in Alberta (Strong, 1986).

The research literature has very few contributions regarding drylines in Alberta. Knott and Taylor (2000) performed a detailed analysis of surface dewpoint temperature fields

and found a synoptic-scale dryline in south-central Alberta that persisted for several hours on 29 July 1993. The dryline boundary triggered convection in the conditionally unstable environment and two severe storms developed within 30 km of the dryline, including the cell that produced the Holden Tornado (F3 on the Fujita scale of tornado intensity). Dupilka and Reuter (2005) examined the surface moisture fields for three cases of severe tornadic storms in central and southern Alberta – including the 29 July 1993 Holden tornado, the 14 July 2000 Pine Lake tornado (F3), and the 31 July 1987 Edmonton tornado (F4). It was observed that the Pine Lake tornado also initiated and developed along a well-defined dryline. However, in the case of the 1987 Edmonton tornado, the surface moisture field was uniformly moist and no dryline was detected in the vicinity.

1.4 A-GAME and FOPEX Field Projects

The major field projects (i.e. IHOP) studying various aspects of the dryline in the High Plains have many resources that are simply not available at this time for dryline studies in Alberta. However, recent field campaigns in south-central Alberta have provided an excellent opportunity to add to the limited knowledge base for the Alberta dryline, as well as to evaluate a relatively new technique for estimating atmospheric moisture. These two projects, described below, collaborated with the on-going operations of Weather Modification Inc. (WMI) during the most active months of severe weather in Alberta in 2003 and 2004. This resulted in a data set consisting of surface mixing ratio measurements (stationary and mobile observations), upper air sounding data from up to 3

sites in south-central Alberta, and precipitable water estimates retrieved from a network of GPS receivers[1].

The Alberta GPS Atmospheric Moisture Evaluation

The Alberta GPS Atmospheric Moisture Evaluation (A-GAME) project operated by the Department of Geomatics Engineering at the University of Calgary utilized the Southern Alberta Network (SAN) of Global Positioning Satellite (GPS) receivers to examine GPS-derived precipitable water (PW) estimates in southern Alberta. The main objectives of the project were to validate GPS-derived data by comparing them to sounding data and to evaluate the usefulness of GPS-derived data on documenting drylines. Businger et al., (1996) observed that PW data could be used to locate the dryline in the High Plains. A-GAME involved two field campaigns (16-26 July 2003 and 10-16 July 2004) operating in south-central Alberta, over an area of ~40,000 km^2 containing 16 GPS receivers spaced approximately 30-100 km apart (Figure 1.7). A-GAME operated upper air sites in the study area during the field campaigns, launching radiosondes and/or airsondes up to three times a day from Sundre, Olds-Didsbury Airport and Airdrie. The sounding data collected at these sites was employed as verification data to evaluate the GPS-derived PW estimates and aid in modelling techniques for describing the atmospheric moisture distribution (e.g. Hoyle, 2005). This upper air data set was also analyzed to assess the atmospheric potential to support deep convection and identify important features such as the presence of a capping inversion. A vehicle was also equipped with sensors to

[1] A propagation error occurs as a GPS signal passes through the atmosphere, and within this error the delay caused by atmospheric water vapour can be isolated. This isolated delay can then be translated into an estimate for the total integrated atmospheric water vapour, or precipitable water (PW) above a GPS receiver.

measure surface moisture while making transects in and around the Alberta foothills, aiming to detect the dryline boundary at the surface. My participation in A-GAME included collecting data on surface conditions by completing mobile transects, and launching radiosondes for upper-air soundings (see Appendix C).

The Foothills Orographic Precipitation Experiment

The Foothills Orographic Precipitation Experiment (FOPEX) operated by the Climate Research Branch (CRB) of the Meteorological Service of Canada (MSC) in Saskatoon is a separate field project in the Alberta foothills area. The FOPEX researchers aim to determine the relationship between seasonal precipitation and elevation, aspect, and slope in the Alberta foothills[2]. The field observations include a line of 4-6 weather stations in the foothills at different elevations (Figures 1.8, 1.9, 1.10). The FOPEX researchers collaborated with the A-GAME field project by sharing the valuable FOPEX transect data during July and August of 2003 and 2004, and supplying additional field equipment and manpower. During A-GAME 2004 a GPS receiver was co-located with a surface station within the FOPEX transect to evaluate the GPS-derived PW estimates by comparing them with surface mixing ratio in a dryline situation.

1.5 Objectives

Boundary layer convergence zones, such as the dryline, destabilize the lower atmosphere, and are important in the initiation of deep convection (Schaefer, 1986). There is a serious

[2] For additional information on FOPEX, please visit http://www.geo.ucalgary.ca/fopex/ or contact Mr. Craig Smith (craig.smith@ec.gc.ca), of MSC/CRB.

lack of local information on this important feature, which this study attempts to rectify by enhancing our knowledge of the dryline in Alberta with specific field measurements. The validity of applying knowledge of the High Plains dryline to Alberta cases will be addressed with field measurements to compare the basic characteristics of the phenomenon. The primary objectives of this study are stated in terms of 4 questions

1. How many dryline events were recorded during the 2003 and 2004 field campaigns of A-GAME and FOPEX? Specifically, how many dryline events were recorded during July and August of 2003/2004 by the FOPEX transect?
2. Are all Alberta drylines associated with severe thunderstorms? Specifically, are there drylines that do not spawn convection or only weak storms?
3. How intense are drylines in south-central Alberta? Specifically, what are typical spatial gradients of water vapour mixing ratio across the dryline? How do these values compare to drylines in the High Plains of the U.S.?
4. How can the GPS-derived precipitable water estimates be used to document the dryline of 10 July 2004?

These questions can only be answered by examining surface moisture data in the Alberta foothills on a spatial and temporal scale that has not been previously attempted. Mesoscale surface measurements collected during A-GAME along the FOPEX transect and with the mobile transect vehicle over two warm seasons will provide the opportunity to address the lack of Alberta dryline knowledge. Questions 1 and 2 will be answered by analyzing FOPEX and mobile transect data along with synoptic analysis maps, upper air

sounding data and remote sensing imagery. Question 3 will be addressed by analysis of the mobile transect data, including an in depth examination of the mobile transect dryline event of 16 July 2004. A detailed case study with GPS-derived PW data of the 10 July 2004 dryline event in the FOPEX transect will address Question 4.

1.6 Outline

Chapter 2 contains the methodology employed to address the objectives of this study. The process of data analysis required to detect the dryline in the Alberta foothills involves examining surface mixing ratio measurements from FOPEX and mobile transects and subsequently examining available sounding data, synoptic analysis maps, and remote sensing imagery as confirmation. Also, the theory and methodology of deriving moisture estimates using GPS receivers is provided.

Chapter 3 provides the results of surface moisture analysis over the study period, addressing each objective of the study. This includes discussing the rate of occurrence of the dryline in the FOPEX and mobile transects, and any associated thunderstorm development. The case studies examine the mesoscale observations of the dryline in the mobile transect (16 July 2004) and in the FOPEX transect, as well as the usefulness of the GPS-derived moisture estimates (10 July 2004).

Chapter 4 summarizes conclusions drawn from the results of this study. Also, recommendations for future dryline research in Alberta are provided, based on limitations and drawbacks of the A-GAME and FOPEX field projects.

Appendix A provides a brief background to the scales of motion discussed in this study. Appendix B contains a climatology of the FOPEX measurements during July and August of 2003 and 2004. This includes a discussion of the observed mean mixing ratios of the FOPEX stations relative to seasonal, elevation, and diurnal variability. Appendix C contains an article written for the 'Environmental News', a monthly collection of graduate student interests produced by the Environmental Research and Studies Centre of the University of Alberta. This article was written as an introduction to Alberta thunderstorms and describes the impetus for this study.

Chapter 2

Methodology

2.1 Overview

This chapter begins with a review on how a dryline has been identified in the research literature. This leads to our criterion of what constitutes an Alberta dryline event during A-GAME. The initial analysis involved isolating potential dryline events in the mesoscale observations of the FOPEX and mobile transects. An analysis of the synoptic mixing ratio field confirmed the presence of a synoptic-scale moisture gradient in the study area. Upper air analysis and synoptic analysis observations were utilized to study the associated capping lid, and synoptic scale flow patterns over Alberta. For 10 July 2004, the usefulness of GPS-derived PW estimates to document the dryline was examined.

The majority of the data analyzed in this study were provided by the A-GAME and FOPEX field experiments that operated simultaneously over southern Alberta during the summer months of 2003 and 2004. The Meteorological Service of Canada (MSC) supplied additional data, such as synoptic analysis charts, synoptic surface moisture data, and satellite and radar imagery. Weather Modification Inc. (WMI), a hail seeding operation based at Olds-Didsbury Airport (located approximately half-way between Red

Deer and Calgary), provided radar imagery for the study area, as well as additional reports of severe weather.

2.2 Detecting the Dryline

The dryline boundary can be detected by using various types of data. The most common method of detection involves examining water vapor observations across the boundary. Typical data sources for moisture at the surface and in the lower levels of the atmosphere include stationary weather observation sites, mobile observations with one or more vehicles, low flying aircraft equipped with meteorological instruments, and atmospheric sounding data. Also, radiometers and microwave profilers can produce profiles of water vapour in the lower atmosphere. Remote sensing imagery (i.e. satellite, radar) is useful for estimating the location of the dryline boundary when clouds and/or thunderstorms are developing in its vicinity.

Surface Humidity Discontinuities

The dryline boundary can be detected at the surface by examining spatial and temporal trends of moisture variables. Much of the research on drylines over the High Plains uses plots of the dewpoint temperature to locate and track the dryline boundary at the surface, a result of the convenience of using the operational synoptic observations of dewpoint temperature (Schaefer, 1986). The dewpoint temperature is a conserved quantity with respect to isobaric heating or cooling, but is not conserved when a parcel of air undergoes vertical adiabatic motion in the atmosphere. Thus, dewpoint temperatures can vary

significantly with elevation, and the climatological means tend to parallel the terrain contours (Schaefer, 1974). Other measures of surface moisture are also used to identify and study the dryline boundary (i.e. mixing ratio, specific humidity, equivalent potential temperature). Mixing ratio and specific humidity represent the 'mass' of water vapour, and are therefore conservative quantities with respect to elevation change. Consquently, differences in surface moisture measurements of a conserved quantity on either side of the boundary do not arise from differences in elevation. The typical synoptic scale gradient of dewpoint temperature associated with the dryline in the High Plains is 10ºC 100 km^{-1} or more lasting for at least 6 h (Schaefer, 1974). Using dewpoint temperature to identify the dryline boundary requires examining the moisture field beyond a threshold value. Schaefer identified the dryline signature as a 5.5ºC difference in dewpoint temperature between reporting surface weather stations with a minimum dewpoint temperature of 10ºC in the moist air. Due to the lack of dryline studies in Alberta, the local applicability of a High Plains dewpoint temperature threshold value of 10ºC is unknown since differences such as orography affect the climatological mean of dewpoint temperature (the mean dewpoint temperature in July for central Alberta is ~10ºC). However, this criterion translates to a mixing ratio difference of 3 g kg^{-1} or more between adjacent stations. Ziegler and Hane (1993) observed mixing ratio changes of 8 g kg^{-1} over 5 km in their dryline studies and Atkins et al. (1998) found gradients of 3-5.5 g kg^{-1} per 5 km in the High Plains using mesoscale data. Pietrycha and Rasmussen (2004) observed mixing ratio gradients ranging from 0.53 g kg km^{-1} up to an extreme gradient of 16.2 g kg^{-1} km^{-1} (~10ºC dewpoint differential over 185 m). Hoch and Markowski (2005) observed the horizontal changes in specific humidity associated with a dryline to be least

3 g kg^{-1} over 100 km. My investigation of A-GAME measurements of surface humidity will examine whether comparable moisture gradients are observed across the dryline boundary in Alberta. My investigation differs from previous studies in Alberta in that it uses mixing ratio rather than dewpoint temperature, for the aforementioned reasons.

The magnitude of the moisture gradient varies across the dryline. Crawford and Bluestein (1997) observed various dryline passages with changes in dewpoint temperature of quite a different character. Some cases showed a monotonic drop in water vapor content across the boundary, while other cases exhibited step-like changes over the dryline cross-section. They found no correlation between the rate of change in dewpoint temperature and the development of deep convection.

Changes in Surface Wind Direction

In addition to the surface moisture discontinuity, changes in surface wind direction are often associated with a dryline boundary. One of the first dryline studies (Rhea, 1966) identified the dryline as the 'first organized line of veering surface wind'. This is consistent with the conceptual model of Ziegler and Hane (1993) discussed in Section 1.2, where surface winds in the dry air have a westerly component, while surface winds east of the dryline in moist air have an easterly component. Knott and Taylor (2000) studied an Alberta dryline case from an operational standpoint, and observed that drops in moisture correlated well with surface winds veering from southeasterly to southwesterly.

2.3 Identifying a Dryline Event During A-GAME

Mixing ratio was used as a measure of surface moisture to detect the dryline boundary within both the FOPEX transect and over a mobile transect during A-GAME. The mixing ratio of water vapour (r), which is the ratio of the mass of water vapour to the mass of dry air, is conserved with changes of elevation and position (without condensation), and is thus an ideal moisture variable to use over mountains and foothills such as southwest Alberta. Mixing ratio is defined as

$$r = \frac{m_v}{m_d} \tag{1}$$

where m_v is the mass of water vapour and m_d is the mass of dry air. It can also be expressed as

$$r = \frac{0.622\, e}{p - e} \tag{2}$$

where e is the water vapour pressure, and p is the air pressure (both measure in the same units). Mixing ratio and vapour pressure are not directly-measured quantities. Consequently the Goff-Gratch equation (Goff and Gratch, 1946) was employed to calculate the water vapour pressure from temperature, air pressure, and relative humidity data.

Mesoscale Surface Analysis

FOPEX Observations

A FOPEX dryline 'event' in this study was defined as the formation of the dryline boundary within the FOPEX transect. A dryline event also included cases where there was an eastward passage of the dryline boundary through the FOPEX transect, (including

the possible westward retreat of a dryline through the same location). In this study, significant changes in mixing ratio (differences between one or more stations) and correlating wind shifts at the surface were used to recognize the dryline within the FOPEX transect. A possible dryline event within the FOPEX transect was first identified when at least a 3 g kg^{-1} drop in mixing ratio occurred at one or more FOPEX stations in less than 2 h. This difference in mixing ratio is similar to the 10 ºC drop in dewpoint temperature in 2 h observed by Knott and Taylor (2000). Additionally, if the dryline formed between FOPEX stations, the difference between two adjacent stations had to be at least 3 g kg^{-1}, with a convergent wind field. After identifying potential dryline events, a detailed analysis was made of the synoptic surface moisture and wind fields, local upper air data, synoptic analysis charts and remote sensing images, as discussed in Synoptic Analysis below.

The FOPEX stations recorded atmospheric conditions every half-hour including temperature, relative humidity, wind speed and direction, and air pressure. The air temperature, relative humidity, and wind direction and speed were measured every 30 seconds and averaged over 30 minutes. The air pressure was measured once at the end of the 30-minute interval. During July and August of 2003, stations AB2 and AB4 were not equipped with pressure sensors, and thus the pressure for these sites was estimated using nearby FOPEX sites (AB1 and AB3, and AB3 and AB5, respectively). The surface pressure for AB2 and AB4 was calculated with an isothermal version of the hydrostatic equation (3) using both nearby stations when possible. The isothermal hydrostatic equation is expressed as

$$p = p_o e^{-\frac{gz}{RT}} \quad (3)$$

with p is the pressure (Pa), p_o is the measured FOPEX station pressure (Pa), z is the geopotential height (m), g is the acceleration due to gravity (9.8 m s^{-2}), R is the dry air gas constant (287 J kg^{-1} K^{-1}), and T is the mean temperature of the layer (K). The approximated surface pressure for the unequipped stations was the average of the two calculated values (the average difference between the calculated pressures using the nearby stations was around 1 hPa). Using nearby pressure calculations to approximate these stations was useful and suitable for calculating accurate mixing ratio values for AB2 and AB4. It would require a rise or fall in pressure of 150 hPa to make a difference of ~1 g kg^{-1} in mixing ratio. Thus a pressure error of 10 hPa within the FOPEX transect would result in a maximum error in mixing ratio of around 0.08 g kg^{-1}. (This method of using nearby stations to approximate air pressure was not required for the 2004 field campaign, as AB2 was decommissioned and AB4 was equipped with a pressure sensor).

The FOPEX surface data set was analyzed for July and August of 2003 and 2004, a total of 122 days. In 2003, the FOPEX transect consisted of 6 stations (AB0 to AB5, Table 2.1), and in 2004 this was reduced to four stations when AB2 and AB5 were decommissioned. For both summers, the four permanent stations had an excellent data recovery rate of 100% for each station (Table 2.2).

Mobile Transect Observations

A mobile transect dryline event was defined as the detection of the dryline boundary one or more times during a mobile transect. The dryline boundary was identified as a change in mixing ratio of at least ~3 g kg^{-1} between moist and dry surface air. According to the conceptual model of Ziegler and Hane (1993), the width of the dryline at the surface is of the order of 10 km. Strong moisture gradients across the dryline boundary have been observed over a distance ranging from a few hundred meters to 5 km (Pietrycha and Rasmussen, 2004). Thus, the changes in mixing ratio associated with the dryline were expected over a distance on the scale of tens of kilometers. Mobile observations were monitored in real-time so as to plan the transect route relative to dryline position and width. Possible dryline events observed by the mobile transects were further analyzed with synoptic scale data and the FOPEX data was also analyzed for the mobile transect events.

The A-GAME field programs in 2003 and 2004 lasted a few weeks. Sensors were installed in a vehicle (Figure 2.1) to perform mobile transects into the foothills. In 2003, the vehicle was equipped with a 21X datalogger and temperature and humidity sensor (HMP45C), provided by Campbell Scientific Inc. A Setra pressure sensor (SBP270) was added to the system in 2004. No wind observations were taken during the mobile transects. The temperature/relative humidity sensor was mounted in a radiation shield with brackets onto a length of PVC tube (approx. 1.5 m) outside a rear window of the vehicle. The sensors were placed at a distance of approximately 0.2 m away from and 0.4 m above the car roof. The equipment took measurements every 1 s and averaged

them over 1 minute, outputting temperature, relative humidity, and water vapour pressure (computed by the datalogger program). During the 2003 field campaign, the surface pressure from nearby weather stations (either in FOPEX or synoptic sites operated by MSC) was used to approximate the surface pressure over the mobile transect using (3), and (2) was used to calculate mixing ratio.

Tests of the equipment were carried out at different vehicle speeds, and it was observed that sensor response and values of temperature and humidity were similar at all speeds up to 110 km h^{-1}, a value significantly higher than the speed at which the mobile transects were actually performed (averaging between 50 km h^{-1} and 90 km h^{-1}). A total of 19 transects were completed over 13 days during the A-GAME field program (11 in 2003 and 8 in 2004). Equipment problems affected two of the mobile transects. Typical transects would commence at mid-day from the Sundre area and head westward into the foothills as far north as Rocky Mountain House, or as far south as Mountain-Aire Lodge (Figure 1.7).

Synoptic Analysis

Upon completing the examination of the mesoscale moisture measurements, potential dryline cases were then analyzed on the synoptic scale, utilizing surface moisture and wind data, sounding data, and synoptic analysis charts at 850 hPa, 500 hPa, and 250 hPa. Also, remote sensing imagery supplemented this process by providing information on nearby thunderstorms and possible outflow boundaries influencing the moisture

measurements in the FOPEX or mobile transects, and observing any convective initiation near the dryline.

Surface Moisture and Wind Analysis

In order to confirm the event detected by the mesoscale data were indeed drylines, the synoptic-scale surface moisture data were examined to identify whether moisture gradients persisted in the study area for at least 6 h. The Meteorological Service of Canada provides a public archive of hourly surface data observations (www.climate.weatheroffice.ec.gc.ca) for a number of weather stations in southern Alberta. Contoured maps of mixing ratio (with observations of wind data) were produced using various MSC weather sites (Table 2.3) to assess the distribution of surface humidity on the synoptic scale in the A-GAME field project area. The FOPEX mixing ratio and wind observations were also included in these contour maps (Figure 2.2), since the relatively high density of the FOPEX stations would aid in identifying mesoscale surface gradients in the FOPEX area within a significantly less dense synoptic network of stations (in the study area, there was approximately one synoptic station per 8000 km^2). The purpose of plotting synoptic mixing ratio was to observe the surface moisture distribution in the area and the diurnal evolution of the moisture field. The purpose of including the FOPEX data within the synoptic maps was to illustrate that significant moisture gradients on the mesoscale could go undetected within the network of synoptic sites in southern Alberta. Thus, these contour maps of synoptic mixing ratio were carefully interpreted.

Sounding Analysis

During the A-GAME field campaigns, three upper air sites were located in the study area at Sundre, Olds-Didsbury Airport, and Airdrie. At least one sounding was launched daily from each of these sites during A-GAME. Several days had multiple soundings from each site. The official dates for the A-GAME field campaigns were 15-26 July 2003, and 10-16 July 2004, but several additional radiosondes were launched on potential severe weather days outside the official field program dates. During 2003 a total of 79 soundings were made (24 airsondes launched from Sundre, 24 radiosondes from Olds-Didsbury, and 31 radiosondes from Airdrie). The Sundre airsonde site was not operated during 2004, but a total of 40 radiosondes were launched (24 from Olds-Didsbury, and 16 from Airdrie). Upper air data from any of these sites are suitable to represent the dryline environment for this analysis, as they were close to the foothills and the FOPEX transect area. Also, when surface winds had an easterly component (which is the typical setting for dryline/capping lid development in southern Alberta), these sites were considered upwind of the storm initiation area along the foothills.

The most significant feature on a sounding profile related to the dryline is the capping lid: a temperature inversion in the lower atmosphere creating a stable layer of air above the unstable boundary layer (as discussed in Chapter 1). Another advantage of employing the mixing ratio as a moisture measurement is that due to its conservative nature, the mixing ratio just above the boundary layer (top of capping lid) is expected to be similar to that measured at the surface west of the dryline because the air is of the same origin (see Section 1.2). Thus, for potential dryline events, the mixing ratio above the capping lid

and the mixing ratio measured in the dry air west of the dryline (as observed by FOPEX or mobile transect) were compared when available.

The temperature, dewpoint temperature, mixing ratio, and wind profiles from the soundings were examined on dryline events detected within the FOPEX transect. Three common severe weather indices were calculated using the sounding data on a dryline day to assess the potential for convection: Convective Available Potential Energy (CAPE), Convective INhibition (CIN), and the Lifted Index (LI). The CAPE is a measure (in units J kg^{-1}) of the maximum potential kinetic energy that a parcel can acquire using the parcel theory (Holton, 1992). Observations of Alberta thunderstorms show that typical mean Convective Available Potential Energy (CAPE) values for Alberta storms range between ~400 J kg^{-1} for single cell storms, to ~850 J kg^{-1} for multicell storms, to ~1400 J kg^{-1} for supercell storms (Brimelow et al., 2002). Convective INhibition (CIN) is equal to the amount of energy required (J kg^{-1}) for a parcel to ascend to the level of free convection. CIN is often referred to as the negative buoyant energy or –CAPE. One can speculate that low-level convergence is strongly forcing thunderstorms to develop within an area where significant CIN has been observed (Rasmussen and Blanchard, 1998). The Lifted Index (LI), a measure of the instability of the air mass, is the difference between the temperature of an air parcel that is lifted adiabatically from the surface to 500 hPa and the air temperature observed at 500 hPa i.e., T_e-T_p (Galway, 1956). Positive values of LI are indicative of a stable atmosphere, while negative values indicate instability and the potential for thunderstorms.

Synoptic Chart Analysis

Certain synoptic features figure into the conceptual model of Alberta thunderstorms (Section 1.3) and the development of a capping lid and the associated dryline. Rhea (1966) observed an approaching shortwave trough was most often associated with drylines in the High Plains, and this is similarly observed on thunderstorm days over south-central Alberta as described by the multi-scale conceptual model. Synoptic conditions over Alberta on potential days with a dryline were examined using MSC operational analysis maps at the standard levels of 250 hPa, 500 hPa, and 850 hPa at 1200 UTC and 0000 UTC. Important features on these synoptic charts include approaching short-waves, large-scale ascent/descent, cooling aloft, and the presence of jet maxima. Also examined was the synoptic analysis at the surface; important features on surface maps include the location of thermal fronts, and the observed wind and pressure fields.

Remote Sensing Imagery Analysis

Radar and satellite imagery were examined for cloud cover and convective development along the Alberta foothills for each potential dryline event. Heavy precipitation in the FOPEX and/or mobile transect areas was noted for the possible influence of outflow boundaries in the area on moisture and wind observations. If a dryline event was confirmed in south-central Alberta, the remote sensing imagery was further examined for convective development within the vicinity of the dryline. Weather Modification Inc. (WMI) supplied radar images from a C-band radar located at the Olds-Didsbury Airport, which is a prime location for monitoring storms that initiate along the foothills. Additional radar imagery from the Strathmore radar operated by MSC was required to

observe storms beyond the range of the WMI radar. The Constant Altitude Plan Position Indicator (CAPPI) radar reflectivity images provided information on storm activity over most of southern Alberta. Cloud cover and convective development in Alberta were also examined with Geostationary Orbital Earth Satellite (GOES) visible satellite images.

GPS-derived Precipitable Water Observations

An additional objective of this study is to evaluate Precipitable Water (PW) estimates collected using a relatively new technique of retrieving vertically-integrated atmospheric moisture from GPS signals. PW is defined as the total integrated atmospheric water vapour in a vertical column of unit-cross sectional area between two layers (Huschke, 1959). In this study it represents the PW from the surface to the top of the atmosphere, and is expressed in mm of water. The dryline is a 'boundary layer' phenomenon, which is the lowest layer of the troposphere that is directly influenced by forcings at the Earth's surface and is capped with a temperature inversion (Stull, 1988). The height of capping inversion east of the dryline in Alberta during the summer months is ~750 hPa (Figure 1.6). Changes in boundary layer moisture can influence the PW significantly as up to 50% of the total PW is contained below 750 hPa (Strong, 2005a). However it must also be noted that changes in boundary layer moisture can be countered to some effect by the evolution of the moisture in the entire column aloft (for example, drying aloft can be countered by moistening at the surface and the PW will not change as significantly as one may expect).

Precipitable water measurements in Alberta are typically retrieved from upper air sounding data. The single operational sounding site is located at Stony Plain in central Alberta and the daily 1200 and 0000 UTC observations at this location cannot be applied to document the dryline in this study. The accuracy of GPS-derived PW measurements versus PW retrieved from sounding data is similar (Smith et al., 2001). A GPS signal can be used to estimate PW at a very high temporal resolution (for this study it was estimated at hourly intervals), for a fraction of the expense of hourly launches of weather balloons to obtain precipitable water measurements from sounding data. Businger et al. (1996) found that the estimation of dryline position using PW values was improved when the synoptic scale measurements (from upper air sites) were supplemented with GPS-derived PW observations from a relatively high-density network of GPS receivers as part of GPS/STORM in the High Plains (Rocken et al., 1995). They found that time series PW data was only useful in combination with other data sources, such as remote sensing imagery, for forecasting on a short-term basis.

The SAN is a high-density network of GPS receivers in south-central Alberta that provided GPS-derived PW data during A-GAME. A GPS receiver was co-located at FOPEX station AB4 and the data collected from this site (and nearby Sundre) was examined on 10 July 2004. Hourly values of GPS-derived PW were compared to trends in mixing ratio measurements at this site and at Sundre where a GPS receiver is located within 2 km of a MSC surface observation station. The purpose of evaluating the GPS-derived PW estimates on either side of the dryline boundary against surface mixing ratio

was to determine whether the presence of dryline is noticeable in the PW estimates at the same time it is recognized in the mixing ratio data.

Additional information on GPS technology

Using GPS signals to measure atmospheric water vapour in the atmosphere is a promising, economic and robust new technique that offers consistently high quality data at a high temporal resolution (Bengtsson et al., 2003). As a signal is transmitted through the atmosphere to a receiver on Earth from one or more of the ~27 orbiting GPS satellites, ranging errors occur as a result of orbital prediction inaccuracies, ionospheric effects, and propagation of the signal through the troposphere (Hoyle, 2005). [The 'troposphere' referred to by GPS researchers is in actuality the troposphere and stratosphere combined, therefore discussion of 'tropospheric' effects concerns the lower atmosphere up to ~40 km above the Earth's surface (Hoyle, 2005)]. Orbital errors occur as a result of estimating the position of the GPS satellite above the Earth, and are solved by using multiple satellites and receivers to obtain exact positioning. Free electrons in the upper atmosphere cause ionospheric errors, the effects of which are mitigated by using multiple frequencies of the GPS signal to one receiver (for more information, see Kaplan, (1996)). Propagation errors occurring as the signal passes through the troposphere contain two components: hydrostatic (influenced by air temperature and air pressure) and wet delay (influenced by air temperature and water vapour pressure). While the hydrostatic delay (responsible for 90% of the error caused by the troposphere) can be mitigated with accurate surface pressure measurements, to estimate the wet delay requires a network of GPS receivers. This remaining delay in the propagation of

microwave radiation to the receiver on Earth is a result of the sensitivity of the atmospheric refractivity to the presence of water vapour, and is almost proportional to amount of water vapour along the path of the signal (Businger et al., 1996). Figure 2.3 shows the typical process that occurs between receiving a GPS signal and derived precipitable water data. As orbital and ionospheric sources of error are removed through calculations, the remaining signal error (referred to as the 'total slant tropospheric delay') contains the hydrostatic and wet delay components. The first step to converting the signal into a precipitable water estimate is to correct the hydrostatic delay with accurate surface pressure measurements for all GPS signals within a network of receivers, such as the SAN. Data from this network can be put into a model and used to describe local water vapour in the atmosphere vertically and horizontally (Hoyle, 2005). The output data, referred to as the zenith wet delay, is multiplied by a conversion factor and in final form represents the total integrated water vapour, or PW, from the surface to the top of the atmosphere above that receiver.

2.4 Summary

Mesoscale measurements, such as those provided by the FOPEX and mobile transects, have not previously been used to analyze Alberta drylines. Crawford and Bluestein (1997) argue that mesoscale measurements are valuable to document characteristics of the dryline (such as local variations in the magnitude of the moisture gradient). My thesis aims to improve our understanding of convective storm initiation in Alberta. The focus is on documenting the frequency of dryline events and the association of the dryline with

convection. I also measure the magnitude of humidity gradients, and compare GPS-derived PW estimates with dryline location.

Chapter 3

Results

3.1 Overview

The A-GAME and FOPEX field projects provided an excellent data set of surface moisture observations over south-central Alberta during July and August of 2003 and July and August of 2004. The FOPEX transect results provided continuous observations over the entire study period, and this data set was supplemented when possible by mobile transects performed within 80 km of the FOPEX transect. Using the methods described in Chapter 2, the entire data set was analyzed and a total of 7 dryline events were observed during A-GAME. Two dryline events were examined in further detail, one dryline case observed with the mobile transect (16 July 2004) and a FOPEX dryline event (10 July 2004). The mobile transect case study showcases observations of the moisture gradient across the dryline on temporal and spatial scales not previously attempted in Alberta. The FOPEX dryline event case study compared the GPS-derived PW values with the dryline location.

3.2 FOPEX Dryline Signature

This section illustrates with an example how a dryline events was identified in FOPEX. As discussed in Section 2.3, a dryline signature in the FOPEX mixing ratio and wind

observations was defined in this project as a drop in mixing ratio at the western-most station (AB4) on Limestone Mountain ridge, together with a shift in wind direction (to a westerly component), possibly followed by similar drops in mixing ratio and wind shifts at stations at lower elevations to the east. The difference in mixing ratio values between stations in the dry air and moist air was required to be at least 3 g kg^{-1}. This was considered to be the standard FOPEX dryline passage signature (the reverse being a retreat in the dryline). A veering (backing) shift in wind direction was also typically associated with the advance (retreat) of the dryline. This is displayed in Figure 3.1, where the dryline boundary formed within the FOPEX transect on 25 July 2004. A nearby sounding at Olds-Didsbury Airport confirmed the presence of a capping lid above south-central Alberta at 1800 UTC (not shown). The dryline was distinguishable between AB3 and AB4 in the early afternoon (1800 UTC). The station in the dry air (AB4) had a mixing ratio of ~5 g kg^{-1} and westerly winds, while the stations in the moist air had mixing ratio values ~10 g kg^{-1} and easterly winds. As the dryline migrated east of AB3 and AB1, significant drops in mixing ratio corresponded with abrupt westerly shifts in wind direction at both stations. The dryline stayed between AB1 and AB0 for 6 hrs and retreated westward through the transect by 0330 UTC, after which all FOPEX stations had mixing ratio values of at least 8 g kg^{-1}. Winds in the moist air after the dryline retreat were variable.

3.3 Dryline Events Observed During A-GAME

As described in Chapter 2, FOPEX data was examined for July and August of 2003/2004 by plotting mixing ratio and wind direction data on time series charts to easily detect any surface boundaries within the transect. The mobile transect data was examined in real time for noticeable variation in surface humidity and later analyzed as a time series. Synoptic analysis charts and radar and satellite imagery were subsequently examined for active weather in the foothills. Dryline cases were identified after ruling out other possible boundaries present in the FOPEX and mobile transect area, such as outflow boundaries from nearby thunderstorms, and synoptic-scale frontal systems.

Over the entire study period a total of 7 dryline events were observed in the FOPEX and/or the mobile transects. Of the 122 days examined during the two summer seasons, 6 days (~5%) exhibited dryline characteristics in the FOPEX transect. Two dryline events were detected with the mobile transect vehicle (once each in 2003 and 2004) out of a total of 17 transects (performed over 12 days during the A-GAME campaigns of 2003 and 2004). One dryline event was detected by both the FOPEX and mobile transects (17 July 2003).

The 7 A-GAME dryline cases are listed in Table 3.1. For all cases, the presence of a capping lid was noted, as well as flow patterns at 500 hPa and at the surface, and radar and satellite imagery was examined for thunderstorm development in the vicinity of the dryline. The surface wind direction in each case had an easterly component at 1800 UTC in south-central Alberta. In each case where sounding data were available from either

Olds-Didsbury Airport or Airdrie, a capping inversion was observed between 1800-1900 UTC. Three days exhibited classic Alberta thunderstorm synoptic conditions: an approaching 500 hPa trough (southwesterly flow aloft), easterly surface winds, and a capping inversion (12 August 2003 is not considered here due to the absence of local sounding data).

Discussion of FOPEX Dryline Events

In this study, the FOPEX transect observed an average of 3 dryline events annually at one location. Peterson (1983) found that a single station located in the center of a High Plains study area (West Texas) detected an average of 12 dryline events per year, or 40% of the drylines that were annually observed in the entire study area, roughly four times the size of the area of focus in this study. If one were to suppose the 3 FOPEX cases represented 40% of the drylines that occur in south-central Alberta annually, it would translate to ~7 dryline cases per year in this area. However, it is important to note that the FOPEX transect may not be in the optimal position for detecting the Alberta dryline. Paruk and Blackwell (1994) found that the highest frequency of hail events per year in Alberta occurred in the area south of the FOPEX line, in agreement with earlier studies (e.g., Wojtiw, 1975). Given that a significant proportion of these events would satisfy the conceptual model of Alberta thunderstorms (Strong, 1986; Smith and Yau, 1993b) and based on results of thunderstorm development in proximity to the dryline by Rhea (1966) (as discussed in Section 1.2), it can be expected that the dryline would likely be more prevalent and detected more often in that area south of the FOPEX line. Also, the furthest east the dryline advanced within the FOPEX transect was between AB1 and AB0

(this occurred in 3 cases). Strong (2005b) reasons that most drylines sweep eastward from the mountains *south* of the Red Deer River (see Figure 1.7) due to variations in foothills topography, as foothill peaks decrease south of Limestone Mountain (resulting in reduced orographic blocking and convergence). Thus, it is possible that mesoscale surface measurements in the foothills south of the FOPEX area may have resulted in a higher frequency of dryline detection. Determining the ability of the FOPEX transect to accurately reflect overall dryline activity in Alberta would also require more than two seasons of data in order to reduce the influence of annual fluctuations in thunderstorm activity in Alberta on the results.

3.4 Thunderstorm Formation in the Dryline Vicinity During A-GAME

Radar imagery was examined for each A-GAME dryline event for thunderstorm development along the foothills in the vicinity of the dryline location (determined by analysis of synoptic mixing ratio field). Of the A-GAME dryline cases, thunderstorms developed near the dryline in 5 of 7 cases (~71%), which is in agreement with the 70% of drylines associated with nearby thunderstorm development observed by Rhea (1966). No thunderstorms developed in the vicinity of the dryline on 17 July 2003 and 25 July 2004. Weak or short-lived thunderstorms developed on three days (30 July 2003, 12 August 2003, 16 July 2004). Thunderstorms that developed in the dryline vicinity produced hail on two days in south-central Alberta (walnut-sized hail on 20 July 2003, marble-sized hail on 10 July 2004). These results show that a dryline in the Alberta foothills is associated with various levels of convective development (or lack thereof) in the vicinity

of the dryline, and not just severe weather (as could be implied by the lack of discussion of a fair-weather dryline situation in Alberta in the research literature).

3.5 Moisture Gradients Observed by Mobile Transects

Two mobile transects performed during A-GAME detected the dryline in the Alberta foothills. The 17 July 2003 mobile transect was sampled north of the FOPEX transect, and the dryline was detected in FOPEX as well. The 16 July 2004 mobile transect (discussed in more detail in Section 3.6) was performed south of the FOPEX transect, where a dryline passage was not observed. Both of these mobile transects provide excellent information on the Alberta dryline, as measurements such as these have not been previously collected in Canada. The data indicate that the magnitude of surface moisture gradients associated with the dryline in Alberta are similar to those observed over the High Plains of the U.S. On 17 July 2003, the mobile transect west of Rocky Mountain house detected a moisture gradient of 0.92 g kg^{-1} km^{-1} across the dryline boundary upon the first traverse, and upon the second traverse almost 45 minutes later, a similar gradient was observed in a similar location as before. On 16 July 2004, the mobile transect traversed the dryline at 4 separate locations within 45 minutes, and sampled moisture gradients ranging from 0.90 g kg^{-1} km^{-1} to 4.27 g kg^{-1} km^{-1}. The moisture gradients observed during the A-GAME mobile transects are within the range observed by various dryline studies of the High Plains of the U.S. For example, Pietrycha and Rasmussen (2004) observed the moisture gradient across a dryline to

between 0.53–16.2 g kg^{-1} km^{-1}, Atkins et al. (1998) observed gradients ranging between 0.6-1.1 g kg^{-1} km^{-1}, and Ziegler and Hane (1993) measured 1.6 g kg^{-1} km^{-1}.

These two mobile cases also demonstrate that the FOPEX transect will not detect every dryline case in south-central Alberta, and overall, the majority of the mobile transect cases did not detect a dryline (2 of 17 transects observed a dryline). Manpower and financial constraints limited the mobile transects performed during the A-GAME field campaigns of July 2003 and 2004. Another possible reason for the lack of detection of the dryline is that it did not migrate far east onto the plains of south-central Alberta and limited road access in and around the western foothills prevented its detection.

3.6 Case Study of 16 July 2004 Dryline Sampled by Mobile Transect

This section describes the case study of 16 July 2004. For this case, data were sampled at a high spatial and temporal resolution allowing a detailed examination of the dryline as the mobile transect traversed the dryline 4 times south of the FOPEX transect. The dryline did not pass through the FOPEX transect on this day. The surface mixing ratio and wind fields were examined for south-central Alberta, along with synoptic analysis charts and two soundings released from Olds-Didsbury Airport at 1800 and 2200 UTC. Cloud and storm development was examined with remote sensing imagery (radar and satellite) over southern Alberta.

Synoptic Chart Analysis

The upper-air flow pattern at 1200 UTC 16 July 2004 revealed a 500 hPa trough off the coast of British Columbia and west-southwesterly flow over southwestern Alberta as a ridge was over eastern Alberta (Figure 3.2). Over the next 12 hrs the 500 hPa ridge intensified over Alberta. The 500 hPa flow above central Alberta at 1200 UTC was west-southwesterly at 8 m s^{-1} (15 knots) and this became westerly by 0000 UTC at 13 m s^{-1} (25 knots). The 500 hPa temperature level remained constant over central Alberta between 1200 UTC and 0000 UTC, and the moisture levels increased slightly over this time. A 250 hPa jet maximum was observed off the coast of British Columbia at 1200 UTC and it tracked northeast to interior British Columbia by 0000 UTC, while at this level the flow shifted from southwesterly to northwesterly over central Alberta by 0000 UTC. The 1200 UTC surface pressure analysis revealed no major surface pressure systems in Alberta, while by 0000 UTC a surface low developed in southern British Columbia. Surface flow at 0000 UTC through interior Alberta was southeasterly at 5 m s^{-1}. Surface flow with an easterly component in south-central Alberta results in convergence along the foothills. Maximum surface temperatures achieved on this day in south-central Alberta were ~30°C in the Calgary area, and slightly lower at ~27°C in the Red Deer area. The upper-level synoptic situation on this day did not nicely fit the multi-scale conceptual model of Alberta thunderstorms, as the building of the 500 hPa ridge on this day reduced the upper-level support for the development of organized convection.

Upper Air Data Analysis

Two radiosondes were released this day from Olds-Didsbury Airport, at 1800 UTC (Figure 3.3) and 2200 UTC (Figure 3.4). At 1800 UTC, surface winds at Olds-Didsbury Airport were light southeasterly and the temperature and dewpoint were 22.6°C and 16.6°C, respectively. The capping lid was detected at ~825 hPa (750 m AGL), where the temperature increased 1°C and above the capping lid the dewpoint temperature dropped ~10°C. The mixing ratio above the lid was 6.6 g kg^{-1}, while at the surface it was 13.3 g kg^{-1}. Winds abruptly shifted from southeasterly to southwesterly at the capping lid, and remained westerly aloft. Maximum wind speed (~26 m s^{-1}) was observed at 220 hPa.

A second sounding was released from Olds-Didsbury Airport at 2200 UTC, where the surface temperature and dewpoint had risen to 26.8°C and 18.8°C, respectively. The capping inversion had been eroded significantly as the temperature profile did not indicate that an inversion was present, however above the boundary layer (~820 hPa), the dewpoint temperature dropped ~10°C while the temperature dropped only slightly at this height (~800 m AGL). The mixing ratio above the boundary layer was 4.5 g kg^{-1}, while at the surface it was 15.4 g kg^{-1}. Unfortunately, no wind data were collected for this sounding apart from surface observations (light and southeasterly).

The stability indices calculated for the soundings of 16 July 2004 (Table 3.2) showed significant instability in the area with the potential for deep convection. The 1800 UTC sounding analysis revealed a CAPE of 2500 J kg^{-1}, CIN of –120 J kg^{-1} and LI of –6.8. By 2200 UTC, surface warming increased the instability in the area significantly, with CAPE

increasing to 4180 J kg^{-1}, CIN at –12 J kg^{-1}, and a LI of –10.2. The CAPE values of both soundings are associated with the development of supercell thunderstorms in Alberta (Brimelow et al., 2002). A comparison of the temperature and dewpoint profiles (Figure 3.5) of the soundings at 1800 and 2200 UTC showed that the depth of the boundary layer increased as it warmed significantly between 1800 and 2200 UTC. The 2200 UTC temperature profile is similar to that of 1800 UTC until ~400 hPa; however, above that level the temperature at 2200 UTC was warmer than 1800 UTC. Above 600 hPa, the dewpoint at 2200 UTC was also significantly higher than at 1800 UTC. These stabilizing changes in the upper atmosphere were likely a factor in the lack of sustained deep convection on this day.

FOPEX Surface Moisture and Wind Analysis

Mixing ratio trends for the FOPEX stations between 1300-0230 UTC are displayed in Figure 3.6. No significant moisture gradients were observed within the FOPEX transect on this day, as mixing ratios increased at all FOPEX stations throughout the day. At 1300 UTC the mixing ratio values within the transect ranged between ~7 and 10 g kg^{-1}. Later in the day, the range increased to ~10 to 15 g kg^{-1}.

FOPEX station AB0 (Figure 3.7a) was the only station on this day to observe relatively consistent winds between 1300 and 0230 UTC as the wind had an easterly component throughout the day. Station AB1 (Figure 3.7b) recorded the maximum mixing ratio levels observed on this day, up to ~16 g kg^{-1} between 2130 and 0230 UTC. The winds at AB1 were quite variable until 2100 UTC, when they became consistently northwesterly.

At AB3 (Figure 3.7c), winds were variable until 2000 UTC, when they became southeasterly/easterly winds. At the AB4 site on Limestone Mountain ridge (Figure 3.7d), winds were variable until 1930 UTC, after which they became southeasterly.

The Dryline and Related Storms

The mixing ratio and wind data collected on the synoptic scale and by FOPEX was plotted on 3-hourly contour maps from 1200 to 0300 UTC for 16-17 July 2004 (Figure 3.8). At 1200 UTC, the moisture field was fairly uniform, with drier air near the FOPEX transect and Red Deer. Winds were light and variable early in the morning, and became southerly with an eastern component in south-central Alberta by 1500 UTC as the moisture gradient from west to east in the study area developed. By 1800 UTC, winds were southeasterly in the moist air, while westerly in the dry air in the southwest. By 2100 UTC a strong moisture gradient was observed south of FOPEX, with only one synoptic station located in the dry air (Bow Valley, ~7 g kg^{-1}). As discussed above, the FOPEX transect was in moist air during the day, and the mixing ratio plots at 2100 and 0000 UTC indicate that Limestone Mountain was an area of enhanced moisture convergence, with higher mixing ratio values observed at higher elevations in the FOPEX transect than at AB0. By 0300 UTC, the dryline retreated westward to the extreme southwest of the study area as winds became light and variable.

The mobile transect began at 1930 UTC at the Olds-Didsbury Airport and encountered dry air more than 70 km west in the foothills near Mountain-Aire Lodge. The vehicle was traveling approximately 50 km hr^{-1} when it crossed the dryline boundary detecting

significantly dry air at 2050 UTC (Figure 3.9). The observed moisture gradient upon this first traverse of the dryline was 0.90 g kg^{-1} km^{-1} and the vehicle proceeded for a few kilometers west of the dryline before turning back eastward to retrace the last few kilometers of the path. Moist air was not encountered at the same position as before (therefore the boundary must have been moving eastwards in the ~15 minutes between observations). Figure 3.10 shows the contoured mixing ratio field for the remainder of the mobile transect as the vehicle turned northwest where moist air was encountered again. This gradient however was significantly stronger; in about 1 km the mixing ratio jumped ~3 g kg^{-1} (a gradient of 3.13 g kg^{-1} km^{-1}). The vehicle was in moist air for about 2 km when the mixing ratio dropped ~4 g kg^{-1} in less than 1 km (a gradient of 4.27 g kg^{-1} km^{-1}). The vehicle, now in dry air (~6 g kg^{-1}), proceeded northwest for 11 km until it turned eastward and encountered moist air yet again. This last traverse of the dryline boundary into relatively moist air was at a similar gradient as the first, increasing at 1.04 g kg^{-1} km^{-1}. Localized variations are common with any surface variable, including moisture. The strong moisture gradients observed were likely a result of localized moisture convergence, but unfortunately no wind data are available to support this hypothesis.

As observed in Figure 3.8d, the location of the strongest moisture gradient observed at 2100 UTC with synoptic and FOPEX mixing ratio data was south of the FOPEX transect on 16 July 2004. It was in this area that the mobile transect detected the dryline boundary. For comparison purposes, the contour map of the synoptic mixing ratio field without the high resolution mobile transect data at 2100 UTC is displayed beside the

surface mixing ratio field as observed with the inclusion of the mobile transect observations (Figure 3.11). While the mixing ratio field without the mobile transect data (Figure 3.11a) did accurately depict the same area of a less intense moisture gradient, the inclusion of mobile transect data (Figure 3.11b) clearly displayed the actual strength of the moisture gradient and dryline position (as one would expect with a finer spatial resolution).

Cumulonimbus clouds (Figure 3.12) were observed to the east of the dry air along the foothills during the entire mobile transect, as observed in the satellite imagery (Figure 3.13). Radar images at the time of the transect show storm cells developing along the foothills (Figure 3.14). An examination of the radar imagery on this day showed that three significant cells initiated along the foothills between 2000 and 2200 UTC. However all three cells had relatively short lifespans and dissipated within ~50 km of the initiation zone.

Case Study Summary

The 16 July 2004 mobile transect dryline case provided high-resolution spatial and temporal measurements of the moisture gradient across the dryline. The general synoptic conditions for this day resulted in convergence along the foothills (easterly winds at the surface) and westerly winds aloft. The dryline was detected by the mobile transect south of the FOPEX transect (where it was not observed) and was traversed 4 times, measuring moisture gradient magnitudes ranging from 0.9–4.3 g kg^{-1} km^{-1}. The sounding analysis revealed significant instability (CAPE up to 4180 J kg^{-1}) in the area, as cumulonimbus

clouds developed 20 km east of the dryline along the foothills in the mid-afternoon. However, evolving atmospheric conditions inhibited any sustained deep convection in south-central Alberta as upper level support for severe thunderstorms in Alberta was lacking.

3.7 GPS-derived Precipitable Water Observations During 10 July 2004 FOPEX Dryline Event

A complete data set of GPS-derived PW estimates was not available throughout A-GAME at the FOPEX transect site location AB4. Of the 6 drylines detected by the FOPEX transect, only one event had complete PW data (10 July 2004). This case was examined in detail. Surface moisture data, synoptic conditions and sounding data were examined. Radar and satellite imagery were used to observe cloud and storm development. The GPS-derived PW measurements were evaluated at FOPEX station AB4 and Sundre.

Synoptic Chart Analysis

The upper-air flow pattern at 1200 UTC 10 July 2004 revealed a 500 hPa trough over the southwestern British Columbia and zonal flow over the eastern Alberta through to Manitoba (Figure 3.15). Over the next 12 hrs the 500 hPa low over southwestern BC tracked slightly east, while a ridge developed over Saskatchewan. The 500 hPa flow above central Alberta at 1200 UTC was westerly at 10 m s^{-1} (20 knots) and this became southwesterly by 0000 UTC as the trough approached. The 500 hPa temperature and

moisture levels did not vary over central Alberta between 1200 UTC and 0000 UTC. A 250 hPa jet maximum over southeastern BC at 1200 UTC, moved into south-central Alberta by 0000 UTC, resulting in a strong southwesterly flow of 31 m s^{-1}, and placing the left-exit zone, conducive to storm formation (Uccellini and Johnson, 1979), over central Alberta shortly thereafter. The 1200 UTC 10 July 2004 surface pressure analysis revealed a surface high over extreme southern Alberta, giving way to a low pressure centre by 0000 UTC, and a moderate (5 m s^{-1}) southeasterly flow through central Alberta. Surface flow with an easterly component in south-central Alberta results in convergence along the foothills. Maximum temperatures achieved on this day in south-central Alberta were ~23°C. Along with the development of an 850 hPa low over southwestern Alberta by 0000 UTC (not shown), the upper-level support for the surface low led to a classic thunderstorm day for Alberta.

Sounding Analysis

Two radiosondes were launched over south-central Alberta on 10 July 2004; sounding data were collected at 1900 UTC from Airdrie (Figure 3.16) and at 2400 UTC from the Olds-Didsbury Airport (Figure 3.17). Due to the easterly component of the surface flow in south-central Alberta, the Airdrie sounding provided representative sounding data east of the dryline boundary for the pre-thunderstorm environment of 10 July 2004. The 2400 UTC Olds-Didsbury sounding was launched after thunderstorms were observed in the area.

At 1900 UTC a sounding analysis revealed an atmosphere conducive to severe weather development with a capping inversion in place above an unstable relatively moist boundary layer. The capping inversion was observed between 845 hPa (401 m above ground level (AGL)) and 835 hPa (501 m AGL), where the air temperature increased by 1.3°C to 15.5°C and the dewpoint temperature dropped significantly from 6.2°C to –1.9°C. The average mixing ratio in the boundary layer beneath the capping lid was ~7 g kg^{-1}, while above the capping lid (~830 hPa) it was significantly lower at ~4 g kg^{-1}. The stable layer at 835 hPa, in an otherwise conditionally unstable atmosphere, capped the boundary layer in south-central Alberta and allowed latent heat energy to build up at the surface during the afternoon of 10 July 2004. The 1900 UTC wind profile showed light southeasterly winds from the surface up to the capping inversion, while above the capping inversion wind directions ranged between 200°-221° with speeds steadily increasing to a maximum of 27 m s^{-1} at 255 hPa. The mean winds from surface to 6 km AGL were 214° at 13 m s^{-1} while from the surface to 0.5 km they were 178° at 5 m s^{-1}.

The radiosonde launched 5 h later from Olds-Didsbury Airport collected sounding data ~50 km north of the Airdrie, and thus reflected the evolution of atmospheric conditions both temporally and spatially between these sites. Comparing the two soundings, the 2400 UTC lower atmosphere (up to 800 hPa) was considerably warmer and drier than at 1900 UTC. At 850 hPa, the observed air and dewpoint temperatures at 1900 UTC were and 14.6°C and 6.9°C respectively, while at 2400 UTC they were 19.8°C and –6.2°C, respectively. The capping inversion feature and instability present on the 1900 UTC sounding from Airdrie was not observed on the Olds-Didsbury sounding at 2400 UTC.

As discussed below, storms passed through the area around 2300 UTC, suggesting that the capping inversion was removed in the area by that time. By 2400 UTC, zero CAPE was computed for a parcel lifted from the surface, and a nocturnal inversion was already forming over the area (as the surface air temperature was 1.2°C cooler than that measured at 48 m AGL). The wind profile measured at 2400 UTC was similar to that observed at Airdrie at 1900 UTC, with southeasterly winds at the surface and southwesterly winds aloft.

Table 3.3 displays three standard severe weather indices calculated for the soundings of 10 July 2004. The CAPE for the 1900 UTC sounding was 1270 J kg^{-1}, while the CIN was -70 J kg^{-1}, indicating potential for multicell thunderstorms to develop. There was no CAPE or CIN observed with the 2400 UTC sounding. At 1900 UTC, the LI was –6.6, indicating support for deep convection, while the post-thunderstorm environment at 2400 UTC the LI was a stable value of 0.2. It is clear that the instability and potential for convective development indicated by the 1900 UTC sounding was realized in south-central Alberta prior to the release of the 2400 UTC radiosonde at Olds-Didsbury Airport. The post-thunderstorm environment at 2400 UTC was stable, with warmer and drier air at the surface compared to the 1900 UTC sounding – likely influenced significantly by the environmental mixing caused by thunderstorms.

FOPEX Surface Moisture and Wind Analysis

Mixing ratio trends for the FOPEX stations between 1200-0300 UTC are displayed in Figure 3.18. Significant moisture gradients were observed within the FOPEX transect

between 1930 and 0130 UTC. Mixing ratios increased at the lower elevation stations, AB0 and AB1, from 8 to 10 g kg^{-1} by 1900 UTC, then remained steady into the evening. Winds at AB0 and AB1 (Figures 3.19a, 3.19b) show a consistent easterly component through most of this period, averaging 123° and 113°, respectively.

At AB3, easterly winds (averaging 119°) switched briefly to southwesterly at 2330 UTC, which coincided with mixing ratio dropping from 9 to 5 g kg^{-1}, the minimum value measured at the station at that day (Figure 3.19c). The wind direction fluctuated during the dry episode (from 248° to 43°), most likely a result of turbulent mixing that can be observed west of the dryline (Hane et al., 1997). Once mixing ratio values at AB3 returned to 8 g kg^{-1}, the wind direction switched back to easterly and the rapid fluctuations in wind direction ceased.

At the AB4 site on Limestone Mountain ridge, mixing ratio values were lower than at the other stations during early afternoon (around 6 g kg^{-1}), and decreased throughout the afternoon to a minimum of 4.4 g kg^{-1} at 2330 UTC. These relatively low mixing ratios at AB4 were accompanied by southwesterly winds, averaging 206° until 0100 UTC (Figure 3.19d), which was advecting drier air from higher elevations over the Rocky Mountains west of Limestone Mountain. After 0100 UTC, winds shifted abruptly to northeasterly at AB4, resulting in the observed increase in mixing ratio (from 6 to 8 g kg^{-1}) as moist air was brought upslope from the lower foothills to the northeast.

These mixing ratio and wind direction graphs for the FOPEX transect are interpreted as follows: the dryline boundary formed between stations AB3 and AB4 late in the morning as moisture converged along the foothills under easterly surface winds. The dryline then advanced eastward past AB3 by 2330 UTC, and retreated westward past AB3 and AB4 out of the FOPEX transect by 0130 UTC.

The inclusion of a small, closely-spaced line of stations (FOPEX) within the relatively coarse-resolution surface synoptic grid provided excellent data for the detection of drylines. Plots of the 2100 UTC surface mixing ratio values in south-central Alberta without and with the FOPEX data included are displayed in Figures 3.20a and 3.20b, respectively. Both contour maps show moisture highest in the north and southeast areas, with decreasing mixing ratio values westward. Without the FOPEX data, the contoured moisture gradient is evenly spaced out in the western part of the region. When the FOPEX data are included, a significantly tighter moisture gradient is observed west of Sundre, as well as a bulge of moisture to the north of Sundre. As observed by Pietrycha and Rasmussen (2004), dryline features on the finer-scale that are not adequately resolved with synoptic data alone can be very important (as already observed with mobile transect data in Section 3.6), and in this instance the FOPEX data resolved a tighter moisture gradient and northward bulge in the dryline. This reinforces the importance of mesoscale data, such as the FOPEX transect provides, for studying features such as the dryline in Alberta.

The Dryline and Related Storms

The evolution of the surface moisture and wind fields between 1200 and 0300 UTC is displayed in Figure 3.21. At 1200 UTC (Figure 3.21a) the winds in south-central Alberta were light and variable and mixing ratio values were slightly lower in the western area of the region. By 1500 UTC the surface map analysis revealed a typical surface moisture set-up on a thunderstorm day in Alberta, with moisture converging along the foothills due to the easterly component of the surface winds. A drier area was observed around Drumheller at 1800 UTC, while peaks in surface moisture were observed north of Red Deer and in the southeast near Brooks. By 2100 UTC, the moisture gradient was at a maximum in the western part of the foothills region, reflecting the convergence of moisture over the foothills against the advancing dryline. Westerly winds were observed at the driest stations (AB4 and Bow Valley WXA). At 0000 UTC the dryline was still present along the foothills and bulging slightly eastward south of the FOPEX sites. The strength of the moisture gradient across the dryline weakened significantly to become undetectable in the area by 0300 UTC, as all stations in the area recorded mixing ratios ~7 g kg^{-1}. The peaks in moisture were observed further to the east in the area, and winds were variable and relatively light in most of south-central Alberta.

Storms developed and remained over the region between 2000 and 0200 UTC. The 1.5-km CAPPI images from Strathmore radar (operated by MSC) were examined in order to observe storm development along the foothills on this day. Two significant storm cells developed over the study area on this day (Figure 3.23) – the first cell was detected on radar at 2010 UTC about 30 km north of the FOPEX transect near Rocky Mountain

House (WRM). It tracked eastward until about 0100 UTC when it began to weaken and dissipate. This was the most intense cell observed on this day, and developed within the vicinity of the bulge in the dryline north of the FOPEX transect (see Figure 3.21d). A bulge in the dryline is a favored area of thunderstorm development because it results in maximum convergence as the winds in the moist air wrap around the dry air (Schaefer, 1986). MSC issued several severe thunderstorm warnings for this storm in the Rocky Mountain House area and as far east as Red Deer. The storm produced heavy rainfall, marble-sized hail (1.3-1.9 cm in diameter), and funnel clouds.

The other storm observed in the study area developed 40 km northwest of Calgary at 2100 UTC. This cell tracked northeastwards towards Olds, but had weakened significantly before reaching Olds by 2400 UTC. The examination of the radar images confirm that the radiosonde launched at Olds-Didsbury Airport at 2400 UTC was indeed representative of the post-thunderstorm environment.

Visible satellite images of Alberta are displayed in Figure 3.23. At 1931 UTC prior to storm development, areas directly east of the Alberta foothills in south-central Alberta were in cloud-free air, while cloud was observed over the foothills and Rocky Mountains, and also in southeastern Alberta. By 2301 UTC, mature storms were present over south-central Alberta, with three distinct significant storms and associated anvils identifiable on the satellite image. The two southern-most storms in the satellite image were the Rocky Mountain House storm and the storm that developed northwest of Calgary.

GPS-derived Precipitable Water Analysis

Hourly observations of mixing ratio and GPS-derived PW were collected at AB4 and Sundre on 10-11 July 2004. As discussed above, the dryline formed east of FOPEX station AB4 during the afternoon of 10 July 2004, resulting in relatively low mixing ratio values at AB4 of ~ 5 g kg^{-1} (Figure 3.24a). East of the dryline in the moist air, Sundre recorded mixing ratio values ~ 9 g kg^{-1} (Figure 3.24b). The PW values east of the dryline at Sundre were significantly higher than AB4 by 1900 UTC, and up until 0200 UTC the average difference in PW between the two locations was 7.5 mm. The largest difference between Sundre and AB4 PW values (11.4 mm) was observed at 2000 UTC. The mean difference in mixing ratio between the two locations from 1900-0200 UTC was 3.7 g kg^{-1}.

In comparing PW values with surface vapour mixing ratio values it is important to emphasize that PW is a vertically-integrated measure of atmospheric humidity, whereas the mixing ratio observations are in situ surface measurements. However most of the temporal variability of the vapour within a given column occurs near the surface. It is thus of interest to determine whether trends in the hourly surface measurements coincide with similar trends in the hourly PW values. The correlation between mixing ratio and PW values was calculated for each site on either side of the dryline boundary between 1200 and 0300 UTC. The correlation coefficient between mixing ratio values and PW at AB4 over this period was –0.52, indicating a negatively correlated relationship between mixing ratio and PW. The correlation coefficient calculated for the same time period at the Sundre location was 0.13, indicating a slightly positive correlation. While examining

trends of mixing ratio values was effective for detecting the dryline boundary at the surface on this day, the correlation results showed that examining trends of GPS-derived PW measurements in a similar manner was not as effective for tracking the dryline boundary. When the mixing ratio at AB4 rose significantly upon the retreat of the dryline west of the FOPEX transect at 0200 UTC, the PW dropped at AB4.

Similar to Businger et al. (1996), an additional data source (in this case, mixing ratio data) was used in conjunction with the PW data. The retreat of the dryline west past AB4 was reflected in the mixing ratio data, but the PW data did not clearly indicate that both AB4 and Sundre were in moist air by 0200 UTC. While examining PW *trends* was not useful on this day, comparing PW values between the specific locations did indicate that AB4 and Sundre were on opposite sides of the dryline boundary during the afternoon. The extremely limited data (only one case) prevents a conclusion on the usefulness GPS-derived PW in dryline studies, and further exploration is warranted over a longer time period with more dryline cases.

Summary of findings

This case study of 10 July 2004 is a good example of dryline development on a typical non-severe Alberta thunderstorm day (maximum hail size under 2 cm). Correlating wind shifts with changes in moisture indicated the presence of the dryline boundary within the FOPEX transect, with the associated capping inversion over south-central Alberta detected by the radiosonde released from Airdrie at 1900 UTC. Upper-level dynamics combined with the surface flow resulted in convergence along the foothills and the

removal of the capping inversion in that area. The unstable atmosphere combined with significant CAPE (~1270 J kg^{-1}) led to the development of non-severe thunderstorms along the foothills by 2100 UTC. The most intense storm observed in south-central Alberta formed along the foothills within 50 km of the dryline that was detected by the FOPEX transect. Examining trends of GPS-derived PW values did not prove useful compared to mixing ratio for detecting the dryline boundary at FOPEX transect site AB4, yet comparing PW values with Sundre did indicate that AB4 was west of the dryline.

3.8 Summary and Conclusions

The analysis of the A-GAME mobile transect and FOPEX stationary transect mixing ratio observations during July and August of 2003 and 2004 yielded 7 dryline cases (6 in FOPEX and 2 in the mobile transect). The synoptic setting on the majority of the dryline days fit the multi-scale conceptual model for Alberta thunderstorms. Adding to the established knowledge that severe thunderstorms in Alberta can be observed with and without a dryline (Dupilka and Reuter, 2005), it was observed in this study that drylines are also observed in Alberta on days with non-severe thunderstorms, no thunderstorms, and on days with no potential for thunderstorms.

The value of mesoscale measurements of the dryline boundary is apparent for studying the dryline in Alberta. The 16 July 2004 mobile transect and 10 July 2004 FOPEX dryline case studies included plots of mesoscale data within the MSC operational synoptic observation network and revealed that mesoscale measurements are necessary in

Alberta to determine the magnitude of the moisture gradient and location of the dryline. The multiple traverses of the dryline on 16 July 2004 with the mobile transect vehicle confirmed that the magnitude of the moisture gradient across the dryline is similar to that observed in the High Plains of the U.S. The examination of the GPS-derived PW measurements on 10 July 2004 during a FOPEX transect dryline episode showed that these measurements have the potential to be useful in the Alberta foothills for estimating the location of the drylines.

Chapter 4

Conclusions and Recommendations

4.1 Discussion and Conclusions

The dryline is a mesoscale convergence zone, defined as a sharp moisture gradient across a narrow zone between relatively moist air and relatively dry air (Schaefer, 1986). This thesis documents an investigation of drylines that occurred in south-central Alberta during the summers of 2003 and 2004. The A-GAME and FOPEX field projects provided good opportunities for developing a data set suitable for a dryline study in south-central Alberta. Surface moisture measurements, collected by the FOPEX transect of weather stations and the A-GAME vehicle equipped for mobile transects, provided the basis for this investigation. Upper-air sounding data collected from various sites in the study region provided information on the capping lid, as well as assessing the potential for deep convection. Also, these field projects provided the first opportunity to evaluate GPS-derived moisture measurements in a dryline situation in Alberta.

Table 4.1 lists data that summarizes some major findings of this thesis. These data are compared with values presented in the research literature in previous studies. The first objective of this thesis was to determine the frequency of dryline occurrence. During July and August of 2003, 4 dryline events were detected, characterized by water vapour mixing ratio changes equal to or larger than 3 g kg^{-1} over the specified time and/or spatial

scales. In the following year, 3 dryline events were detected during July and August. There were 6 dryline events detected in a total 4 months in the FOPEX transect. In comparison with the High Plains, Peterson (1983) examined dryline events in West Texas over 10 years and found that in the center of the study area (Lubbock, Texas), ~12 events were recorded within a 3-month spring season.

The second objective of this thesis was to clarify whether all Alberta drylines are associated with severe convective storms, or whether drylines can occur with weak convection or without any convection. Of the 7 dryline cases, only 2 events/days were not associated with convective activity in the vicinity of the dryline. Of the 5 remaining cases, storms that initiated near the dryline produced hail in 2 cases (walnut-sized hail on 20 July 2003, marble-sized hail on 10 July 2004). Three other dryline events had weak or short-lived convection develop in the vicinity of the dryline (30 July 2003, 12 August 2003, 16 July 2004). Severe storms in Alberta can be associated with and without a dryline (Dupilka and Reuter, 2005), and the results of this investigation indicate that a dryline can be present in the Alberta foothills without triggering convection. Therefore, it can be said that the dryline alone is neither necessary nor sufficient for severe thunderstorm development in Alberta.

The third objective of this thesis was to quantify the magnitude of water vapour mixing ratio gradients across drylines. This component of our investigation was based on data from two mobile transects (17 July 2003, 16 July 2004). On 17 July 2003, the humidity gradient across the quasi-stationary dryline was close to 0.9 g kg^{-1} km^{-1}. Measurements

were taken twice about 40 minutes apart and at both times the gradient of mixing ratio was of the same magnitude. In contrast, on 16 July 2004, the vapour mixing ratio gradient varied in magnitude during the 4 different transects that were sampled. The humidity gradients measured were 0.9 g kg^{-1} km^{-1}, 1.0 g kg^{-1} km^{-1}, 3.1 g kg^{-1} km^{-1}, and 4.3 g kg^{-1} km^{-1}. This is similar to the results of Pietrycha and Rasmussen (2004), who also observed a significant range in the magnitude of the moisture gradient magnitude across the dryline in the High Plains. They measured multiple transects of the dryline boundary and observed a range in magnitudes of moisture gradients between 0.53 g kg^{-1} km^{-1} and 16.2 g kg^{-1} km^{-1}.

The final objective of my thesis was to use the GPS-derived Precipitable Water (PW) estimates to document drylines. Only one event (10 July 2004) had both GPS data and FOPEX data. The data showed that the GPS-derived PW estimates on the dry side of the dryline were much smaller than the PW values recorded on the moist side. A mean difference of 7.5 mm in PW was documented during the dryline event. This case suggests that GPS-derived PW estimates can aid in locating drylines. This finding is consistent with the results of Businger et al., (1996), who came to a similar conclusion regarding the ability of PW measurements to document the dryline position.

4.2 Limitations of this Study and Recommendations for Future Work

While this study provided new information on the Alberta dryline, the number of recorded drylines was limited with only 122 days of FOPEX observations, and 18 days of

A-GAME field observations. For example, Hoch and Markowski (2005) used 30 years of data to compile their dryline climatology for the U.S. Great Plains. A climatology would be valuable to forecasters - knowledge of the typical dryline location and frequency of development could help identifying favoured areas of thunderstorm initiation when a dryline is present. However, a sufficiently dense network of operational weather stations is not currently in place for such a study. As observed in the detailed analysis of the 16 July 2004 and 10 July 2004 dryline events, these synoptic-scale surface moisture measurements do not necessarily adequately resolve the actual dryline boundary. Thus, a mesoscale network such as FOPEX is required in southern Alberta for dryline detection at the surface.

In this study, the evaluation of the GPS-derived PW measurements in a dryline situation in the Alberta foothills was restricted to a single case. In future studies continuous GPS-derived PW data for the entire study period would be optimal, as would co-locating a GPS-receiver with a mesonet of surface sites. Observations of the PW gradient across the dryline boundary in high spatial resolution within in the FOPEX transect would be a valuable addition to the knowledge base of Alberta drylines.

The location of both the mobile and FOPEX surface transects was also a potentially inhibiting factor in dryline detection during this study. As discussed by Strong (2005b), the FOPEX transect may not be in the optimal location for detecting the Alberta dryline. Strong indicates that drylines may sweep further eastward onto the Alberta Plains further south of the FOPEX transect because of differences in topography (lower foothills peaks

south of Limestone Mountain). Thus, a mesoscale surface station transect further south (i.e. near Sundre) may detect more drylines as they migrate further onto the Plains. Road accessibility for mobile transects was also a restrictive issue for data collection in this study. As building roads in remote areas of the foothills is not a likely solution, low-level flight observations from aircraft are desirable to collect humidity data in remote areas.

Tables

Table 2.1. Location and elevations (ASL) of each station in the FOPEX surface transect in south-central Alberta.

Site	Location	Latitude	Longitude	Altitude (m)
AB0	Caroline	52.09	-114.87	1070
AB1	Clearwater Ranger Station	51.99	-115.24	1280
AB2	Marble Mountain East	51.90	-115.19	1440
AB3	Marble Mountain West	51.90	-115.23	1640
AB4	Limestone Mountain East	51.89	-115.37	1950
AB5	Limestone Ridge	51.92	-115.42	2120

Table 2.2. Data recovery rates for the surface stations of the FOPEX transect in south-central Alberta during July and August of 2003 and 2004 (a total of 122 days). Sites AB2 and AB5 were decommissioned during for 2004 months.

Site	2003	2004
AB0	100%	100%
AB1	100%	100%
AB2	94.7%	-
AB3	100%	100%
AB4	100%	100%
AB5	36.7%	-

Table 2.3. Location and elevations (ASL) for all Meteorological Service of Canada weather stations used to plot the synoptic surface mixing ratio field in southern Alberta. Abbreviations are displayed only for sites within the A-GAME and FOPEX field operations (Figure 2.2) as only these will appear on the synoptic mixing ratio analysis maps.

Site	Abbreviation	Latitude	Longitude	Altitude (m)
Banff		51.18	-115.55	1397
Bow Valley	WXA	51.07	-115.07	1298
Brooks	WBO	50.55	-111.85	747
Calgary	YYC	51.10	-114.02	1084
Camrose		53.02	-112.82	739
Coronation		52.07	-111.45	791
Drumheller	WDZ	51.42	-112.67	678
Edmonton		53.32	-113.57	723
Lethbridge		49.62	-112.80	929
Medicine Hat		50.02	-110.72	717
Nordegg		52.47	-116.07	1362
Pincher Creek		49.52	-113.97	1190
Red Deer	YQF	52.17	-113.88	905
Rocky Mountain House	WRM	52.42	-114.90	988
Springbank	YBW	51.10	-114.37	1200
Sundre	WAV	51.77	-114.67	1114
Vegreville		53.52	-112.10	639

Table 3.1. All dryline events detected during A-GAME by the FOPEX transect and/or mobile transects in July and August of 2003/2004. The upper level flow over south-central Alberta was observed at 500 hPa at 1200 UTC and/or 1800 UTC, similarly the surface flow in south-central Alberta was examined from 1200 to 1800 UTC. The stations in dry air listed represent the farthest east that the dryline advanced to during the day in FOPEX (note no cases observed the dryline passing beyond AB0).

Date	Capping Inversion Detected? (Sounding Location)	Upper level flow	Surface flow (zonal component)	Stations in dry air	Thunderstorms developed along foothills?
17 Jul 2003	Yes (Olds-Didsbury)	NW	E	AB4, AB3, AB1 (Mobile)	No
20 Jul 2003	Yes (Olds-Didsbury)	SW	E	AB4	Yes
30 Jul 2003	-	NW	E	AB4	Yes
12 Aug 2003	-	SW	E	AB4, AB3, AB1	Yes
10 Jul 2004	Yes (Airdrie)	SW	E	AB4, AB3	Yes
16 Jul 2004	Yes (Olds-Didsbury)	W	E	(Mobile)	Yes
25 Jul 2004	Yes (Olds-Didsbury)	SW	E	AB4, AB3, AB1	No

Table 3.2. Stability indices for the 16 July 2004 soundings at Olds-Didsbury Airport at 1800 and 2200 UTC.

Stability Index	1800 UTC	2200 UTC
CAPE (J kg^{-1})	2498	4175
CIN (J kg^{-1})	-120	12
Lifted Index (LI)	-6.8	-10.2

Table 3.3. Stability indices for the 10 July 2004 soundings at Airdrie at 1900 UTC and at Olds-Didsbury Airport at 2400 UTC.

Stability Index	1900 UTC	2400 UTC
CAPE (J kg^{-1})	1273	0
CIN (J kg^{-1})	-69	0
Lifted Index (LI)	-6.6	0.2

Table 4.1. Major findings of this dryline study in south-central Alberta specific to each objective of described in Section 1.5.

Objective	Observed in Alberta during A-GAME	Observed in previous projects
Number of events at one location during A-GAME	6 events in FOPEX over 4 months (17 Jul 03, 20 Jul 03, 30 Jul 03, 12 Aug 03, 10 Jul 04, 25 Jul 04)	~12 cases in 3 months at Lubbock, TX (Peterson, 1983)
Convective initiation in the dryline vicinity	-no convective activity (17 Jul 03, 25 Jul 04) -weak to moderate convection (30 Jul 03, 12 Aug 03, 16 Jul 04) -deep convection (20 Jul 03, 10 Jul 04)	Severe tornadic storms in Alberta (Knott and Taylor, 2000; Dupilka and Reuter, 2005)
Strength of moisture gradient across a dryline	0.9-4.3 g kg^{-1} km^{-1} (16 Jul 04) 0.9 g kg^{-1} km^{-1} (17 Jul 03)	0.53-16.2 g kg^{-1} km^{-1} (Pietrycha and Rasmussen, 2004)
Comparison of GPS-derived PW estimates and dryline location	PW estimates on moist side of dryline an average of 7.5 mm higher than on dry side (10 Jul 04)	PW improved estimation of dryline location (Businger et al., 1996)

Figures

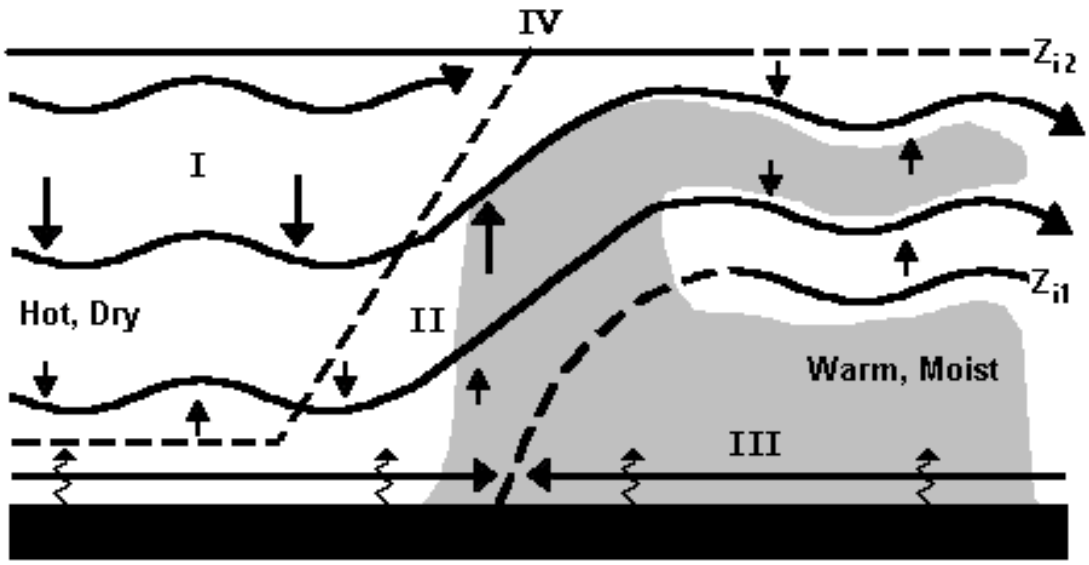

Figure 1.1. The conceptual model of a typical Great Plains dryline offered by Ziegler and Hane (1993). This model involves four distinct air masses (I to IV), the vertical/horizontal motion (arrows), air flow (streamlines), moisture discontinuities (dashed lines) and inversions (solid lines). The stable air above the inversion (IV) is from the same source as the dry air west of the dryline (I). The gray shaded area east of the dryline (III) indicates high moisture content, and along with moist air east of the boundary at the surface, there is also an elevated moist layer extending further east downwind of the dryline. The intersection of mixing zone (II) with the surface is considered to be the surface dryline boundary, and has a width of approximately 10 km. The depth of the moist boundary layer varies with proximity to the dryline boundary (after Ziegler and Hane, 1993).

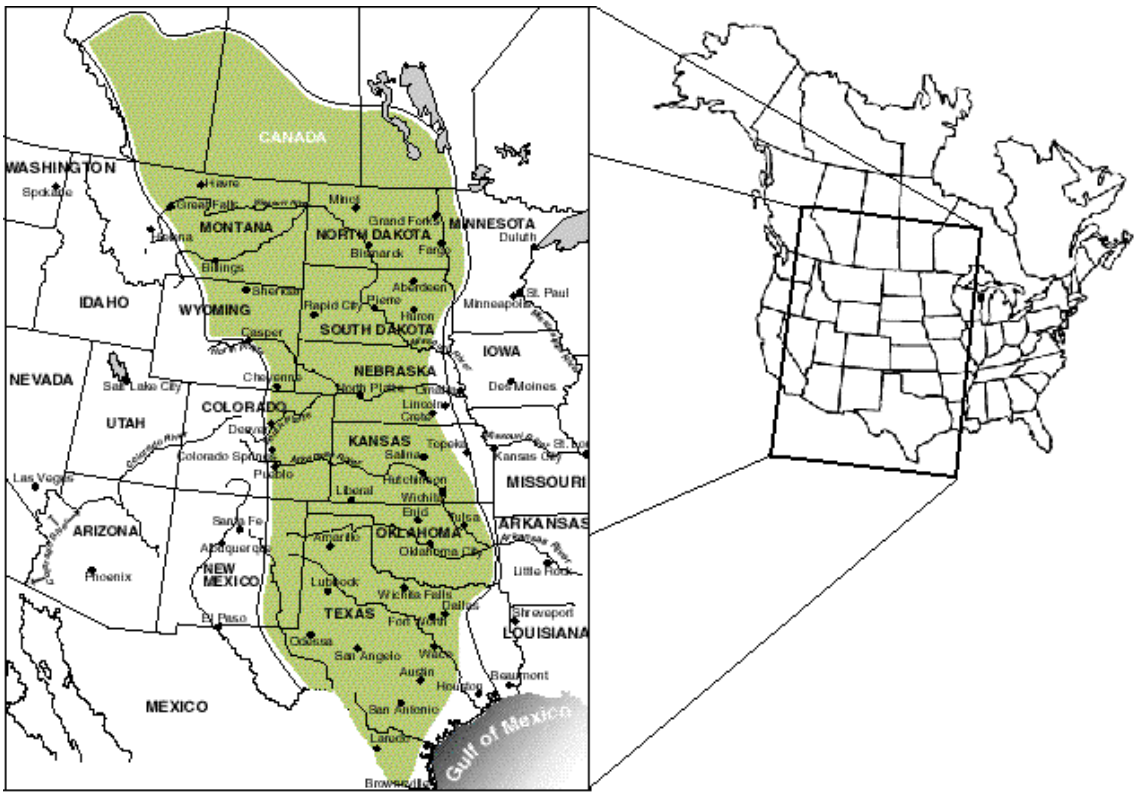

Figure 1.2. A map of the Great Plains (or High Plains) in the lee of the Rocky Mountains, extending from central Alberta south to Texas and Oklahoma (from Birdsall and Florin, 1999)

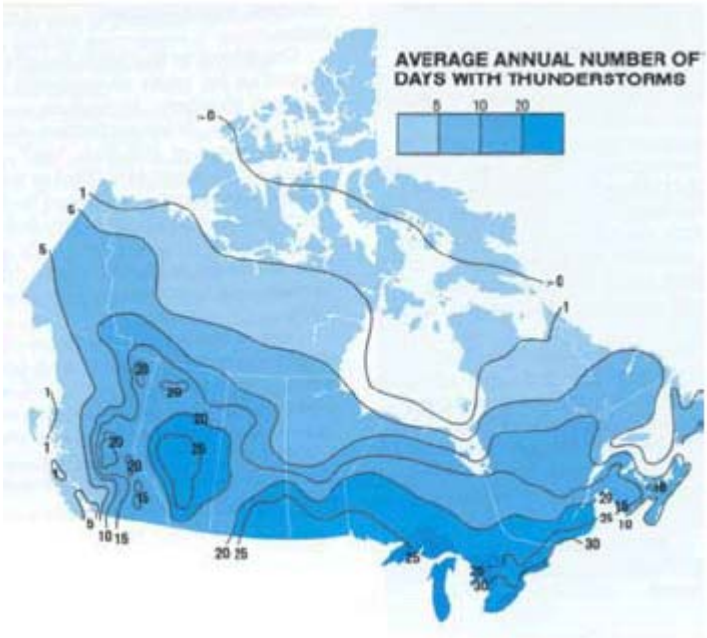

Figure 1.3. The average annual number of days with thunderstorms in Canada. Peaks in thunderstorm activity are observed in southern Ontario and interior Alberta (from Phillips, 1990).

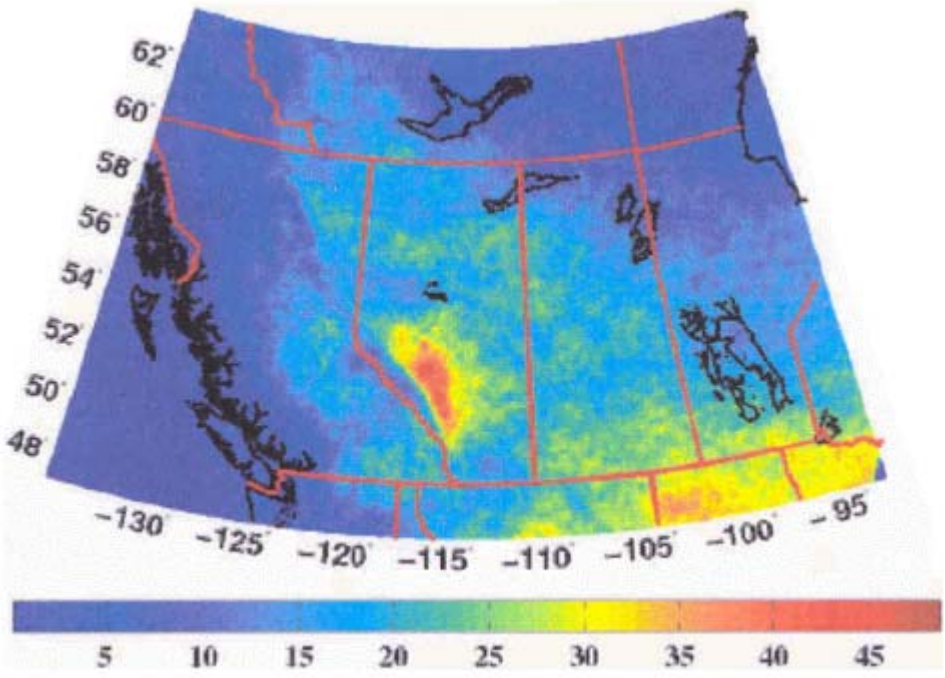

Figure 1.4. The annual mean number of days with lightning (per 400 km^2 grid cell) in Western Canada. Similar to Figure 1.3, the peak lightning activity is observed over the foothills in the lee of the Rocky Mountains and southern Ontario (not shown) (from Burrows et al., 2002).

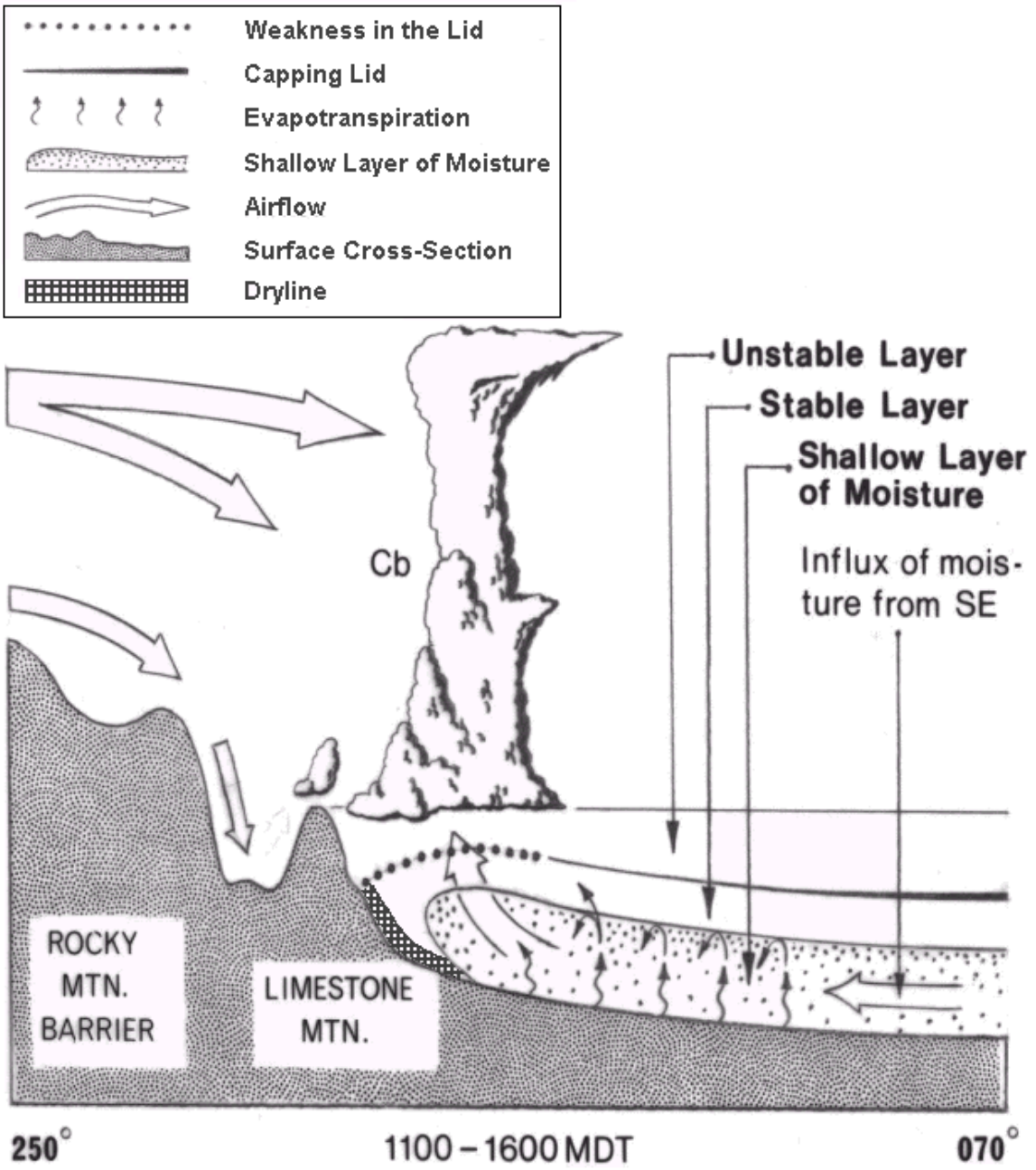

Figure 1.5. The conceptual model of Alberta thunderstorm development along the foothills between 1100-1600 MDT (-0600 UTC). Facing the foothills (from southwest to northeast) the boundary layer convergence at the surface east of Limestone mountain results in the formation of the capping lid and dryline (the intersection of the capping lid with the surface, the estimated location of the dryline is labeled). Cumulonimbus (Cb) clouds can develop along the foothills in such a situation (after Strong, 1986).

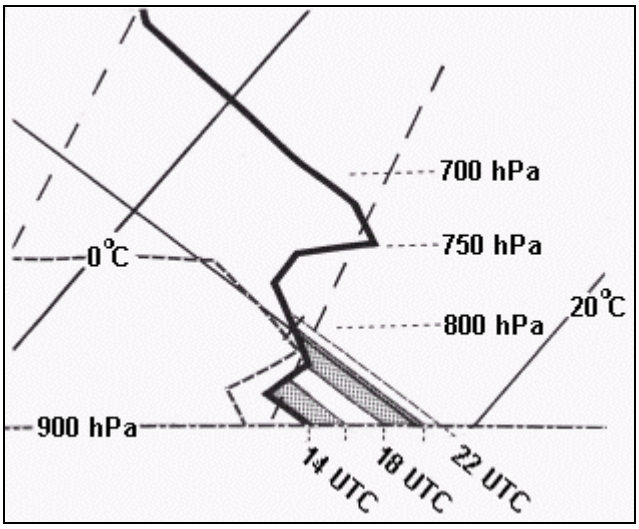

Figure 1.6. The evolution of boundary layer temperature beneath a capping inversion between 1400 UTC and 2200 UTC on a typical thunderstorm day in central Alberta. At the surface the air is warm and relatively moist, while above the stable capping inversion (displayed here at typical height of 750 hPa) the air is significantly drier. Daytime heating and mixing in the unstable boundary layer can lead to the erosion of the capping inversion and deep convection (from Strong, 1986).

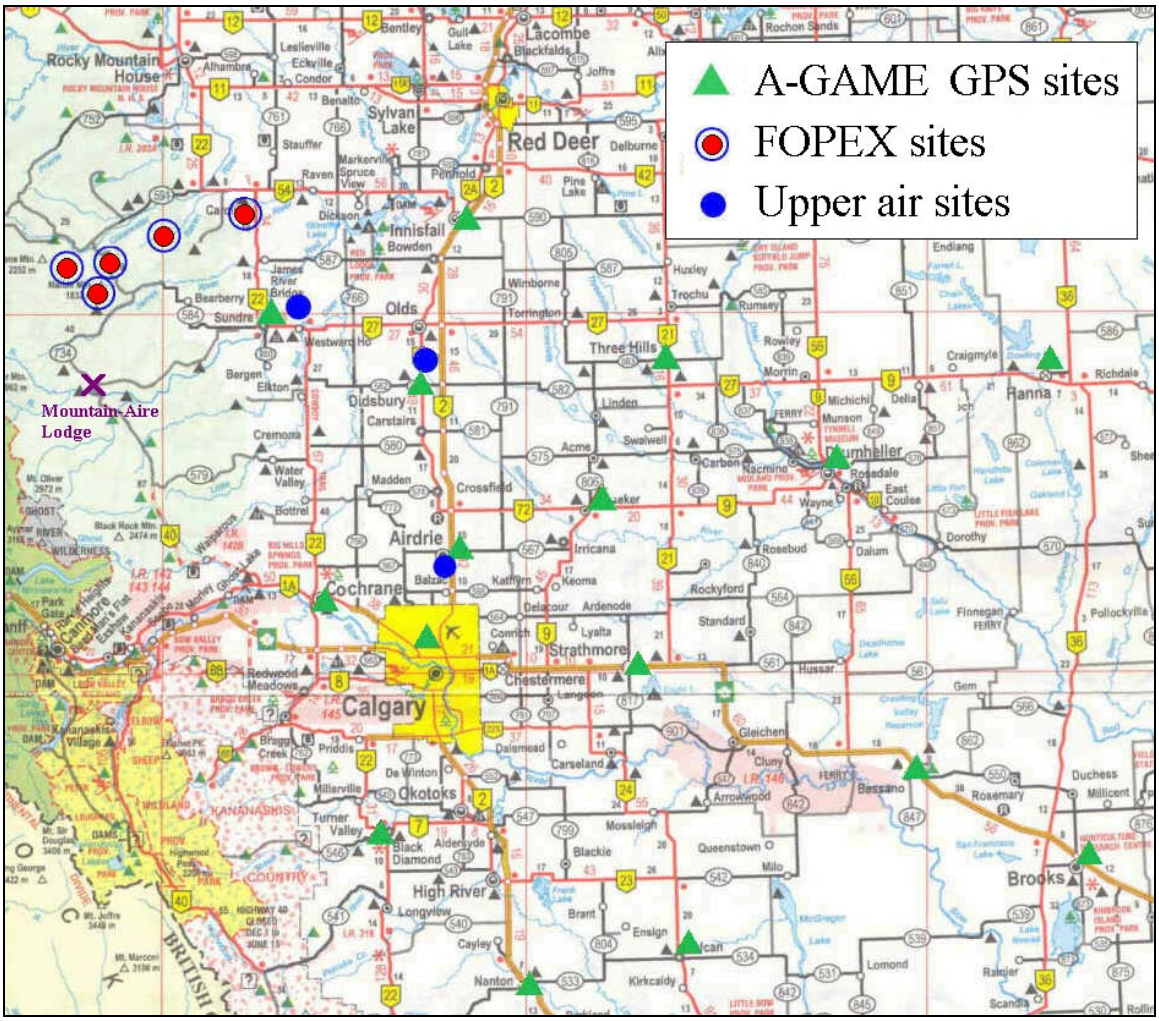

Figure 1.7. The A-GAME study area in south-central Alberta. Labeled are the 16 GPS-receivers of the Southern Alberta Network, upper air locations, and approximate locations of the FOPEX transect weather stations (note station AB5 is not labeled). Mountain-Aire Lodge, (along the Red Deer River) a standard checkpoint for the mobile surface transects, is also labeled (**X**).

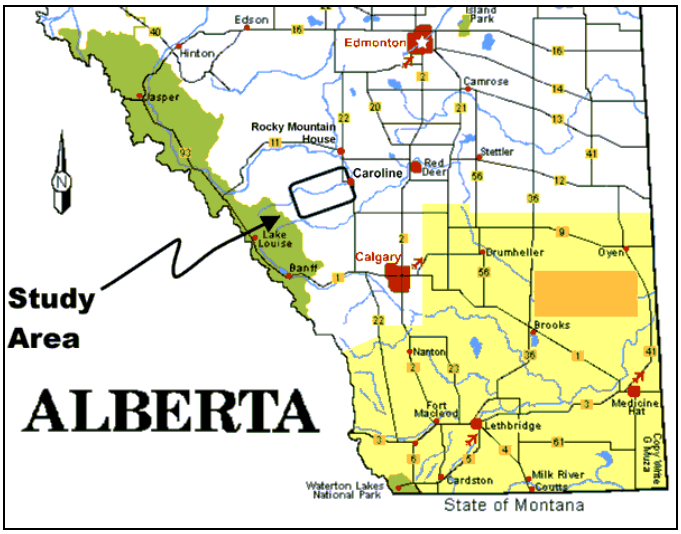

Figure 1.8. The Foothills Orographic Precipitation Experiment (FOPEX) study area in south central Alberta (with permission, from http://www.geo.ucalgary.ca/fopex/).

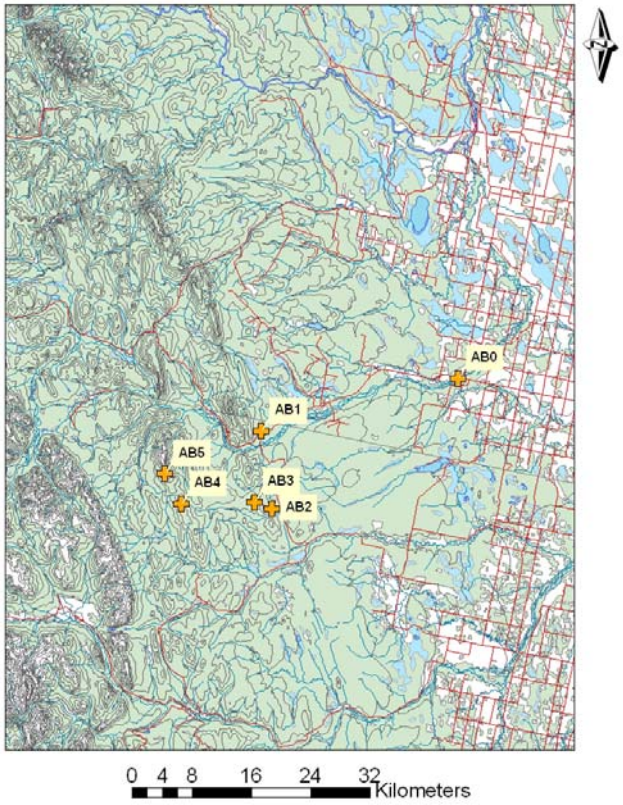

Figure 1.9. The locations of the FOPEX surface weather stations on a topographical map of south-central Alberta. Station AB0 is located at Caroline (labeled in Figure 1.7), while station AB5 is located on Limestone Mountain (with permission, from Mr. Craig Smith, Climate Research Branch of the Meteorological Service of Canada).

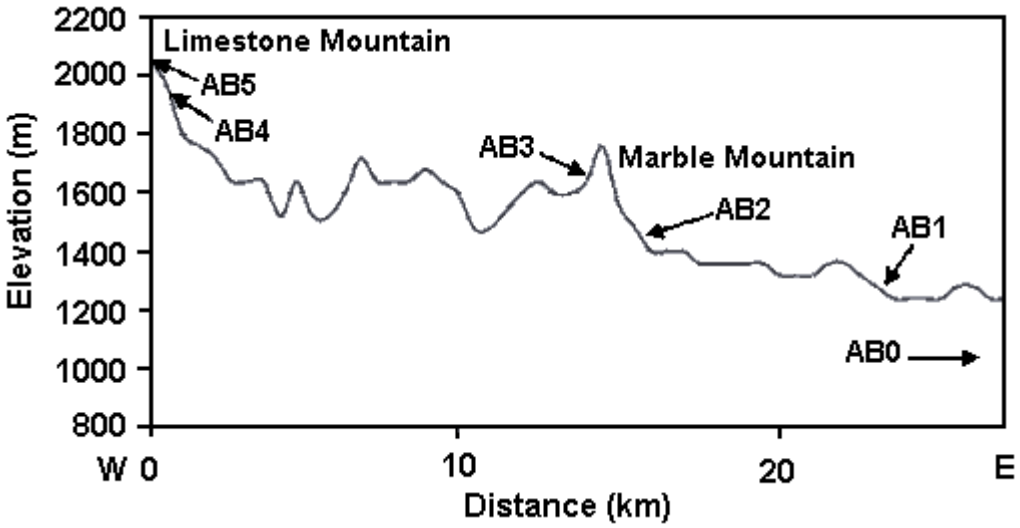

Figure 1.10. The elevation profile of the FOPEX transect in south-central Alberta (with permission, from http://www.geo.ucalgary.ca/fopex/). Limestone and Marble Mountain (foothills peaks) are labeled.

Figure 2.1. A temperature and relative humidity sensor mounted onto an economy-sized vehicle to perform mobile transects during the A-GAME field project in July 2003 (with a similar set-up for July 2004). The radiation shield containing the sensor was secured to a vertical length of PVC pipe above a rear window. For the July 2004 A-GAME field campaign, a pressure sensor was located on the back seat of the vehicle.

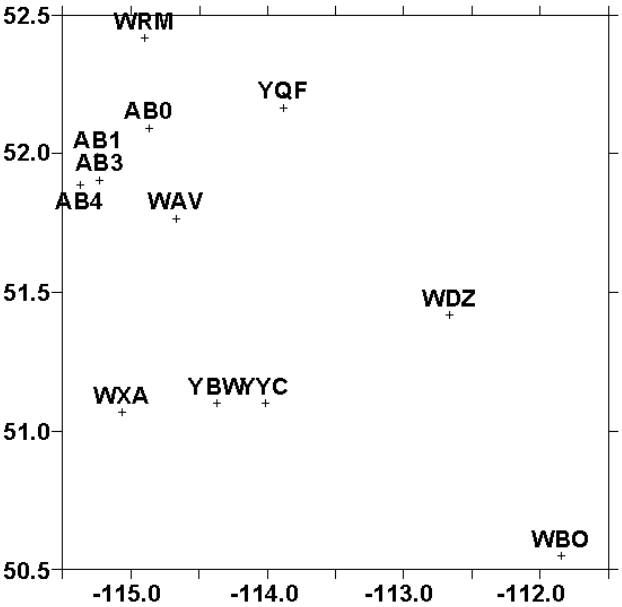

Figure 2.2. Labeled synoptic observation sites (both MSC and FOPEX weather stations) employed for synoptic mixing ratio and wind field analysis during A-GAME dryline events within the south-central Alberta study area. Complete site descriptions are provided in Table 2.1 (FOPEX) and Table 2.3 (MSC).

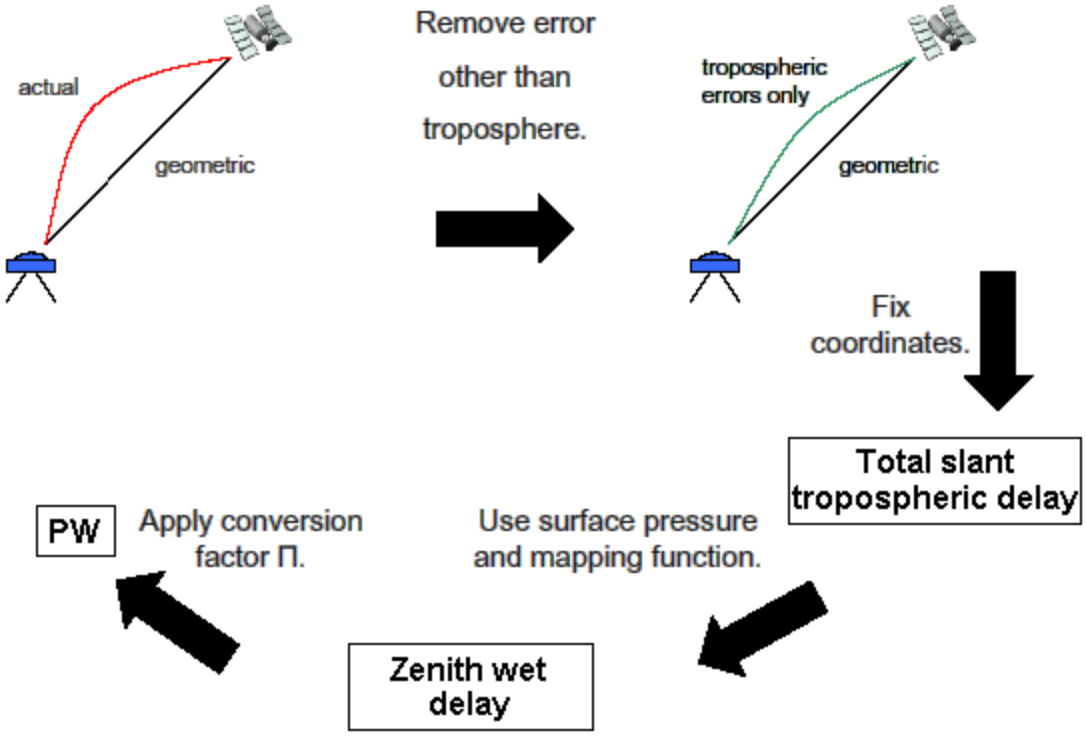

Figure 2.3. The process of retrieving an atmospheric moisture measurement (precipitable water, PW) by isolating errors in a GPS signal (from Hoyle, 2005).

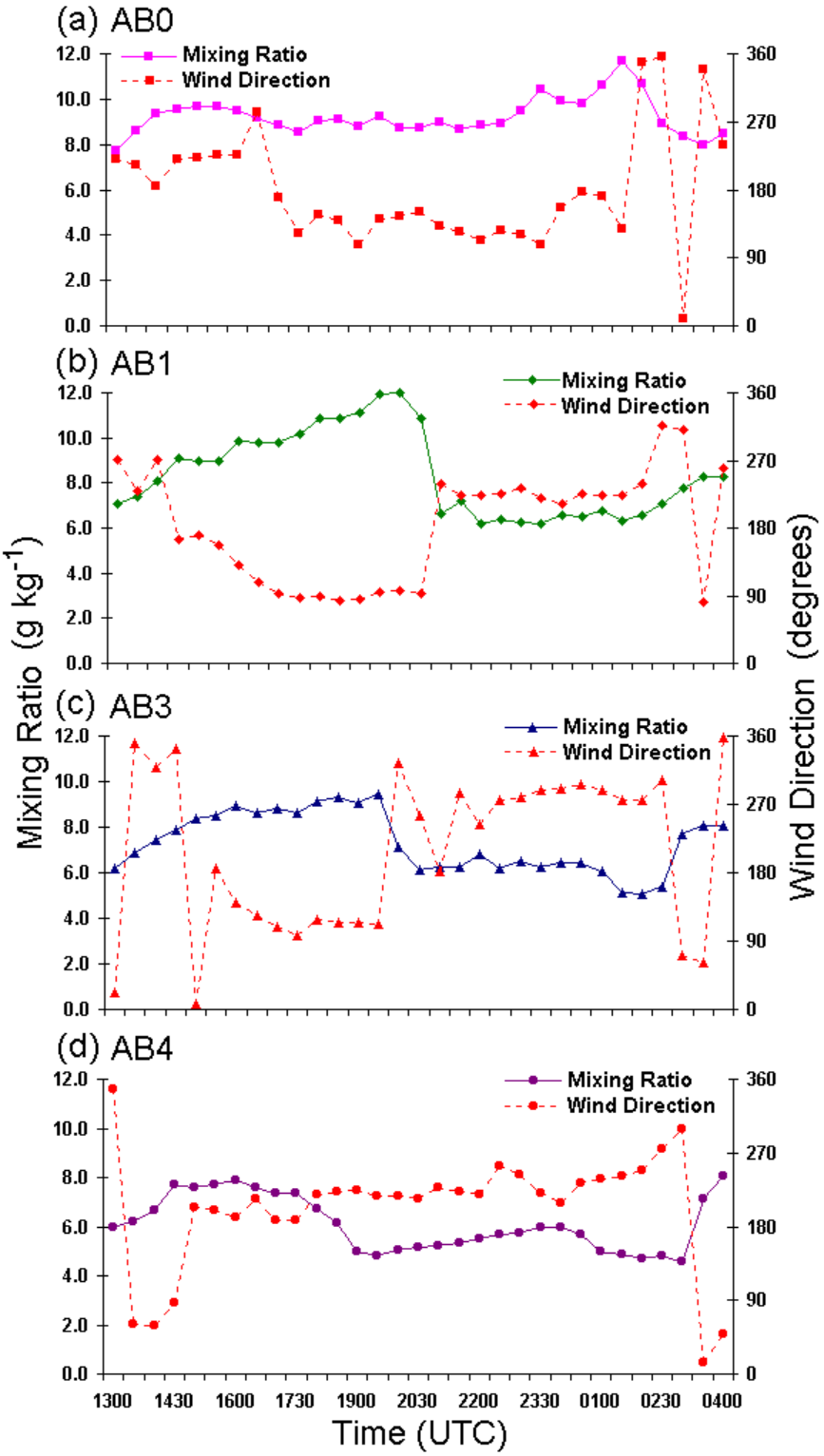

Figure 3.1. A typical FOPEX dryline signature, observed 25 July 2004. The dryline boundary formed between AB3 and AB4 by 1800 UTC and by 2100 UTC, AB1, AB3, and AB4 were on the west side of the dryline boundary while AB0 was east of the dryline. Beginning at 0230 UTC, wind shifts to an easterly component correspond with rises in mixing ratio in the 'dry air' signaled the dryline retreat west of the FOPEX transect by 0330 UTC.

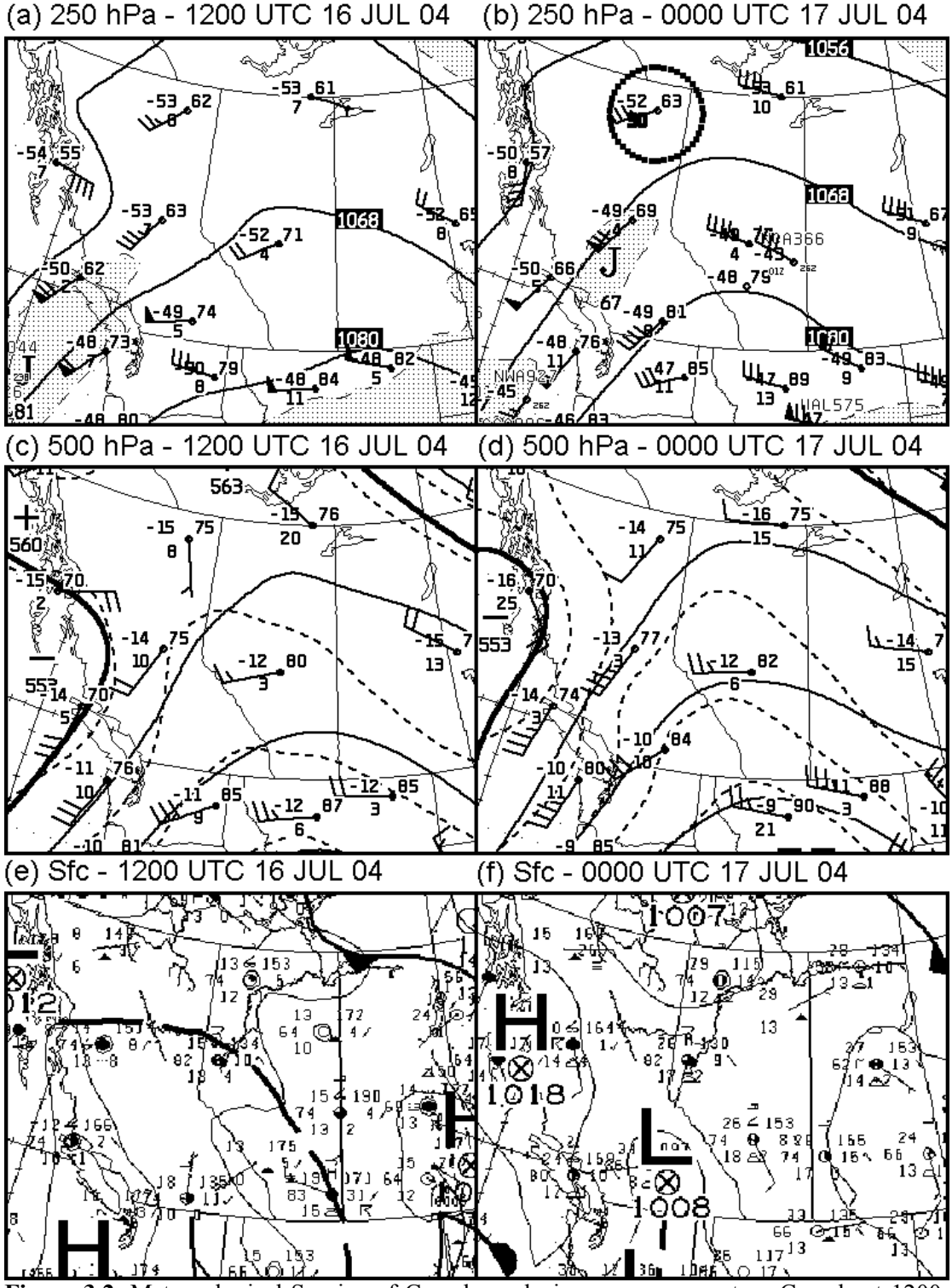

Figure 3.2. Meteorological Service of Canada analysis maps over western Canada at 1200 and 0000 UTC on 16-17 July 2004 at 250 hPa, 500 hPa, and at the surface.

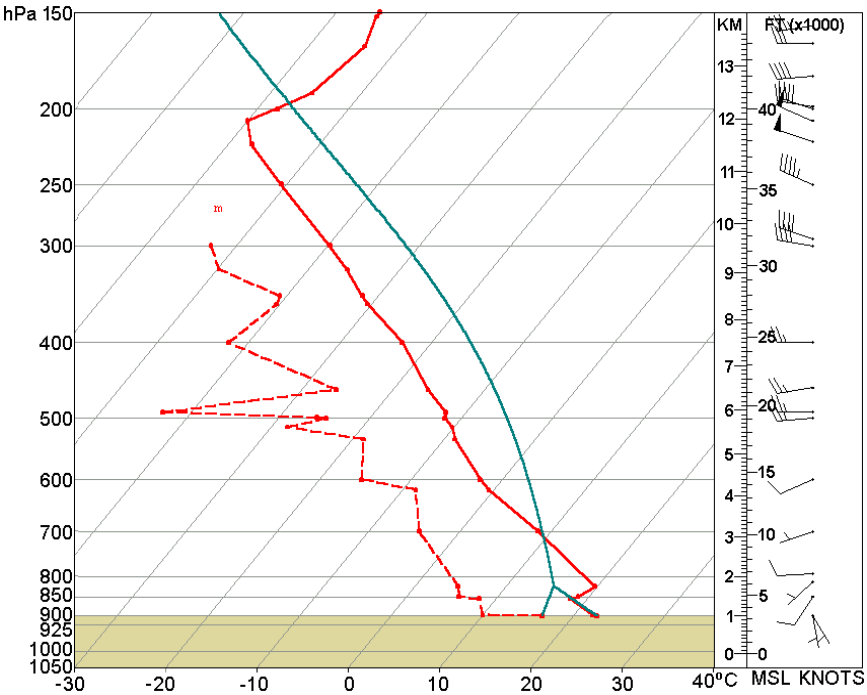

Figure 3.3. The Skew-T Log P diagram of the 1800 UTC Olds-Didsbury Airport sounding on 16 July 2004. The temperature (solid red line), dewpoint (dotted red line), and wind profiles (in knots) are displayed along with the pseudoadiabat (solid blue line) based on temperature and dewpoint observed at the surface.

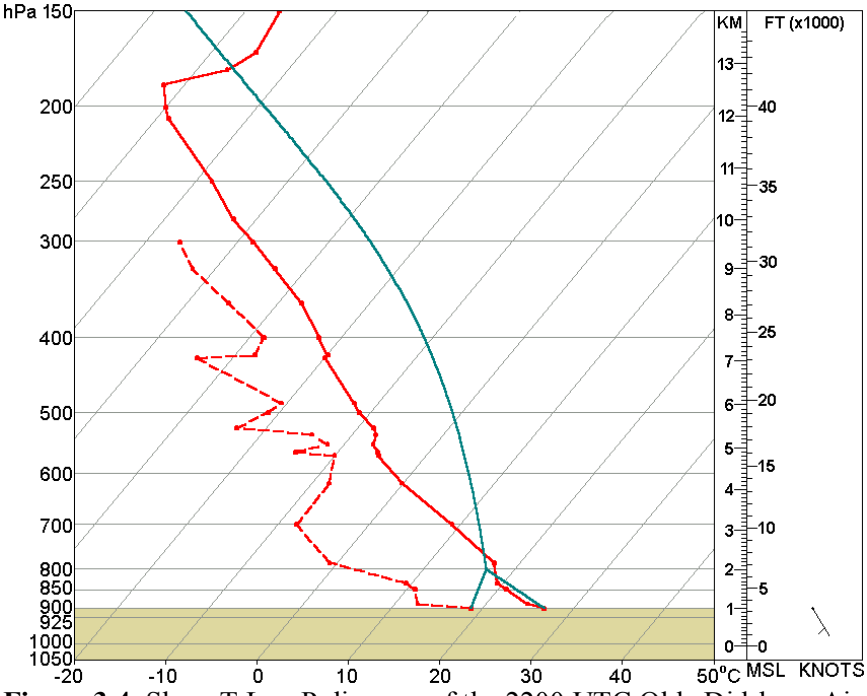

Figure 3.4. Skew-T Log P diagram of the 2200 UTC Olds-Didsbury Airport sounding on 16 July 2004. The temperature (solid red line), dewpoint (dotted red line), and wind profiles (in knots) are displayed along with the pseudoadiabat (solid blue line) based on temperature and dewpoint observed at the surface). No wind data was recorded for this sounding.

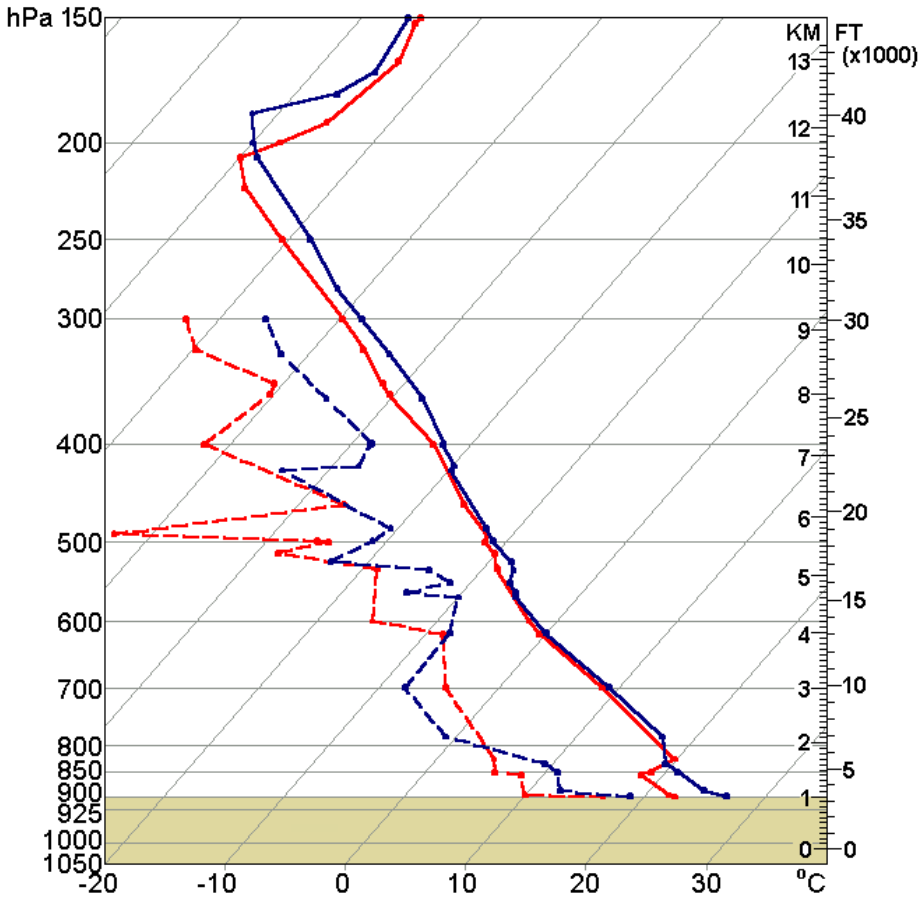

Figure 3.5. A comparison of the 1800 UTC (lighter) and 2200 UTC (darker) Olds-Didsbury Airport soundings on 16 July 2004. The temperature (solid line) and dewpoint (dotted line) are displayed.

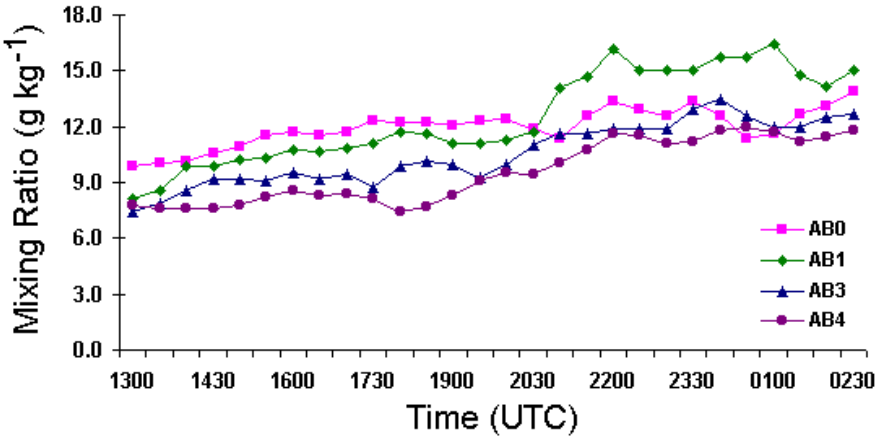

Figure 3.6. The surface mixing ratio values (g kg^{-1}) measured by FOPEX stations on 16-17 July 2004 from 1300 UTC to 0230 UTC.

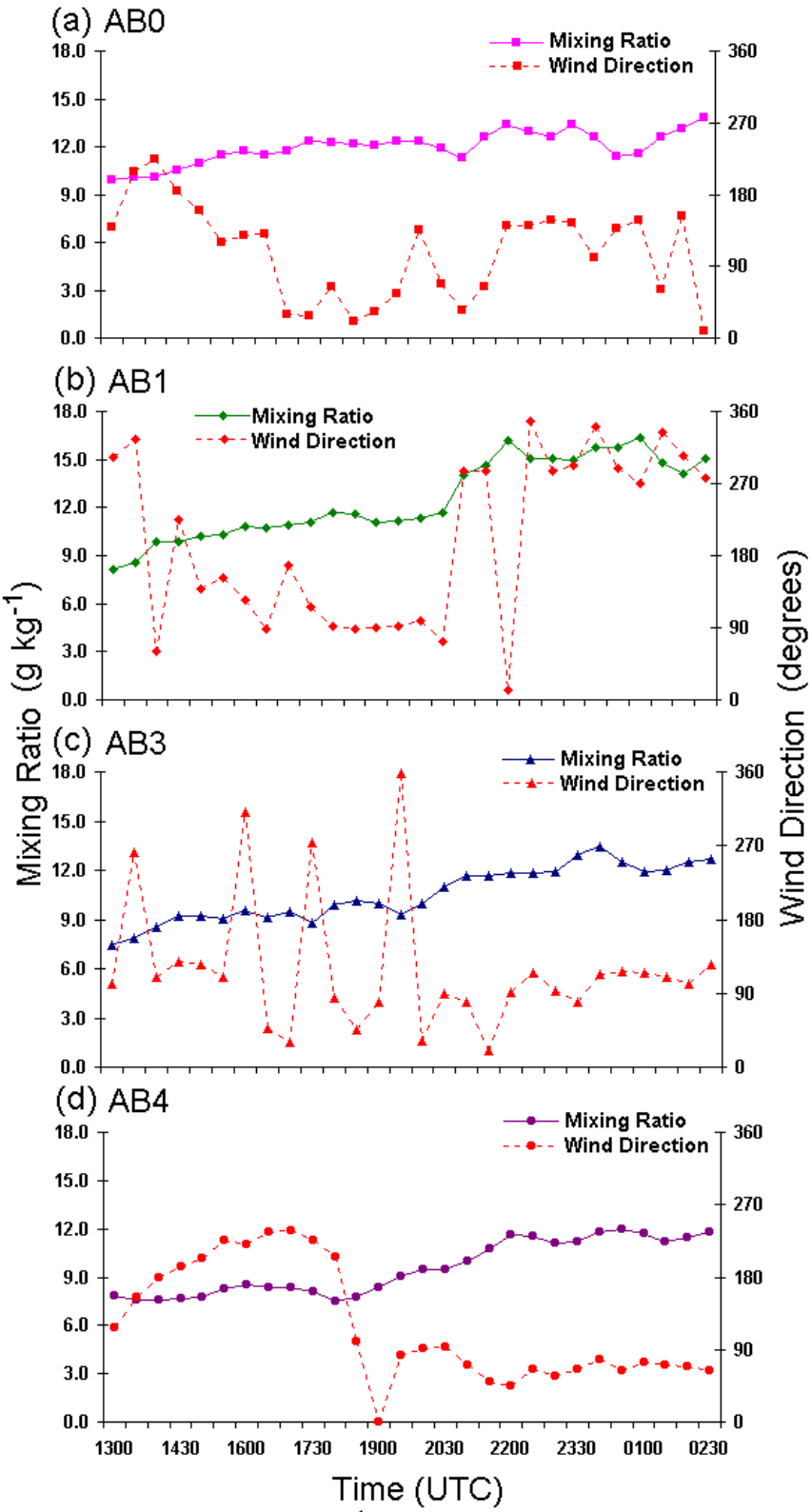

Figure 3.7. Mixing ratio (g kg^{-1}) and wind direction (degrees) measurements for each station in the FOPEX transect on 16-17 July 2004 from 1300 UTC to 0230 UTC. The dryline was not detected on this day in the FOPEX transect.

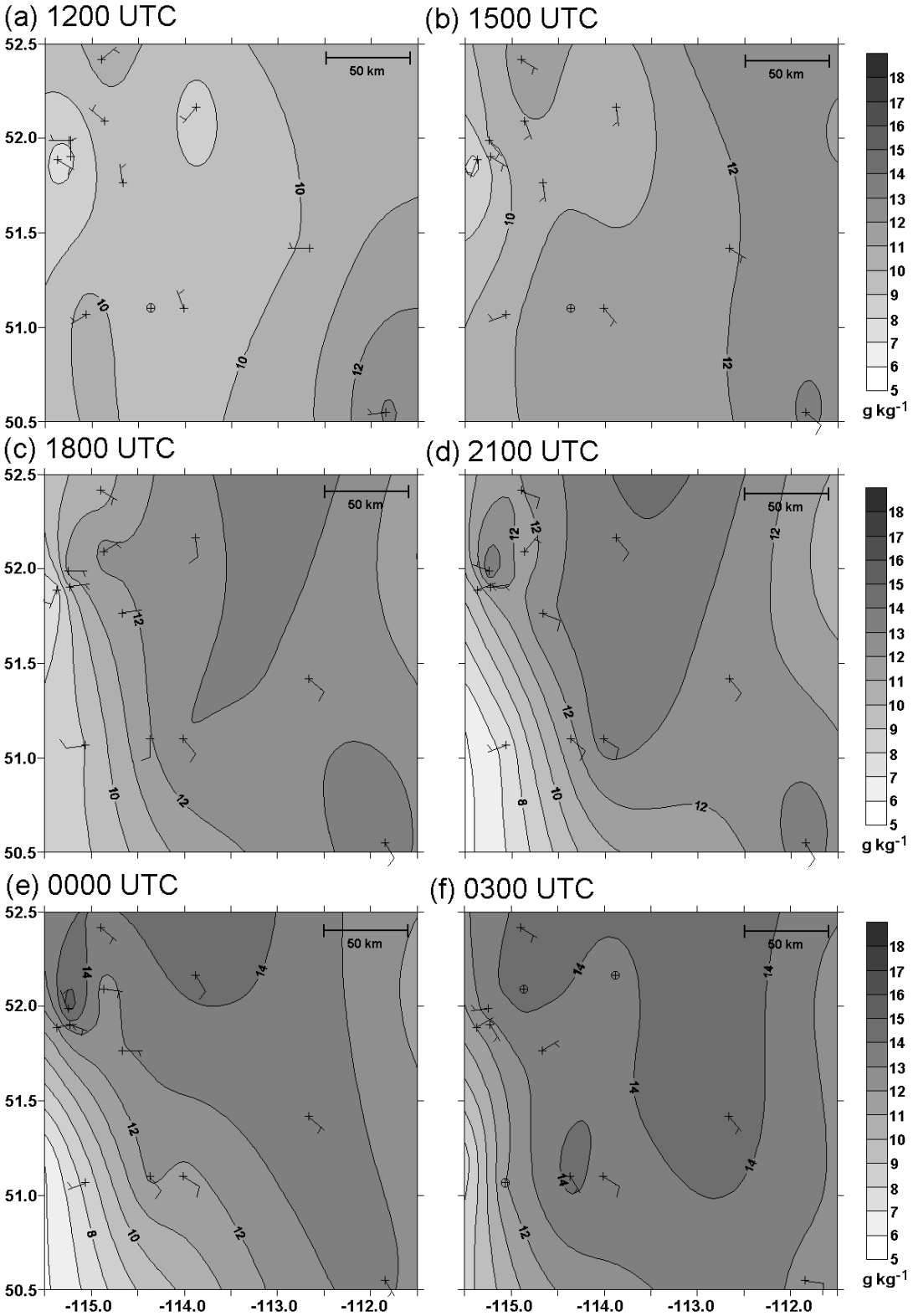

Figure 3.8. Contoured synoptic mixing ratio data (g kg^{-1}) and wind data (kn) from MSC weather stations and the FOPEX transect in south-central Alberta every 3 hrs from 1200 UTC to 0300 UTC on 16-17 July 2004. (For site labels, see Figure 2.2).

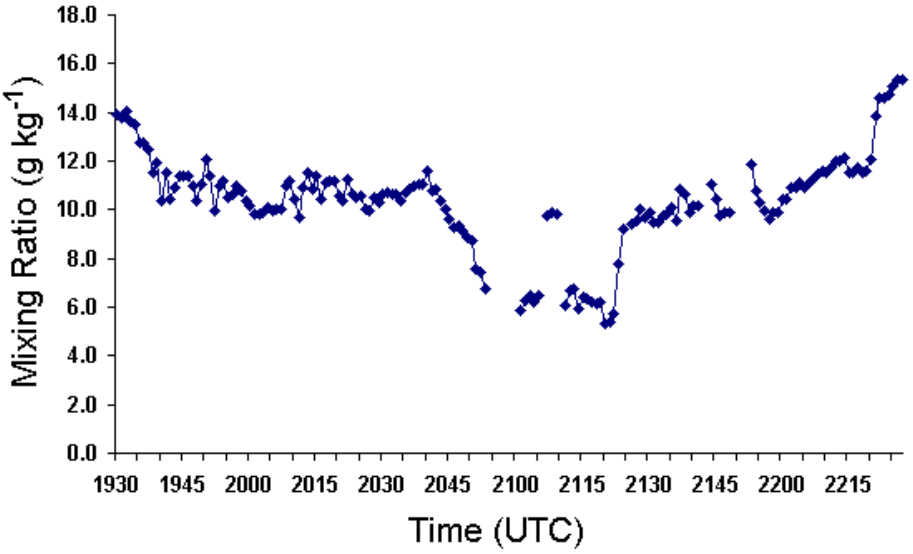

Figure 3.9. The surface mixing ratio trend recorded by a mobile transect on 16 July 2004 in south-central Alberta. Four traverses of the dryline boundary were completed, at 2050, 2106, 2110, and 2122 UTC. (Spaces in the data represent time when the vehicle was stationary, which lead to insufficient ventilation for the temperature and relative humidity sensor).

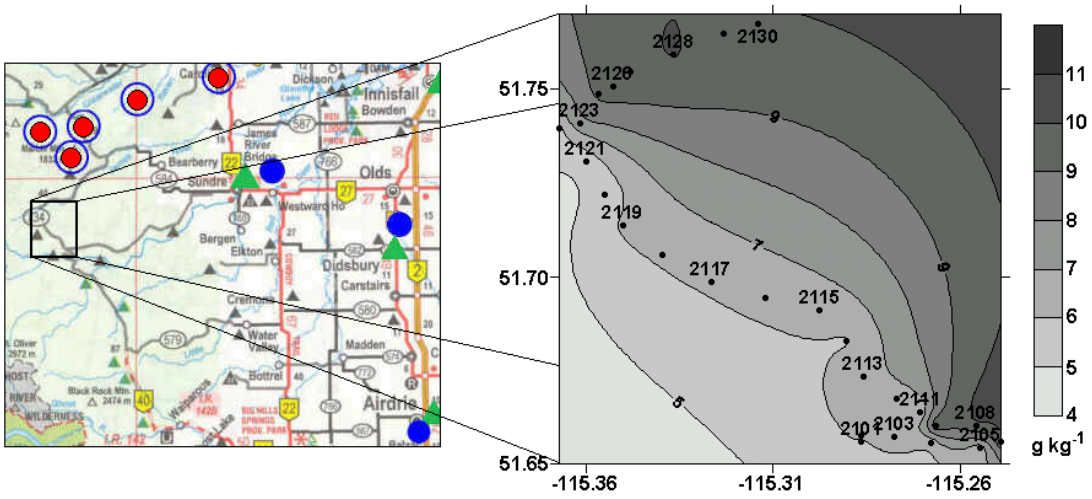

Figure 3.10. Mobile transect location relative to the FOPEX transect (left, as labeled in Figure 1.7) and the contoured plot of the mixing ratio field (right) measured by the mobile transect vehicle south of the FOPEX transect between 2101-2130 UTC on 16 July 2004. Each point (every other is labeled with a time stamp) represents a 1-minute average measurement of mixing ratio. The contour map displays 3 (of a total of 4) traverses of the dryline boundary on this day.

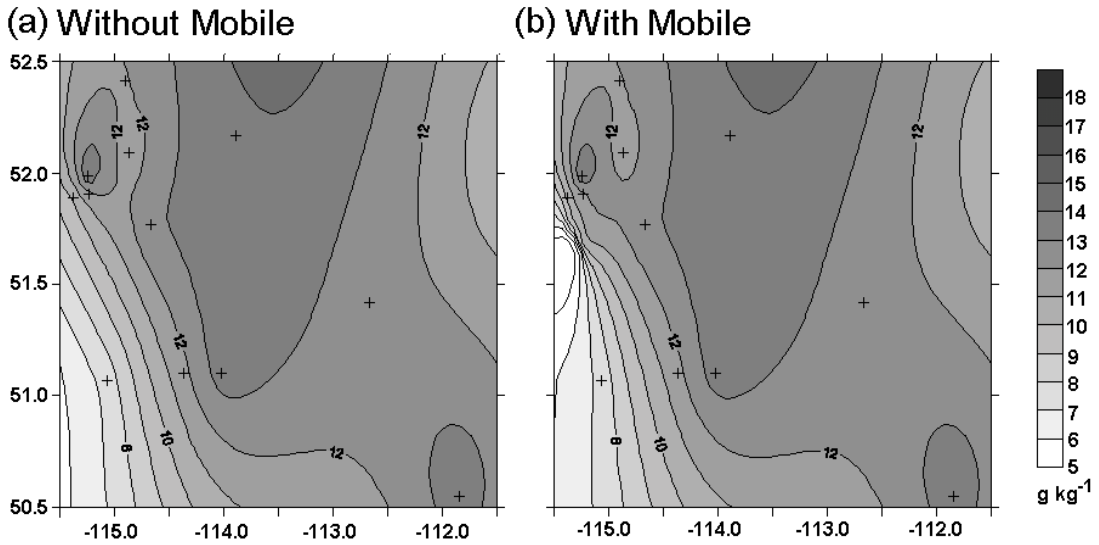

Figure 3.11. A comparison of the surface mixing ratio (g kg^{-1}) distribution at 2100 UTC 16 July 2004 in south-central Alberta (a) without mobile transect data and (b) with mobile transect mixing ratio data included. (For site labels, see Figure 2.2).

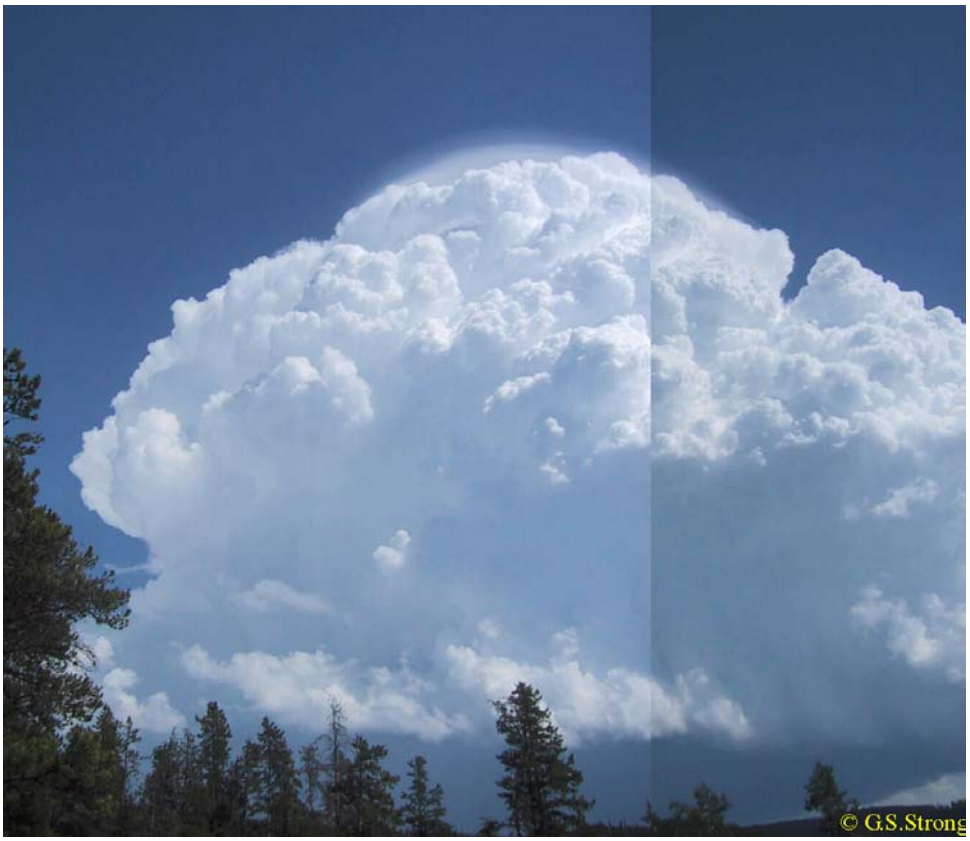

Figure 3.12. A cumulonimbus cloud observed at 2152 UTC on 16 July 2004. The photo was taken from the mobile transect vehicle facing west, and is indicated with a yellow arrow on the 2210 UTC visible satellite image (Figure 3.13) and radar reflectivity image (Figure 3.14). Photo courtesy Geoff Strong.

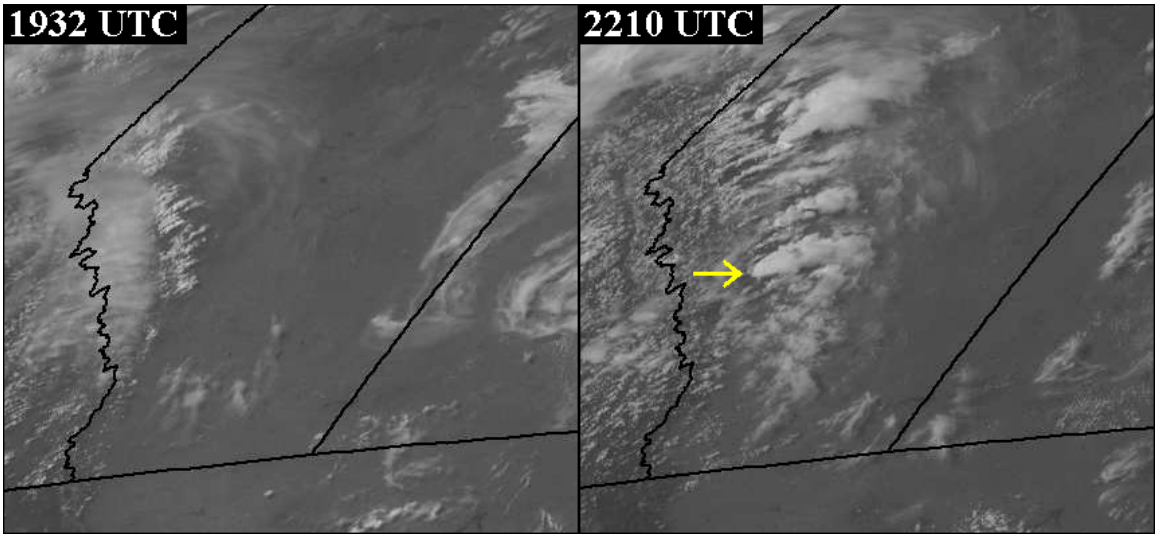

Figure 3.13. Visible satellite image from GOES at 1932 and 2210 UTC over Alberta on 16 July 2004. Storm cells are visible developing along the Alberta foothills by 2210 UTC, and the yellow arrow indicates the thunderstorm photographed during the mobile transect (Figure 3.12).

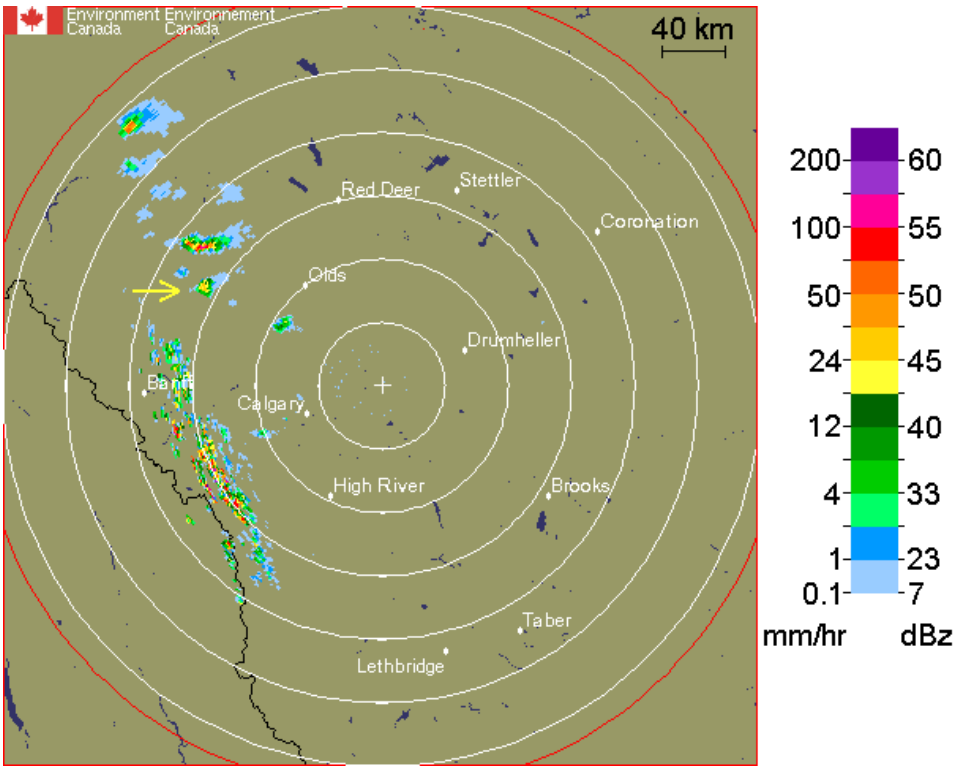

Figure 3.14. The 1.5 km CAPPI radar image from Strathmore radar at 2130 UTC on 16 July 2004. The mobile transect completed on this day was around the storms cells developing along the foothills west of Olds. The arrow indicates the cell photographed in Figure 3.12. This image is courtesy MSC.

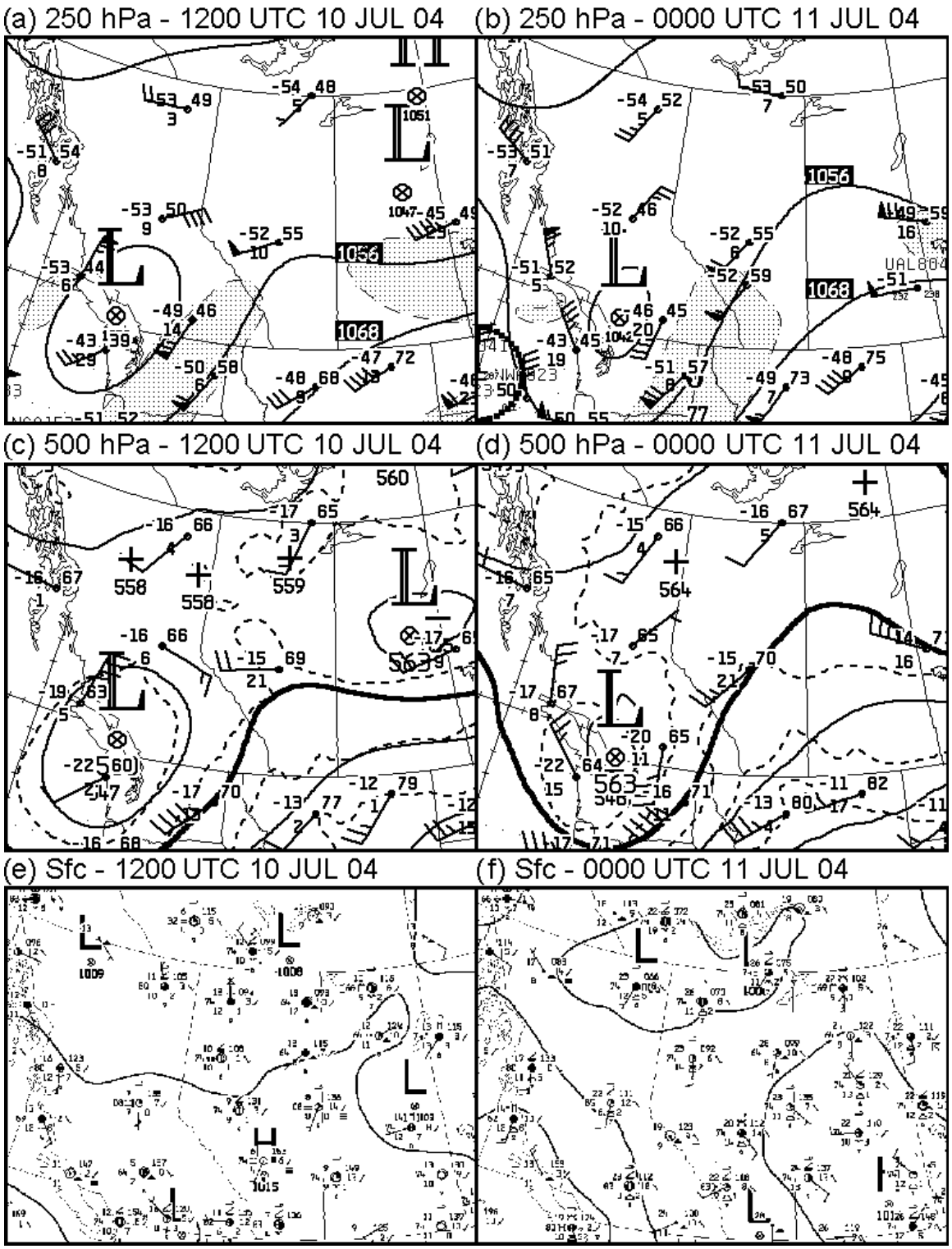

Figure 3.15. The Meteorological Service of Canada synoptic analysis maps over western Canada at 1200 UTC and 0000 UTC on 10-11 July 2004 at 250 hPa, 500 hPa, and at the surface.

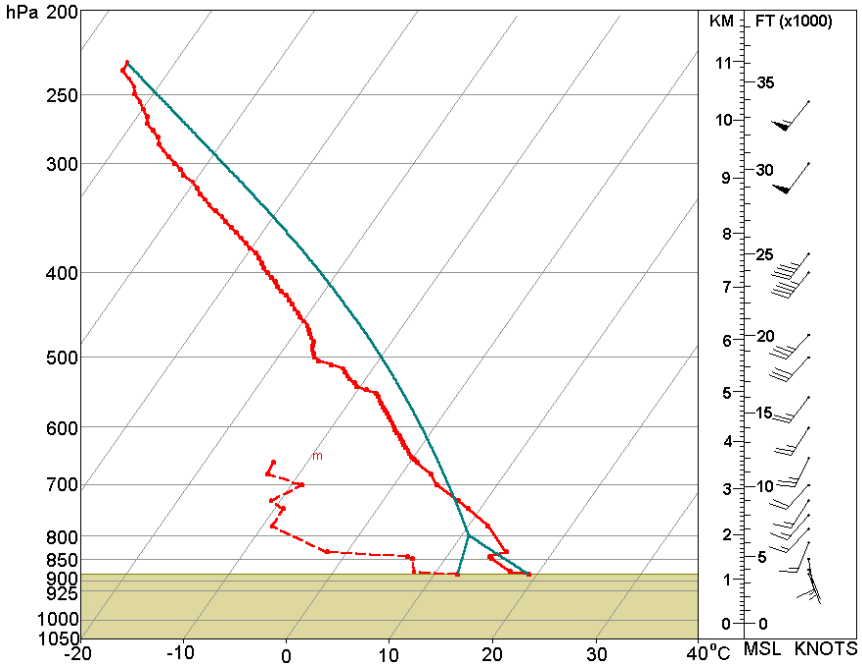

Figure 3.16. The Skew-T Log P diagram of the 1900 UTC Airdrie sounding on 10 July 2004. The temperature (solid red line), dewpoint (dotted red line), and wind profiles (in knots) are displayed along with the pseudoadiabat (solid blue line) based on temperature and dewpoint observed at the surface).

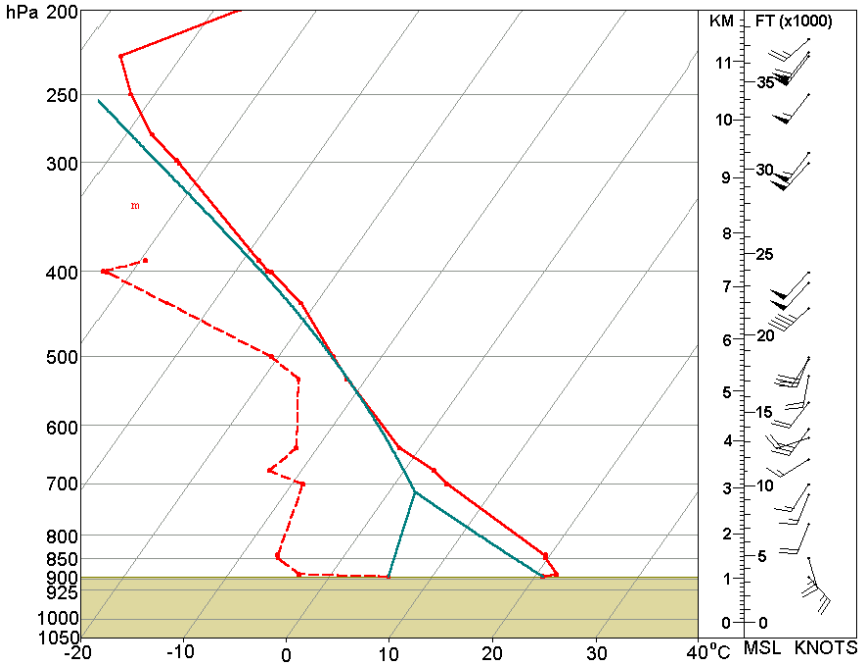

Figure 3.17. The 2400 UTC sounding data of a radiosonde launched from Olds-Didsbury Airport, Alberta on 10 July 2004. The temperature (solid red line), dewpoint (dotted red line), and wind profiles (in knots) are displayed along with the pseudoadiabat (solid blue line) based on temperature and dewpoint observed at the surface.

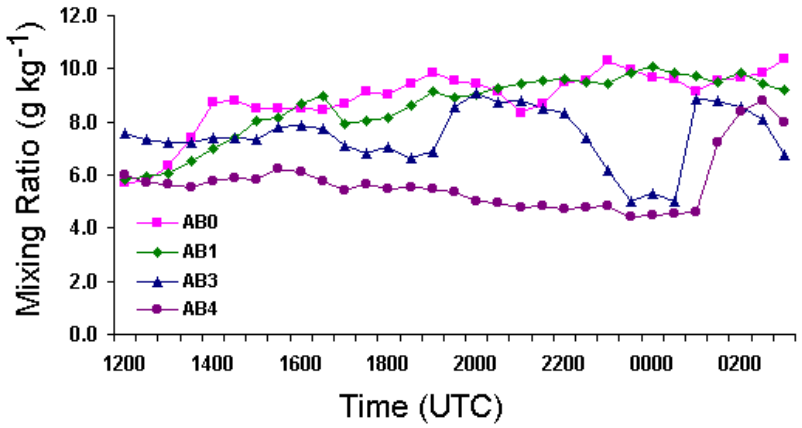

Figure 3.18. The surface mixing ratio values (g kg^{-1}) measured by the four FOPEX stations on 10-11 July 2004 from 1200 - 0300 UTC.

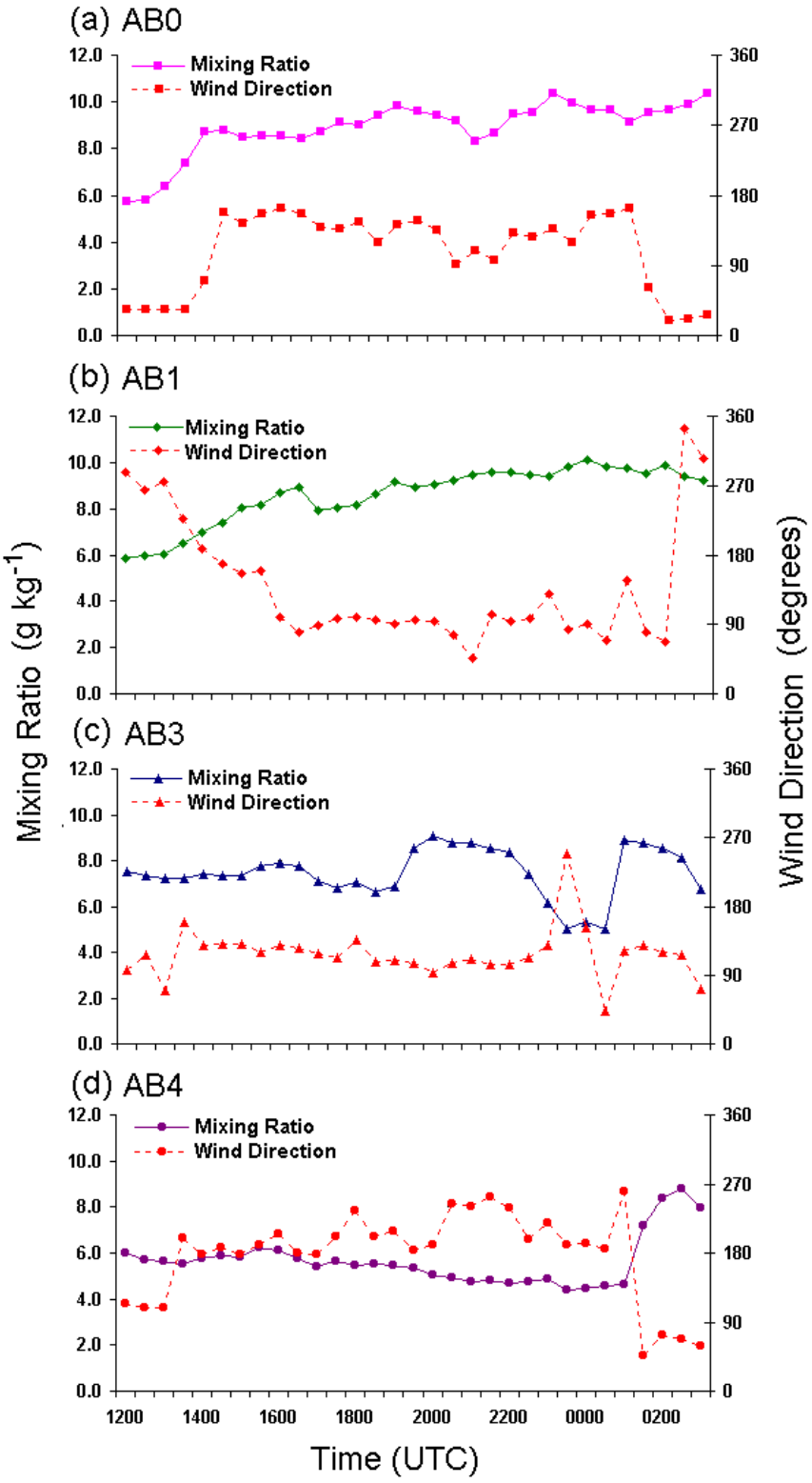

Figure 3.19. Mixing ratio (g kg^{-1}) and wind direction (degrees) measurements for each station in the FOPEX transect on 10-11 July 2004 from 1200 UTC to 0300 UTC.

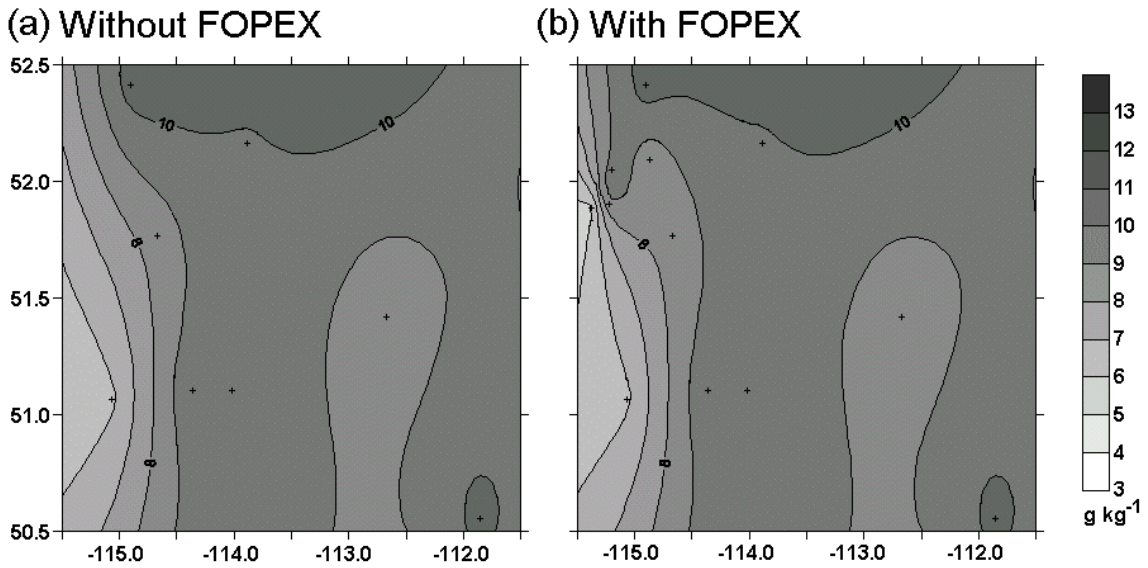

Figure 3.20. A comparison of the surface mixing ratio (g kg^{-1}) distribution at 2100 UTC 10 July 2004 in south-central Alberta (a) without FOPEX and (b) with FOPEX transect mixing ratio data included. (For site labels, see Figure 2.2).

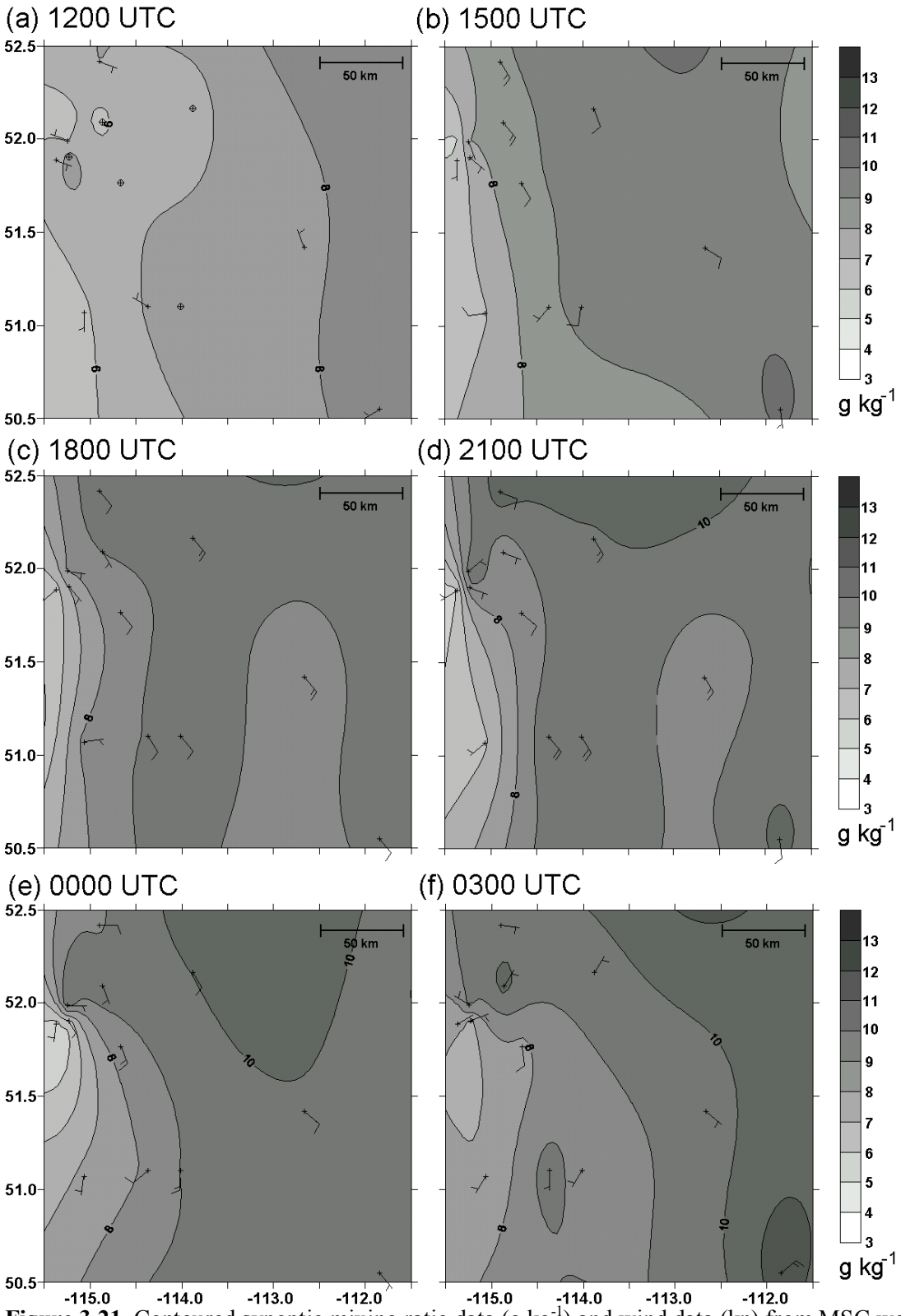

Figure 3.21. Contoured synoptic mixing ratio data (g kg^{-1}) and wind data (kn) from MSC weather stations and the FOPEX transect in south-central Alberta every 3 hrs from 1200 UTC to 0300 UTC on 10-11 July 2004. (For site labels, see Figure 2.2).

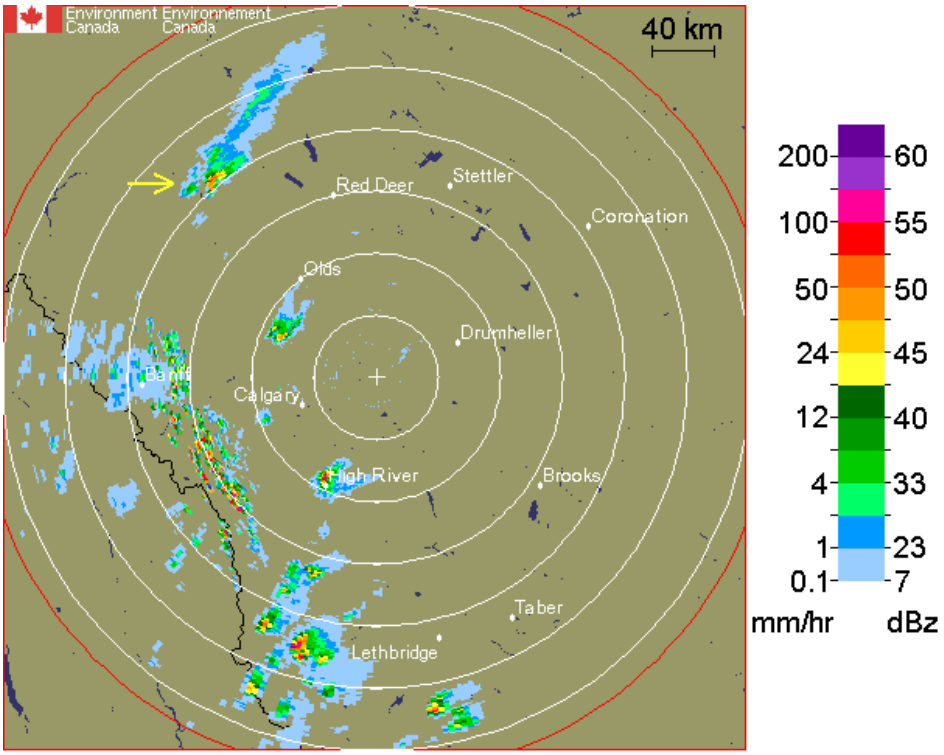

Figure 3.22. The 1.5 km CAPPI radar image from Strathmore radar at 2310 UTC on 10 July 2004. The two northernmost storms on the image are within the study area (active weather was observed in southern and central Alberta as well on this day). The yellow arrow indicates the strongest cell observed on this day in south-central Alberta that initiated near Rocky Mountain House. This image is courtesy MSC.

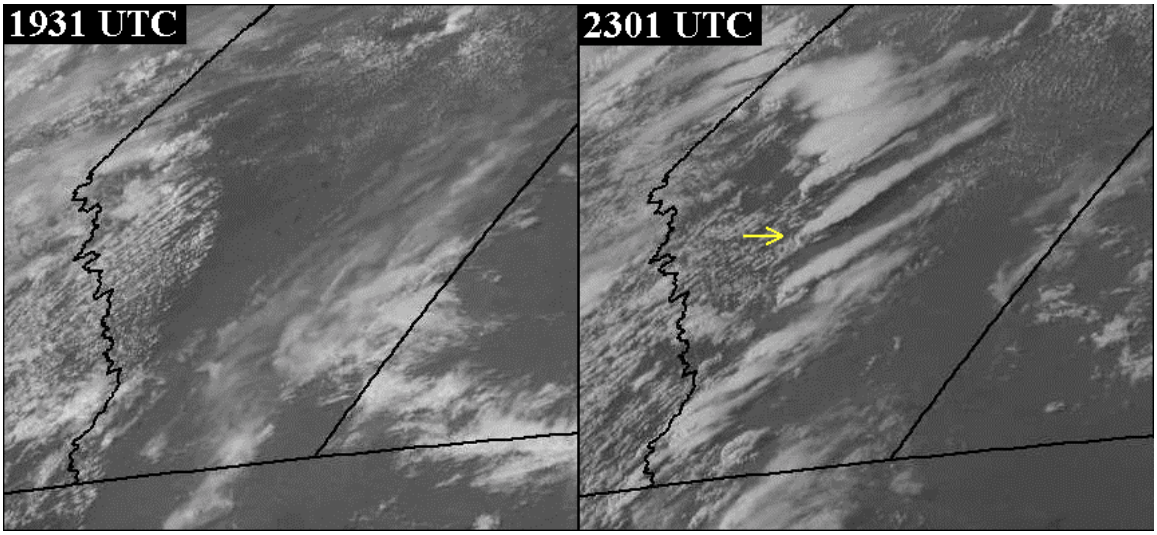

Figure 3.23. The GOES visible satellite images of Alberta at 1931 UTC and 2301 UTC on 10 July 2004. The pre-thunderstorm image at 1931 UTC shows cloud cover over the Rocky Mountains and foothills of Alberta, with clear skies over the interior of south-central Alberta. At 2301 UTC, storms are observed from southern to central Alberta, with the anvils of the storms blowing off to the northeast. The yellow arrow indicates the strongest cell observed on this day in south-central Alberta that initiated near Rocky Mountain House.

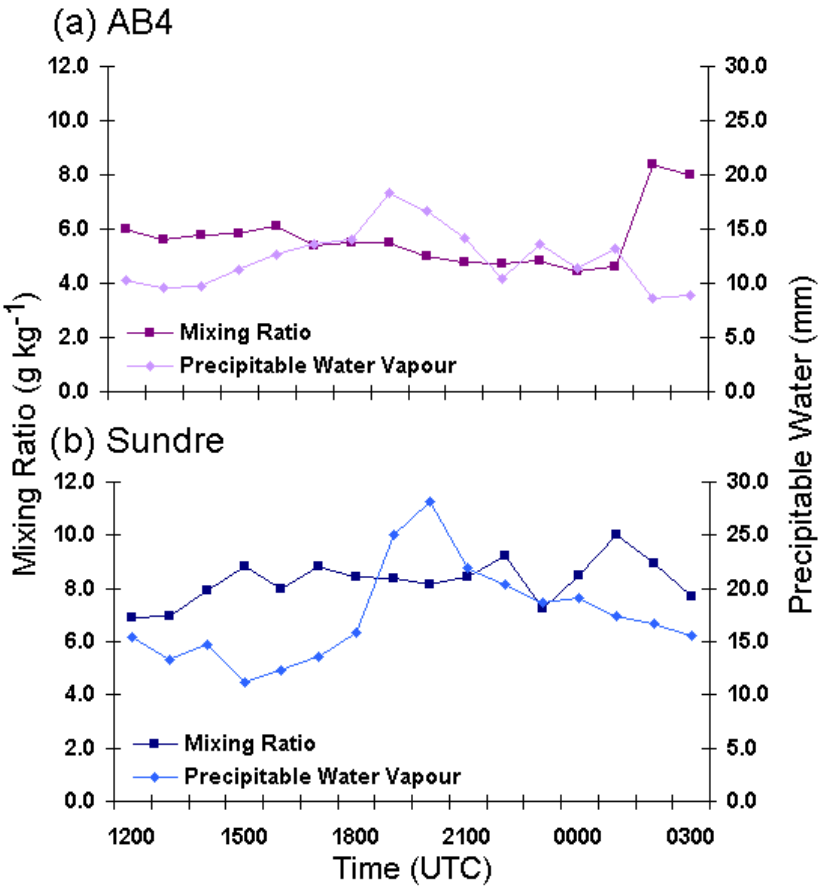

Figure 3.24. Mixing ratio and precipitable water (PW) trends from 1200 to 0300 UTC on 10-11 July 2004 at a) AB4 of the FOPEX transect and b) Sundre.

Bibliography

Aguado, E. and J.E. Burt, 2004: *Understanding Weather & Climate*, 3rd ed. Pearson Education Inc., 560 pp.

Atkins, N.T., R.M. Wakimoto, and C.L. Ziegler, 1998: Observations of the finescale structure of a dryline during VORTEX 95. *Mon. Wea. Rev.*, **126**, 525-550.

Bengtsson, L., G. Robinson, R. Anthes, K. Aonashi, A. Dodson, G. Elgered, G. Gendt, R. Gurney, M. Jietai, C. Mitchell, M. Mlaki, A. Rhodin, P. Silvestrin, R. Ware, R. Watston, and W. Wergen, 2003: The use of GPS measurements for water vapor determination. *Bull. Amer. Meteor. Soc.*, **84**, 1249-1258.

Birdsall, S., and J. Florin, 1999: *Regional Landscapes of the United States and Canada* 4th ed., John Wily & Sons Inc., 450 pp.

Brimelow, J.C., G.W. Reuter, and E.R. Poolman, 2002: Modeling maximum hail size in Alberta thunderstorms. *Wea. Forecasting*, **17**, 1048-1062.

Burrows, W.R., P. King, J.L. Lewis, B. Kochtubajda, B. Snyder, and V. Turcotte, 2002: Lightning occurrence patterns over Canada and adjacent United States from Lighting Detection Network observations. *Atmos.-Ocean*, **40**, 59-81.

Businger, S., S.R. Chiswell, M. Bevis, J. Duan, R.A. Anthes, C. Rocken, R.H. Ware, M. Exner, T. Vanhove, and F.S. Solheim, 1996: The promise of GPS in atmospheric monitoring. *Bull. Amer. Meteor. Soc.,* **77**, 5-18.

Changnon, S.A., 2001: Thunderstorm rainfall in the conterminous United States. *Bull. Amer. Meteor. Soc.*, **82**, 1925-1940.

Concannon, P.R., H.E. Brooks, and C.A. Doswell, III, 2000: Climatological risk of strong and violent tornadoes in the United States. Preprints, *2nd Symposium on Environmental Applications*, Amer. Meteor. Soc., 212-219.

Crawford, T.M., and H.B. Bluestein, 1997: Characteristics of dryline passage during COPS-91. *Mon. Wea. Rev.*, **125**, 463-477.

Doswell, C.A., III, 1980: Synoptic-scale environments associated with High Plains severe thunderstorms. *Bull. Amer. Meteor. Soc.*, **61**, 1388-1400.

Dupilka, M.L. and G.W. Reuter, 2005: An examination of three severe convective storms that produced significant tornadoes in central Alberta. *Submitted to National Weather Digest.*

Fujita, T., 1958: Structure and movement of a dry front. *Bull. Amer. Meteor. Soc*., **39**, 574-582.

Galway, J.G., 1956: The lifted index as a predictor of latent instability. *Bull. Amer. Meteor. Soc.,* **37**, 528-529.

Goff, J.A., and S. Gratch, 1946: Low-pressure properties of water from –160 to 212 F. *Trans. Amer. Soc. Heat. Vent. Eng*., **52**, 95-122.

Gokhale, N.R., 1975: *Hailstorms and Hailstone Growth*, State University of New York Press, 465 pp.

Hane, C.E., R.M. Rabin, T.M. Crawford, H.B. Bluestein, and M.E. Baldwin, 1997: Severe thunderstorm development in relation to along-dryline variability: A case study. *Mon. Wea. Rev*., **125**, 231-251.

_____, _____, _____, _____, and _____, 2000: Severe thunderstorm initiation along the dryline. A mesoscale case study. Preprints, *20th Conf. on Severe Local Storms*, Amer. Meteor. Soc., 80-83.

_____, _____, _____, _____, and _____, 2001: A case study of severe storm development along a dryline within a synoptically active environment. Part I: Dryline motion and an eta model forecast. *Mon. Wea. Rev*., **129**, 2183-2204.

Hoch, J., and P. Markowski, 2005: A climatology of springtime dryline position in the U.S. Great Plains region. *J. Clim*., **18**, 2132-2137.

Holton, J.R., 1992: *An Introduction to Dynamic Meteorology*. Academic Press, 511 pp.

Hoyle, V.A., 2005: Data assimilation for 4-D wet refractivity modeling in a regional GPS network. M.Sc. Thesis, Department of Geomatics Engineering, University of Calgary, 172 pp.

Huschke, R.E, 1959: *Glossary of Meteorology*, 1st ed. Amer. Meteor. Soc., 638 pp.

Kaplan, E.D., 1996: *Understanding GPS Principles and Applications*, Artec House, 554 pp.

Knott, S.R.J., and N.M. Taylor, 2000: Operational aspects of the Alberta severe weather outbreak of 29 July 1993. *Nat. Wea. Digest*, **24**, 11-23.

Krauss, T.W., and J.R. Santos, 2004: Exploratory analysis of the effect of hail suppression operations on precipitation in Alberta. *Atmos. Res.,* **71**, 35-50.

Peckham, S.E., R.B. Wilhelmson, L.J. Wicker, and C.L. Ziegler, 2004: Numerical simulation of the interaction between the dryline and horizontal convective rolls. *Mon. Wea. Rev*., **132**, 1792-1812.

Peterson, R.E., 1983: The West Texas dryline: Occurrence and behaviour. Preprints, *13th Conf. on Severe Local Storms*, Amer. Meteor. Soc., 9-11.

Phillips, D.W., 1990: *The Climates of Canada*, Canadian Government Publishing, 176 pp.

Pietrycha A.E., and E.N. Rasmussen, 2001: Observations of the Great Plains dryline utilizing mobile mesonet data. Preprints, *9th Conf. on Mesoscale Processes*, Amer. Meteor. Soc., 452-456.

_____, and _____, 2004: Finescale surface observations of the dryline: A mobile mesonet perspective. *Wea. Forecasting*, **19**, 1075-1088.

Raddatz, R.L., 1998: Anthropogenic vegetation transformation and the potential for deep convection on the Canadian prairies. *Can. J. Soil Sci*., **78**, 657-666.

Rasmussen, E.N., and D.O. Blanchard, 1998: A baseline climatology of sounding-derived supercell and tornado forecast parameters. *Wea. Forecasting*, **13**, 1148-1164.

Rhea, J.O., 1966: A study of thunderstorm formation along dryline. *J. Appl. Meteor*., **5**, 58-63.

Rocken, C., T. Vanhove, J. Johnson, F. Solheim, R. Ware, M. Bevis, S. Chiswell, and S. Businger, 1995: GPS/STORM – GPS sensing of atmospheric water-vapor for meteorology. *J. Atmos. Ocean Tech*., **12**, 468-478.

Schaefer, J.T., 1973: The motion of the dryline. Preprints, *8th Conf. on Severe Local Storms*, Amer. Meteor. Soc., 104-107.

_____, 1974: The life cycle of the dryline. *J. Appl. Meteor*., **13**, 444-449.

_____, 1986: The dryline. *Mesoscale Meteorology and Forecasting*, P.S. Ray, Ed., Amer. Meteor. Soc., 549-572.

Smith, C.D., F. Seglenieks, B. Proctor, and E.D. Soulis, 2001: Determining total atmospheric precipitable water vapour using two Canadian GPS receivers, *CMOS Bull.,* **29**, 107-114.

Smith, R., J. Paegle, T. Clark, W. Cotton, D. Durran, G. Forbes, J. Marwitz, C. Mass, J. McGinley, H.L. Pan, and M. Ralph, 1997: Local and remote effects of mountains on weather: Research needs and opportunities. *Bull. Amer. Meteor. Soc*., **78**, 877-892.

Smith, S.B., and M.K. Yau, 1993a: The causes of severe convective outbreaks in Alberta. Part I: A comparison of a severe outbreak with two non-severe events. *Mon. Wea. Rev.,* **109**, 1099-1125.

_____, and _____, 1993b: The causes of severe convective outbreaks in Alberta. Part II: Conceptual model and statistical analysis. *Mon. Wea. Rev.,* **109**, 1126-1133.

Strong, G.S., 1982: Hailstorms! - Why Alberta? *Chinook*, Winter/Spring, 21-23.

_____, 1986: Synoptic to mesoscale dynamics of severe thunderstorm environments: A diagnostic study with forecasting implications. Ph.D. Thesis, Department of Geography, University of Alberta, 345 pp.

_____, 1989: LIMEX-85: 1. Processing of data sets from an Alberta mesoscale upper-air experiment. *Clim. Bull.*, **23**, 98-118.

_____, 1997: Atmospheric moisture budget estimates of regional evapotranspiration from RES-91. *Atmos.-Ocean*, **35**, 29-63.

_____, 2000: A multi-scale conceptual model of severe thunderstorms. *CMOS Bull.*, **28**, 45-54.

_____, personal e-mail communication, November 16, 2005a.

_____, L. Hill, R. Goodson, T. Krauss, V. Hoyle, N. Nicholson, S. Skone, C.D. Smith, P. King, and L. deGroot, 2005b: A-GAME: Part II: Evaluation of revised multi-scale Alberta thunderstorm model. *To be submitted to Atmos.-Ocean.*

Stull, R.B., 1988: *An introduction to boundary layer meteorology*. Kluwer Academic Publishers, 666 pp.

Sun, W.Y., 1987: Mesoscale convection along the dryline. *J. Atmos. Sci.*, **44**, 1394-1403.

_____, and C.C. Wu, 1992: Formation and diurnal variation of the dryline. *J. Atmos. Sci.*, **49**, 1606-1619.

Trier, S.B., F. Chen, and K.W. Manning, 2004: A study of the convection initiation in a mesoscale model using high-resolution land surface initial conditions. *Mon. Wea. Rev.*, **132**, 2954-2976.

Uccellini, L.W., and D.R. Johnson, 1979: The coupling of upper and lower tropospheric jet streaks and implications for the development of severe convective storms. *Mon. Wea. Rev.*, **107**, 682-703.

Weckwerth, T.M., D.B. Parsons, S.E. Koch, J.A. Moore, M.A. LeMone, B.B. Demoz, C. Flamant, B. Geerts, J. Wang, and W.F. Feltz, 2004: An overview of the

International H_20 Project (IHOP) and some preliminary highlights. *Bull. Amer. Meteor. Soc*., **85**, 253-277.

Wojtiw, L., 1975: Climatic summaries of hailfall in central Alberta (1957-1973). Alberta Research Atmospheric Science Report 75-1, Edmonton. 102 pp.

Wu, P., J-I. Hamada, S. Mori, Y.I. Tauhid, and M.D. Yamanaka, 2003: Diurnal variation of precipitable water over a mountainous area of Sumatra Island. *J. Appl. Meteor*., **42**, 1107-1115.

Ziegler, C.L., and C.E. Hane, 1993: An observational study of the dryline. *Mon. Wea. Rev*., **121**, 1134-1151.

Appendix A: Scales of Atmospheric Motion

When describing atmospheric phenomena, the scales of motion are defined in both spatial and temporal terms. Synoptic scale processes, such as shortwaves and low and high pressure systems, are phenomena that range in spatial scale from 2000 to 5000 km, affecting a region for 2-7 days. Synoptic data are collected simultaneously over the whole globe, and typically are displayed on weather maps. Mesoscale processes such as sea/land breezes, and thunderstorms take place over spatial scales of the order of 10-1000 km and temporal scales of 3-24 h. The focus of this study, the Alberta dryline, is a mesoscale phenomenon influenced by synoptic scale processes and local topography through scale interactions (Strong, 1986), which link it to the initiation of thunderstorms over the Alberta foothills.

Appendix B: Climatology of FOPEX Observations

In order to better identify the dryline within the FOPEX transect of weather stations, mean mixing ratio values of the stations over the entire study period were examined.

Seasonal Variability

Examination of the FOPEX line of surface stations for the summer months of 2003 and 2004 showed a significant difference in mean mixing ratio between stations and between months (Table A1). Comparing each surface station over each month of the two summers revealed at least a 1.0 g kg^{-1} increase in mean mixing ratio values between 2003 and 2004.

Table A1. Mean mixing ratio values (g kg^{-1}) for each station in the FOPEX transect by month and year (AB2 was decommissioned in 2004). Results for station AB5 are not displayed as a result of the poor data recovery rate from this station in 2003.

FOPEX Station	2003		2004	
	JUL	AUG	JUL	AUG
AB0	7.33	7.55	8.96	8.85
AB1	7.28	7.48	8.75	8.66
AB2	7.17	7.03	-	-
AB3	6.86	7.03	8.24	8.64
AB4	6.29	6.54	7.47	8.01

The Meteorological Service of Canada (MSC) produced imagery depicting departures from normal (the climatological mean for 1951-1980) of surface air temperature (not shown) and precipitation (Figure A1) over Canada. The temperature anomalies for 2003 and 2004 are not displayed because the temperature anomalies in the FOPEX area were similar for both summers. The precipitation patterns however, were below normal over

the FOPEX area in 2003 and near normal during 2004. This was reflected in the FOPEX surface data with the +1 g kg^{-1} increase noted in the FOPEX mixing ratio between 2003 to 2004.

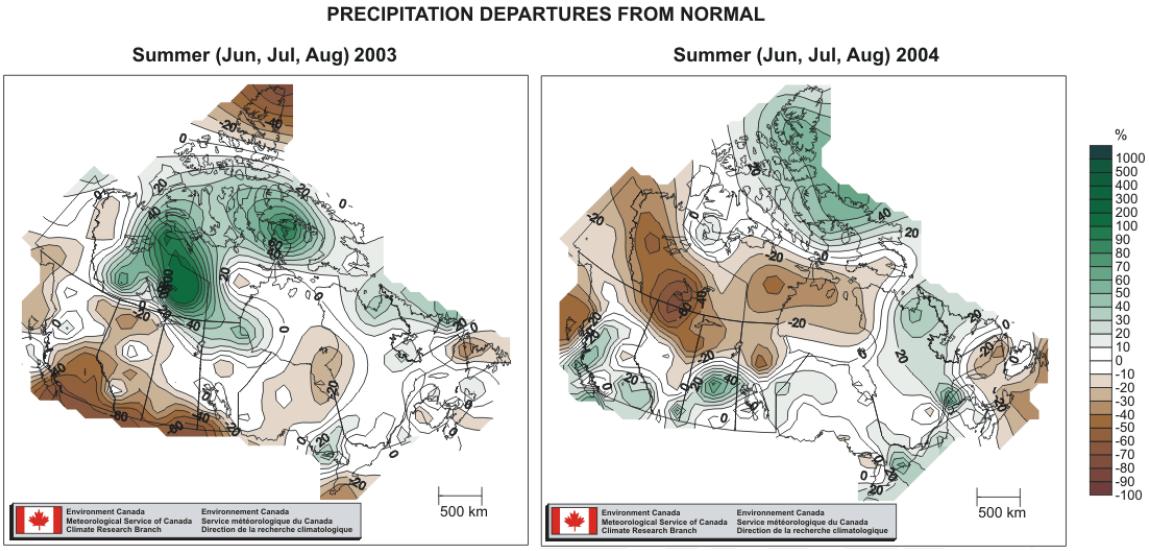

Figure A1. The precipitation anomalies observed during June - August in 2003 and 2004 from the 1951-1980 climatological normal. From the Climate Trends and Variations Bulletin, Meteorological Service of Canada, http://www.msc.ec.gc.ca/ccrm/bulletin/archive_e.cfm.

Elevation Variability

The highest mean mixing ratios in both field seasons were observed at the lowest elevation, AB0, while the lowest mean mixing ratios were observed at the highest station, AB4 on south end of Limestone Mountain ridge (AB5 mean mixing ratio values are not displayed due to poor data recovery from this site). The average difference between the lowest and highest elevation stations was 1.1 g kg^{-1}. This mixing ratio gradient from high to low elevations results from dry air sweeping in from the mountains to the west, contrasting with more humid air at lower elevations on the east side of Limestone Mountain over the foothills.

Diurnal Trend Variability

The mean diurnal patterns of mixing ratio for the FOPEX transect during July and August of 2003 and 2004 are displayed in Figure A2. In 2003, the average daily range above the minimum mixing ratio (typically observed at ~1300 UTC) was 1.1 g kg^{-1} for all stations, while in 2004 this range was slightly higher at 1.9 g kg^{-1}. The rate of increase in mixing ratio is highest after sunrise with solar heating causing evaporation of water at the surface, and it decreases a few hours after sunrise due to increased vertical mixing in the boundary layer (Wu et al., 2003). Overall, mean diurnal trend of mixing ratio within the FOPEX transect for 2003 ranged between values of 6-8 g kg^{-1}, whereas for 2004 it ranged between 7-10 g kg^{-1}. For both summers, the diurnal trend was larger at lower elevations than higher elevations. The lower elevation stations likely observed larger daily fluctuations of mixing ratio due to the proximity to the main source of moisture in the Alberta Plains (evapotranspiration from seasonal crops). Evapotranspiration rates from such crops fluctuate significantly on a daily basis, increasing specific humidity in the boundary layer by up to 8 g kg^{-1} during the day (Raddatz, 1998).

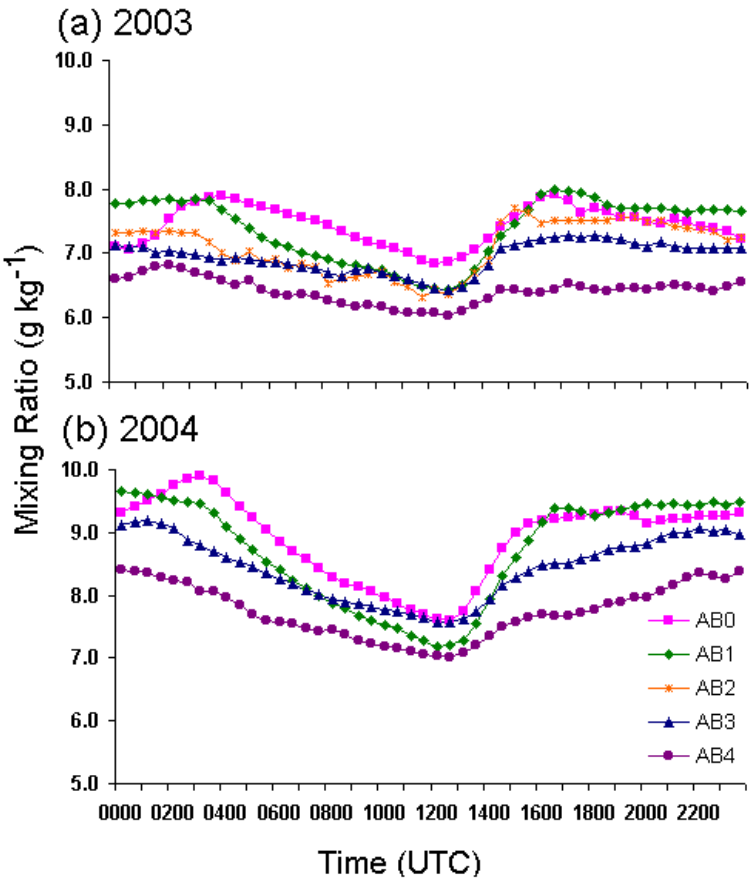

Figure A2. The mean mixing ratio diurnal trend in the FOPEX transect of surface stations in south-central Alberta for July and August of a) 2003 and b) 2004. Stations AB2 and AB5 were decommissioned after 2003 due to logistical constraints.

Appendix C

The following article written by the author appeared in the University of Alberta Environmental Research and Studies Centre (ERSC) publication 'Environment News' in March 2005 (Vol. 5, Issue 2). It is available through the ERSC website, http://www.ualberta.ca/~ersc/.

The Hunt for Dry Air

Lesley Hill
MSc Student
Earth and Atmospheric Sciences
University of Alberta

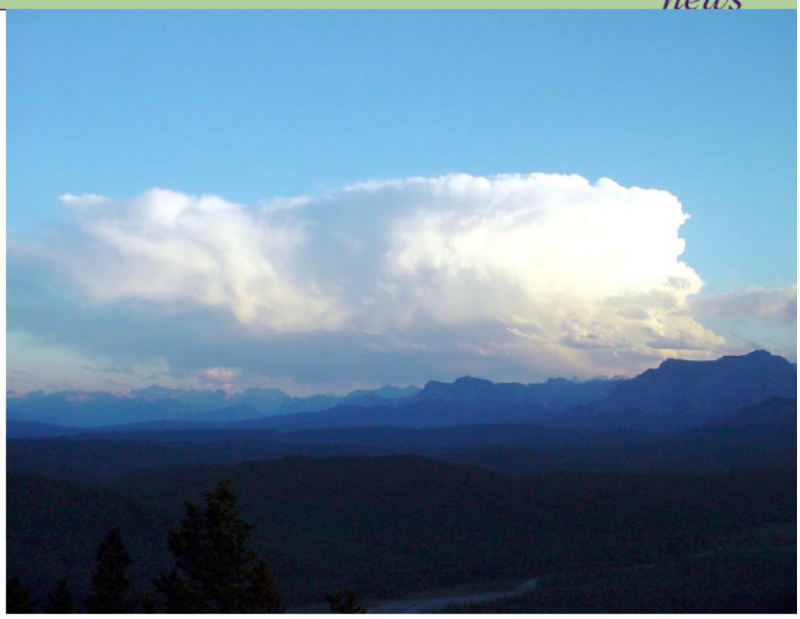

A thunderstorm develops east of the Rocky Mountain barrier over the Alberta foothills on July 16, 2003. The severe storms observed on this day produced golfball-sized hail in south-central Alberta.

(Photo by Victoria Hoyle)

One may ask—why would someone go looking for dry air in Alberta during the summer? You might think it wouldn't be too hard to find considering Alberta is one of the driest provinces in Canada where potential evapotranspiration actually exceeds precipitation. However, when one takes into consideration that moisture levels are relative, not all of Alberta can be considered dry.

Pat King (left) and Lesley Hill equip their vehicle to measure air temperature and relative humidity as they drive into the foothills hoping to detect the dryline.

The effect of the Rocky Mountains on Alberta weather is not limited to causing a rain shadow. The foothills are an important topographical feature that influences the local weather in such a way that Alberta has some of the most frequent and intense thunderstorms in Canada. For example hail is observed in central Alberta on about 50% of summer days. In order to accurately predict the impacts of future climate change on severe weather occurrences in Alberta, it is necessary to first understand the influence of local conditions in thunderstorm development in this unique area of Canada.

On the regional scale, evapotranspiration from the vegetated surface at lower elevations east of the foothills results in relatively moist air when compared with air at higher elevations in the foothills. This contrasting relatively moist air in interior Alberta and dry mountain air is important for the development of an environment conducive to thunderstorm development.

The weather conditions on a typical severe thunderstorm day in Alberta include easterly surface winds (towards the foothills) in central Alberta, and southwesterly winds aloft over the Rockies. This results in dry mountain air blowing down into the foothills to lower elevations, while at the surface winds in central Alberta are advecting moist air towards the foothills. The relatively dry and moist airmasses converge along the foothills.

This area of convergence is known as the dryline—a boundary detectable at the surface as a significant change in moisture over a relatively short distance. The dryline is a weather feature unique to areas in the lee of the Rocky Mountains, most prominently in the

High Plains of the USA. Extensive research on the dryline has been performed in the High Plains, yet very little significant research has been focused on this phenomenon in Alberta. The conceptual model developed for the High Plains can be applied to Alberta, yet the frequency of development and important local influences on thunderstorm development may be different for Alberta.

The value of studying regional differences in dryline behaviour and impacts on thunderstorm initiation is amplified by the growing population in this region of Canada and millions of dollars in hail and wind damage incurred annually in Alberta from severe thunderstorms.

The conceptual model for the dryline focuses on the lower levels of the atmosphere and at the surface there is relatively dry air west of the dryline and moist air east of the dryline. The dry air overrides the moist air at higher levels, which creates an unstable (drier and warmer) layer of air above the moist surface layer east of the dryline. These two layers form a shallow, stable temperature inversion that normally decreases with height. This stable layer is called a capping lid.

The presence of a capping lid allows latent heat energy to build up at the surface as air temperatures rise during the day and mixing occurs. With a capping lid in place, rising parcels of air will not be able to pass above that elevated layer of stable air. If enough energy has built up at the surface (typically by late afternoon), these rising parcels of air will have enough momentum to pass beyond the capping lid, removing or 'breaking' it. These rising parcels of air can quickly turn into large towering cumulus clouds and thunderstorms.

The dryline research that Dr. Geoff Strong (Adjunct Professor, University of Alberta) and I conducted in south-central Alberta during July and August of 2003/2004 is associated with the Alberta GPS Atmospheric Moisture Evaluation (A-GAME) study run by Dr. Susan Skone at the University of Calgary, and a study called Foothills Orographic Precipitation Experiment (FOPEX) conducted by Mr. Craig Smith of the Meteorological Service of Canada (MSC). Our focus was on observing the dryline using both stationary and mobile surface measurements, launching weather balloons to detect a capping lid, and using the GPS data to measure total atmospheric moisture over the region. The stationary surface measurements were collected using six meteorological stations installed for FOPEX at different elevations extending from Caroline to the ridge of Limestone Mountain. One of the objectives of my research is to create a climatology for drylines in southern Alberta, based on dryline detection within this network of surface stations.

The hunt for dry air during the A-GAME field study was carried out using a car equipped to measure temperature and relative humidity, and making mobile surface transects from the Caroline/Sundre area west into the foothills ending at Mountain Aire Lodge. A laptop connected to the sensor allowed us to directly monitor the output as we were driving, and we could observe any significant changes in the moisture level. Although the opportunity to make these mobile observations was limited, these data will be examined as case studies. These case studies will focus on the development of severe weather in south-central Alberta and how it was influenced by the dryline.

This study is an important step towards developing a unique knowledge base for the dryline phenomenon in Canada. Preliminary results show that although the dryline is less prominent than in the High Plains, it is a very important feature over southern Alberta and needs to be closely monitored when the potential for thunderstorms exists.

A familiar scene during the summertime as storms rumble across the prairies.